NASA/CR-2005-213749

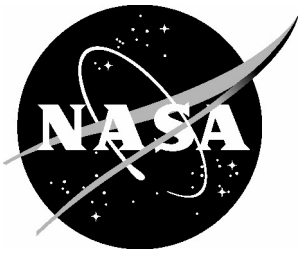

Advanced Energetics for Aeronautical Applications: Volume II

David S. Alexander
MSE Technology Applications, Inc., Butte, Montana

April 2005

The NASA STI Program Office . . . in Profile

Since its founding, NASA has been dedicated to the advancement of aeronautics and space science. The NASA Scientific and Technical Information (STI) Program Office plays a key part in helping NASA maintain this important role.

The NASA STI Program Office is operated by Langley Research Center, the lead center for NASA's scientific and technical information. The NASA STI Program Office provides access to the NASA STI Database, the largest collection of aeronautical and space science STI in the world. The Program Office is also NASA's institutional mechanism for disseminating the results of its research and development activities. These results are published by NASA in the NASA STI Report Series, which includes the following report types:

- TECHNICAL PUBLICATION. Reports of completed research or a major significant phase of research that present the results of NASA programs and include extensive data or theoretical analysis. Includes compilations of significant scientific and technical data and information deemed to be of continuing reference value. NASA counterpart of peer-reviewed formal professional papers, but having less stringent limitations on manuscript length and extent of graphic presentations.

- TECHNICAL MEMORANDUM. Scientific and technical findings that are preliminary or of specialized interest, e.g., quick release reports, working papers, and bibliographies that contain minimal annotation. Does not contain extensive analysis.

- CONTRACTOR REPORT. Scientific and technical findings by NASA-sponsored contractors and grantees.

- CONFERENCE PUBLICATION. Collected papers from scientific and technical conferences, symposia, seminars, or other meetings sponsored or co-sponsored by NASA.

- SPECIAL PUBLICATION. Scientific, technical, or historical information from NASA programs, projects, and missions, often concerned with subjects having substantial public interest.

- TECHNICAL TRANSLATION. English-language translations of foreign scientific and technical material pertinent to NASA's mission.

Specialized services that complement the STI Program Office's diverse offerings include creating custom thesauri, building customized databases, organizing and publishing research results ... even providing videos.

For more information about the NASA STI Program Office, see the following:

- Access the NASA STI Program Home Page at ***http://www.sti.nasa.gov***

- E-mail your question via the Internet to help@sti.nasa.gov

- Fax your question to the NASA STI Help Desk at (301) 621-0134

- Phone the NASA STI Help Desk at (301) 621-0390

- Write to:
  NASA STI Help Desk
  NASA Center for AeroSpace Information
  7121 Standard Drive
  Hanover, MD 21076-1320

NASA/CR-2005-213749

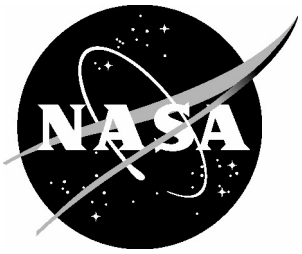

Advanced Energetics for Aeronautical Applications: Volume II

David S. Alexander
MSE Technology Applications, Inc., Butte, Montana

National Aeronautics and
Space Administration

Langley Research Center
Hampton, Virginia 23681-2199

Prepared for Langley Research Center
under Grant NAG1-02048

April 2005

Acknowledgments

The author would like to extend his appreciation to those who have contributed to this report.

In particular, these include, at NASA Langley Research Center, Dennis Bushnell for his vision and leadership and Mark Guynn for his technical contributions. At MSE Technology Applications Inc. (MSE), Dr. Ying-Ming Lee, Dr. Bojana Nikolic-Tirkas, Luke Mauritsen, Chris Ossello, Gloyd Simmons, and Steve Tarrant provided technical contributions; David Micheletti provided project support; and Lisa Barker, Lee Black, Chuck Clavelot, Judy Harvey, and Julie Wyant provided editorial, graphic, and document preparation support.

Work was conducted under Montana Aerospace Development Authority Subcontract No. MADA0001 and National Aeronautics and Space Administration Langley Research Center Grant No. NAG1-02048 at MSE.

Available from:

NASA Center for AeroSpace Information (CASI)
7121 Standard Drive
Hanover, MD 21076-1320
(301) 621-0390

National Technical Information Service (NTIS)
5285 Port Royal Road
Springfield, VA 22161-2171
(703) 605-6000

Contents

Page

Contents (Cont'd)

Contents (Cont'd)

Contents (Cont'd)

Contents (Cont'd)

Page

Figures

Tables

Acronyms and Abbreviations

2-D	two-dimensional
3-D	three-dimensional
ac	alternating current
atm	atmosphere (measurement)
B^{11}	most common boron isotope with atomic weight 11
BSRF	Borderland Sciences Research Foundation
Btu	British thermal unit
°C	degree Celsius
CBFR	Colliding Beam Fusion Reactor
CBFR-SPS	Colliding Beam Fusion Reactor Space Propulsion System
C_L	lift coefficient
cm	centimeter
CNT	carbon nanotube
CR	contractor report
C_μ	momentum coefficient
CW	continuous wave
dc	direct current
DEC	direct energy converter
EM	electromagnetic
°F	degree Fahrenheit
FLOPS	Flight Optimization System
ft	foot/feet
G	acceleration equivalent to the acceleration of gravity at the surface of the Earth
GaSb	gallium antimonide
GE	General Electric
GECAT	Graphical Engine Cycle Analysis Tool
GH_2	gaseous hydrogen
gpm	gallons per minute
GTE	gas turbine engine
GW	gravitational wave
H^1	hydrogen

Acronyms and Abbreviations (Cont'd)

Hz	hertz
He^4	helium 4
HFC	hydrogen fuel cell
HFGW	high frequency gravitational wave
hp	horsepower
ICCF	International Conference on Cold Fusion
ICP-MS	inductively coupled plasma-mass spectrometry
IEC	Inertial Electrostatic Confinement
ID	inside diameter
in	inch
INE	Institute of New Energy
IRI	Integrity Research Institute
K	degree Kelvin
kg	kilogram
kHz	kilohertz
kPa	kilopascal
kV	kilovolt
kW	kilowatt
kWh	kilowatt-hour
L	length
lb	pound
L/D	lift-to-drag
LENR	low energy nuclear reaction
LFGW	low frequency gravitational waves
LH_2	liquid hydrogen
LHe	liquid helium
LMD	longitudinal magneto-dielectric (waves)
m	meter
m^2	square meter
MEMS	micro-electromechanical systems
MeV	megaelectronvolt

Acronyms and Abbreviations (Cont'd)

mH	millihenry
MHz	megahertz
min	minute
mm	millimeter
MSE	MSE Technology Applications, Inc.
MW	megawatt
NASA	National Aeronautics and Space Administration
NASA-LaRC	NASA Langley Research Center
Nb_3Sn	niobium-tin (superconductor wire)
NEPP	NASA Engine Performance Program
NIST	National Institute of Standards and Testing
nmi	nautical mile
OD	outside diameter
P/P	power/propulsion
psi	pound per square inch
PSOFC	planar solid oxide fuel cell
PV	polarizable vacuum
R	rankine
R_e	Reynolds number
RF	radio frequency
s	second
SOFC	solid oxide fuel cell
TEC	thermoelectric converter
TEM	transverse electromagnetic (waves)
TOF-SIMS	time of flight secondary ion mass spectrometry
TPV	thermophotovoltaic
μF	microfarad
USAF	U. S. Air Force
V	volt
W	watt
ZPE	zero point energy

Executive Summary of This Project Prior to This Report

The National Aeronautics and Space Administration (NASA) has identified water vapor emission into the upper atmosphere from commercial transport aircraft, particularly as it relates to the formation of persistent contrails, as a potential environmental problem. Since 1999, MSE Technology Applications, Inc. (MSE) has been working with the NASA Langley Research Center (NASA-LaRC) to investigate the concept of a transport-size emissionless aircraft fueled with liquid hydrogen (LH_2) combined with other possible breakthrough technologies. The goal of the project is to significantly advance air transportation in the next decade and beyond. The power/propulsion (P/P) system currently being studied would be based on hydrogen fuel cells (HFCs) powering electric motors, which drive fans for propulsion. The liquid water reaction product is retained onboard the aircraft until a flight mission is completed.

As of now, NASA-LaRC and MSE have identified P/P system components that, according to the high-level analysis conducted to date, are light enough to make the emissionless aircraft concept feasible. Calculated maximum aircraft ranges (within a maximum weight constraint) and other performance predictions are included in this report.

Carrying liquid water reaction product onboard for the duration of a flight mission imposes a severe weight penalty. If modeling and experiments show that water may be expelled as liquid droplets of an appropriate size and temperature and will not significantly reevaporate in the higher atmosphere nor freeze and form hailstones when falling through the lower atmosphere, the resulting weight relief would greatly accelerate the practical realization of this project. A preliminary calculation showing the magnitude of the resulting benefit of this weight reduction is included in this report.

Even though near-term technology allows for a plausible concept for an emissionless aircraft and therefore a solution to the high-altitude water vapor problem, more advanced technologies presently being investigated in research laboratories may potentially offer more practical solutions. For example, advanced aerodynamics could potentially extend the fuel efficiency of any aircraft; this report describes some leading examples of this type of research.

In the midterm, recently discovered types of nuclear reactions that do not produce penetrating radiation may offer fuel energy densities approximately one million times greater than that of chemical fuels. Examples of these reactions are described. Additionally, recently discovered methods for converting heat to electricity, transferring heat, and storing energy are discussed.

In the long-term, technologies that can only be described as "breakthrough" may potentially be available for producing energy from the very structure of space-time itself or propelling vehicles without using a material propellant to balance momentum. Present research being conducted at multiple locations around the world indicates such technologies may be possible, and this research is presented.

Finally, some topics of "breakthrough physics," which typically precede "breakthrough technology," are presented at an introductory level.

Executive Summary of This Report

The National Aeronautics and Space Administration (NASA) has identified water vapor emission into the upper atmosphere from commercial transport aircraft, particularly as it relates to the formation of persistent contrails, as a potential environmental problem. As a possible solution to this problem, a revolutionary aircraft concept (based upon liquid hydrogen fuel, high temperature fuel cells, electric motors driving fans for propulsion, and retention of reaction product water) was developed, verified with NASA computational flight codes (using stated assumptions) to be a valid concept, and published as NASA/CR-2003-212169. A continuation and extension of that research is published herein; previous conclusions regarding the feasibility of this project remain valid. Applicable near-term concepts described in this current report include: 1) expulsion of reaction product water in a form or by a method that will not harm the environment, 2) using water expelled as vapor (below a "critical" altitude) to augment aircraft propulsion thrust, 3) fabricating planar solid oxide fuel cells (PSOFCs) from materials that could potentially yield a significantly higher electric power density (kilowatt/kilogram), and 4) using the aerodynamic concept known as "circulation control" to extend aircraft range by providing a better match between cruise and takeoff/landing requirements. In addition, conceptual emissionless aircraft performance parameters have been calculated using actual PSOFC electric power density and electrochemical efficiency data from a company that fabricates these devices.

A major limitation to the performance of a conventional aerospace vehicle is the weight of the fuel. Therefore, MSE Technology Applications, Inc. (MSE) investigated revolutionary and breakthrough power production technologies that could potentially allow the creation of aerospace technology far surpassing the state of the art. Such technology (conceptually examined by MSE) includes two distinctly different categories of flight weight fusion reactors. One of these systems is characterized by a radial electric field in a spherical shape; the other is based upon a cylindrical-shaped magnetic field. Both systems react common inexpensive fuels in a plasma state and produce reaction product ions with a very high kinetic energy but do not produce neutrons (or penetrating radiation) or residual radioactive components. The kinetic energy of these fast-moving charged ions produced in these fusion reactions may be readily converted to electric power by known methods. These revolutionary fusion power systems would increase fuel energy density (kilowatt-hour/kilogram) by a factor of approximately one million compared to chemical fuels, and they would be totally emissionless and safe.

As part of this research and at the invitation of NASA Langley Research Center, MSE investigated advanced energetics topics of a more long-term nature. Selected electric concepts such as a deeper understanding of the components of the "electric field," longitudinal electric waves, and scalar waves as well as other advanced physics concepts that are replicable (but not widely known) were examined. Some of these could potentially be developed into advanced power and propulsion technologies or even help access zero point energy, which has a basis firmly established in theoretical physics and a calculated energy density many orders of magnitude greater than currently used sources of energy.

Several additional selected topics in advanced physics (including condensed matter nuclear science and high frequency gravitational waves) were also investigated in order to provide increased understanding of and further insights into some of the research mentioned above.

General Disclaimer

The content of "Advanced Energetics for Aeronautical Applications," both prior and current work, should be considered as a "work-in-progress."

What is reported reflects the current status of investigations and analysis on selected topics.

1. Potential New Aeronautical Energetic Requirement—The "Emissionless Aircraft"—Updated Investigations and Innovations

1.1 Emissionless Aircraft Conceptual Model at the Conclusion of Work Prior to This Report

This section summarizes, in somewhat more detail, the status of the "application side" of the Advanced Energetics for Aeronautical Applications when the prior work was published.

1.1.1 Status of Project Investigations when Prior Work was Published

The following excerpt from the Conclusions section of the prior work is quoted as an introduction to this report.

> *There is now convincing evidence to support observations that water vapor emission into the atmosphere at altitudes above 25,000 ft by conventional hydrocarbon-fueled aircraft is changing climate patterns in local regions, possibly adversely through the formation of contrails. However, the extent of the effect has not been fully determined.*
>
> *Starting with the guideline that any feasible approach could be investigated and considered, and the research performed to date, MSE has determined that a near-emissionless 300 passenger commercial transport aircraft capable of flying substantial distances is conceptually possible. This conclusion was reached by a logical process of eliminating approaches considered to be impractical and assuming there will be modest gains made in areas of technology such as component weight reduction, energy conversion power density, and advanced aeronautics. A numerical analysis based upon the NASA-LaRC FLOPS code, (modified for this application) was used to calculate estimated maximum ranges of the conceptual emissionless aircraft. This analysis, including the energy conversion and aerodynamic assumptions that went into the calculations as well as the calculated ranges and some of the other parameters that are code outputs, have been reported during the course of this study and included herein.*
>
> *The emissionless aircraft concept developed by MSE would use a novel combination of the following technologies, all of which have been developed as hardware (to some degree):*
>
> - *LH_2 fuel carried in insulated tanks;*
> - *high temperature PSOFCs to generate electricity by combining hydrogen with oxygen from ambient air;*
> - *bottoming cycle GTEs coupled to generators to convert heat in the fuel cell exhaust gas into additional electric power;*
> - *ultralight, ultraefficient cryogenic electric motors, coupled to fans, to provide propulsion;*

- *advanced aeronautical technology to maximize the L/D ratio in order to maximize aircraft range;*
- *lightweight, high-strength materials to fabricate appropriate aircraft components, to minimize empty weight and therefore maximize aircraft range; and*
- *novel advanced, lightweight heat transfer technology to remove heat from water vapor produced during flight so that water vapor may be condensed to a liquid and stored onboard for the remainder of a flight mission.*

All of the above technologies have been investigated and reported on by MSE Technology Applications, Inc. (MSE) and are included in this report.

A tentative geometric configuration of major components and systems of the emissionless aircraft was devised within the constraints of technical parameters as currently known.

It was also concluded that if liquid water reaction product could be immediately expelled as liquid droplets of an appropriate size and temperature and would cause no adverse effects either in the atmosphere or on the ground, the resulting weight relief would greatly accelerate the project.

1.1.2 Conceptual Design and Component Placement

Figure 1 illustrates the conceptual design and placement of power/propulsion (P/P) and other components for the National Aeronautics and Space Administration Langley Research Center (NASA-LaRC)/MSE emissionless aircraft.

1.1.3 Calculated Maximum Emissionless Aircraft Ranges

Finally, it is noted that prior work indicated that the calculated range of the emissionless aircraft described by this concept would be 2,568 nautical miles (nmi) for conservative near-term assumptions and as far as 10,715 nmi using long-term assumptions (i.e., technology that is plausible but not yet developed).

1.2 Potential Planar Solid Oxide Fuel Cell Weight Reduction

1.2.1 Introduction

As described previously, planar solid oxide fuel cells (PSOFCs) are the primary source of electric power in the state-of-the-art conceptual emissionless aircraft being investigated. Therefore, it is obvious that any innovation that will increase the density of produced electric power $\left(\frac{\text{kW}}{\text{kg}}\right)$ from the aircraft PSOFCs will be of benefit to ensure project feasibility.

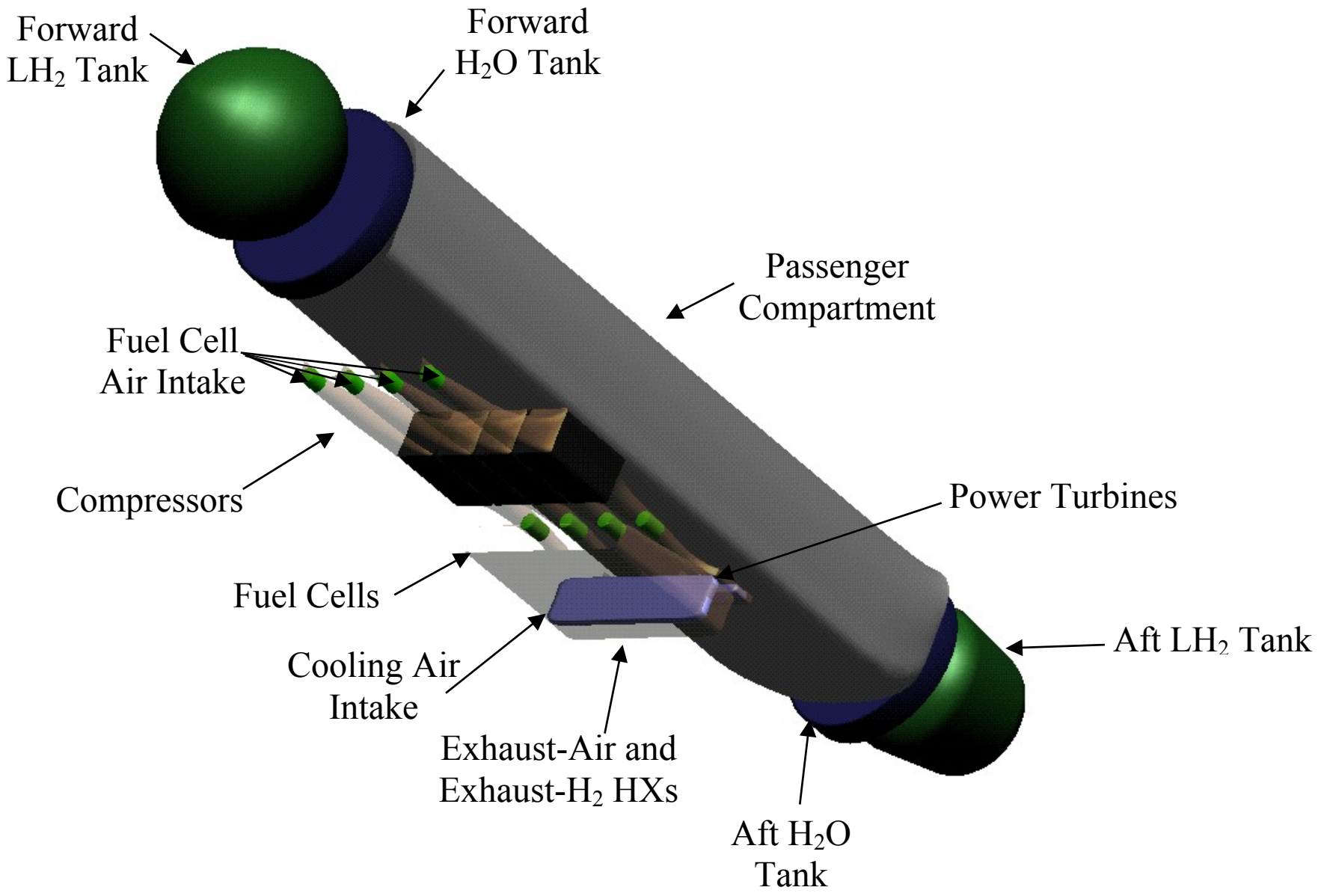

Figure 1. Conceptual design and placement of P/P and other components for the NASA-LaRC/MSE emissionless aircraft.

In order to decrease PSOFC weight, MSE postulated that the stacked plates (and exterior shell) of prototype PSOFCs currently manufactured from traditional stainless steels could instead be potentially produced from the specially developed "superalloys" from which the "hot" components of conventional aircraft turbine engines are produced.

The densities of standard stainless steels and superalloys are similar. It is suggested that (in the PSOFC interior), superalloy metal plates could be significantly thinner than those currently produced from standard stainless steel and that a significant saving in weight and volume would result.

1.2.2 Background Information

NASA-LaRC and MSE had assumed the following PSOFC parameters for aircraft system performance calculations reported in a recent NASA Contractor Report (CR) (Ref. 1, p. 24):

- PSOFC electrochemical efficiency:
  - near-term: 50% cruise, 60% descent; and
  - long-term: 60% cruise, 70% descent.
- PSOFC power density (weight basis):
  - near-term: 1,102 pounds/megawatt (lb/MW) [(2 kilowatt (kW)/kilogram (kg)]; and
  - long-term: 100 lb/MW.

Using these assumed weight-basis power densities, the calculated weight of PSOFCs for the respective near- and long-term scenario assumptions are as follows (Ref. 1, pp. 25-26):

- near-term: 86,139 lb; and
- long-term: 7,975 lb.

Two important points concerning these weights are:

1) Based upon PSOFC parameters known at the time of the previous analysis, no "overrating" of PSOFCs for the climb phase of a flight is allowed compared to the power requirement of the cruise phase of a flight. Therefore, the above weights are sized for the required climb power level.
2) It was assumed for the above-referenced calculations that higher weight reductions were not possible for PSOFCs by substituting (e.g., carbon nanotubes (CNTs) for metals) due to the hot and oxidizing environment.

1.2.3 PSOFC Parameters

One company developing PSOFCs uses circular metal plates with alternate plates coated on one side with a thin layer of a proprietary catalytic oxide material. The plates are sealed to each other over a small radial distance at the center. Spiral grooves on the uncoated plates direct fuel (hydrogen, which enters from the center) and oxidizer (air, which enters from the periphery) respectively. Prototype cells use plates with a 5-inch (in.) diameter. The important parameters relevant to the present investigation are:

- plate material—stainless steel (exclusive of oxide coating); and
- plate thickness—0.083 in.

Additionally, it is noted that:

- the particular alloy of stainless steel used for these plates was not stated;
- these plates were quite rigid (not flexible) at ambient temperature; and
- because the PSOFCs were laboratory prototypes, there has not yet been an attempt by the vendor to ***increase the weight-basis power density*** (i.e., reduce the weight).

1.2.4 PSOFCs Based Upon Superalloys

One can suggest that the metal plates used in this type of PSOFC could be metals specifically designed to maintain dimensional tolerances and strength at significantly high temperatures [e.g., the "nickel superalloys" used in the hot sections of gas turbine engines (GTEs)].

There has been considerable research and development of these types of metals, originating as long ago as 1930. These alloys are created by adding selected combinations of metallic and nonmetallic chemical elements (from a list of ***19*** elements) to a "base" of nickel and then using advanced processing techniques. Such alloys are used to fabricate turbine blades where they must maintain dimensional tolerances while being subjected to high (centrifugal) force and the high temperatures experienced in the turbine section of a GTE (Ref. 2).

The following assumptions can be used when considering to what extent metal weight may be reduced in PSOFCs by using superalloys instead of ordinary stainless steel.

1) The operating temperature inside PSOFCs has been stated to be on the order of 650 degrees Celsius (°C) (or less).
2) The proprietary solid oxide catalytic material will adhere to superalloys as well as it does to stainless steel.
3) There are no adverse chemical, electrical, or electrochemical effects that would occur if stainless steel were replaced with superalloys.
4) Most of the PSOFC weight is from the metal, and "shell" components (also fabricated from superalloys) can have their weight reduced by the same proportion as for cell plates.

Based on the extremely high strength at high temperatures of the nickel-based superalloys, one can postulate that PSOFC plates could be one-fourth the thickness of prototype plates now made from stainless steel. Therefore, because stainless steel and superalloys have nearly equal specific gravities (~8.0) and, using the above-stated assumptions, this is equivalent to stating that in the near-term the PSOFC weight-basis power density is 8.0 kW/kg (equivalent to 276 lb/MW).

1.2.5 Plate Bending and Plasticity Analyses

After initially suggesting that the metal plates in PSOFCs could be significantly thinner if produced from superalloys rather than standard stainless steel, MSE performed both plate bending and plasticity analyses on currently used ceramics and superalloys suggested for the PSOFC application. The results of these analyses are presented in this section.

The goal of this work was to attempt to realistically ***calculate*** the extent that metal plate components of PSOFCs could be reduced in thickness.

When a PSOFC heats from room temperature to operating temperature, any mismatch in coefficients of expansion of internal components will create stress in these components. The amount of stress would be proportional to an amount of bending (deflection) of these respective components if they were not constrained. It is readily possible to calculate material deflection by using:

- known internal geometric configurations of PSOFCs;
- properties of PSOFC materials; and
- standard, accepted methods of performing such calculations.

1.2.6 Calculation Method for Plate Bending and Plasticity Analyses

The fuel cell plates were modeled using ANSYS finite element software. Axisymmetric elements, representing the metal disk and the ceramic layer on one side of the metal disk were used. The stress is induced by the difference in the thermal expansion coefficients of the metal and the ceramic materials. Therefore, the analysis was performed by applying a uniform temperature of 650 ºC and comparing the stress and deflection in the metal plate for several different plate thicknesses (for a constant ceramic thickness between the plates).

It is understood that "ceramic" refers to a multilayer "sandwich" configuration of nickel-zirconia cermet as the anode (fuel side), yttria stabilized zirconia in the middle as the electrolyte (which conducts oxygen anions), and lanthanum strontium manganate as the cathode (air side). A schematic of another type of PSOFC, illustrating these layers, is shown in Figure 2 (Ref. 3). These three materials are produced with different controlled porosities and have similar thermal expansion coefficients [for another type of solid oxide fuel cell (SOFC)] as follows (Ref. 4):

- anode layer—12.5 x 10^{-6} centimeter (cm)/cm per degrees Celsius;
- electrolyte layer—10.5 x 10^{-6} cm/cm per degrees Celsius; and
- cathode layer—11 x 10^{-6} cm/cm per degrees Celsius.

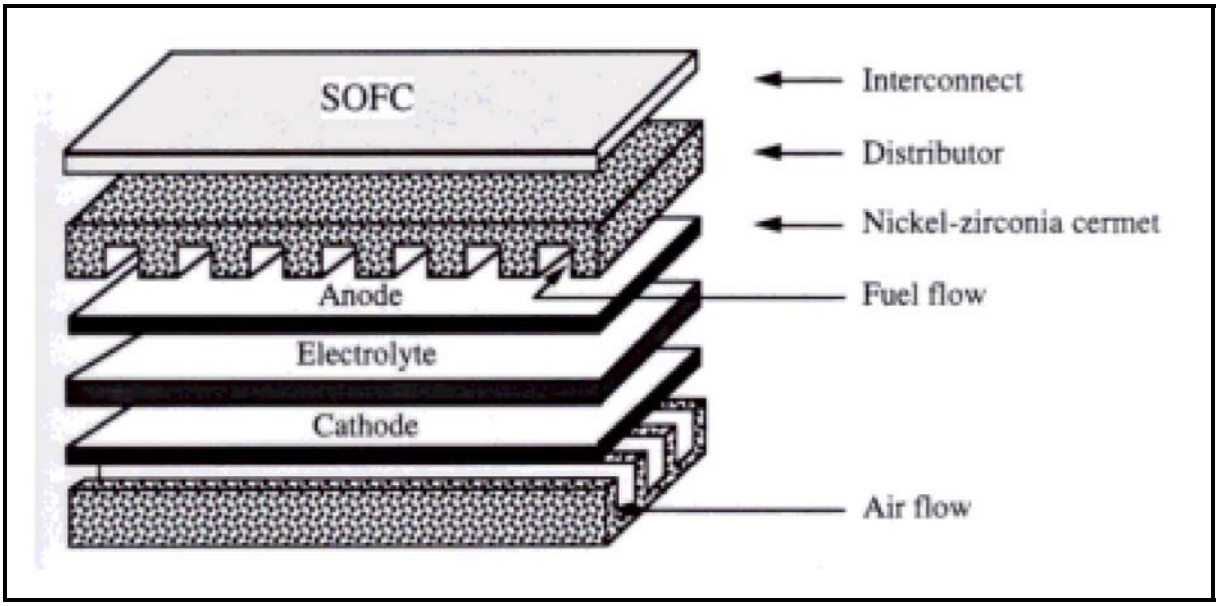

Figure 2. Schematic of a planar SOFC.

For the purposes of this report, this multilayer ceramic structure will be referred to as the "ceramic."

Note that type 301 stainless steel was the representative material used in this analysis, as there are more available property data for type 301 in current references than for other types of stainless steel.

Similarly, Rene 41 was the representative nickel-based superalloy used in this analysis, as there are more available property data in current references than for other types of alloys in the nickel-based "superalloy" family.

Additional material properties (type 301 stainless steel, Rene 41 superalloy, and yttria stabilized zirconia ceramic) that went into the ANSYS calculations were from standard references (Refs. 5, 6, and 7).

1.2.7 Calculation Assumptions

The following parameters and assumptions were included in the deflection calculations explained in the preceding section:

- initial temperature—0 °C (ambient);
- operating temperature—650 °C;
- ceramic properties—those for zirconium oxide stabilized with yttrium oxide (yttria stabilized zirconia) (there are other ceramic components that have similar properties);
- ceramic thickness—0.01 in. in all cases;
- metal plate thickness—0.08, 0.04, 0.02, and 0.01 in (four thicknesses analyzed);
- geometric shape—circular plates;

- interface—ceramic tightly bonded to one side of metal plate;
- plate diameter—5 in;
- center constraint—the plate has a 1-in-diameter hole at its center on which it is rigidly mounted to the rest of the fuel cell assembly; constraint is three dimensions [X, Y, Z axes (for gas seals)];
- edge constraint—the plate has a 5-in. outside diameter (OD) and the outside edge is unconstrained;
- baseline metal—type 301 stainless steel; and
- high temperature metal—Rene 41 nickel alloy.

1.2.8 Calculation Results

The results of the calculations are presented as deflection of the metal plate edge vs. metal plate thickness (for each respective metal) at a temperature of 650 °C, as well as the ratio of these deflections. The deflections resulted in the ceramic being on the "concave" side and metal being on the "convex" side of the resulting shape because each metal has a higher thermal expansion coefficient than ceramic. These values are presented in Table 1 below.

Table 1. PSOFC metal plate deflections vs. metal plate thickness.

Metal Plate Thickness (in)	Deflection, for 301 Stainless Steel (in)	Deflection, for Rene 41 (in)	Ratios of Deflection, Rene 41 to 301 SS
0.08	0.212	0.053	0.250
0.04	0.542	0.153	0.282
0.02	1.093	0.351	0.321
0.01	1.645	0.589	0.358

1.2.9 Preliminary PSOFC Plate Bending Analysis Conclusions

As shown in Table 1, the ratio of deflection of Rene 41 to an equal thickness of type 301 stainless steel is one-quarter for the thickest dimension analyzed to approximately one-third for the thinnest dimension. These would be for an unconstrained situation but imply that in the (PSOFC stack) constrained situation the stainless steel plates could be conceptually replaced with Rene 41 plates approximately one-quarter to one-third as thick. Since the specific gravities (densities) of these respective metals are similar, this would result in a considerable weight savings (provided there are no adverse effects resulting from making such a change).

However, there is a significant problem associated with "plasticity" because in all the cases analyzed, the thermally induced stresses exceeded the yield strength of the metal through the cross-section in at least a portion of the disk. The meaning of this is that (for any material) when the force divided by a cross-sectional area (stress) exceeds the yield strength (which varies with temperature), the dimensions of the material will not return to the starting values when this stress is released (i.e., the material will be permanently stretched or deformed).

It is to be expected that (with temperature cycling) this condition would eventually lead to a separation of the ceramic-metal bond that would cause fuel cell degradation or failure.

The preliminary conclusion from the plasticity analysis (as well as the plate bending analysis which preceded it) is that ***the ceramic and metallic thermal expansion coefficients should match to the greatest extent possible***.

1.2.10 Potential PSOFC Metals

A preliminary search of a materials property database resulted in 144 metals with thermal expansion coefficients (in the PSOFC operational temperature range) within a few percent of the ceramic thermal expansion coefficient used in the calculations described in the preceding sections (Ref. 8).

A preliminary analysis indicates many (but not all) of these metals are titanium alloys. It is understood that chemical and other properties will eliminate many potential candidate metals (e.g., an alloy constituent may migrate into the ceramic layers, over a period of time, driven by the operating temperature and electric field between the layers).

1.3 State-of-the-Art Vendor-Supplied Planar Solid Oxide Fuel Cell Parameters

1.3.1 Introduction

It was previously assumed that PSOFCs had a constant upper limit (weight basis) power density (i.e., could not be overrated for the climb portion of a flight mission). Therefore, PSOFC weight was sized for the approximately 84 MW required for the climb portion of the flight mission, whereas most of the PSOFC weight would then be excess for the much longer cruise phase of a flight mission. MSE has had recent extensive technical discussions with a company that manufactures PSOFCs, and the present understanding is that PSOFCs may be significantly overrated for the climb portion of a flight mission (though at reduced electrochemical efficiency). This report analyzes the consequences of this new information.

1.3.2 Updated PSOFC Parameters

MSE has recently discussed a performance map for PSOFCs operating with hydrogen as fuel and air as oxidizer with a company that develops and manufactures this technology (Ref. 9).[1] For the present analysis, the two relevant parameters are (weight basis) power density and electrochemical efficiency. As with any other electrochemical power production technology, there is an approximately inverse relationship between power density and efficiency.

After MSE explained the P/P requirements of the conceptual MSE/NASA-LaRC emissionless aircraft, the PSOFC manufacturing company stated the following:

[1] Joseph Hartvigsen, Ceramatech, Inc., December 12, 2003.

- Cruise electrochemical efficiency is 55%; the (weight basis) power density (after climb and before descent) is 1 kW/kg.
- The (weight basis) power density (for the relatively short duration of climb) can be as high as 3.33 kW/kg. At this power density, the electrochemical efficiency is 25%. (MSE assumes the actual electrochemical efficiency can be linearly interpolated between 55% at 1.00 kW/kg to 25% at 3.33 kW/kg.)
- Descent electrochemical efficiency is 65%; the (weight basis) power density could be as high as 0.83 kW/kg and maintain this level of electrochemical efficiency (but in fact the required power density for descent is significantly less).

1.3.3 Discussion of Updated PSOFC Parameters

The updated PSOFC parameters are considered current state of the art (near term) and imply the following changes (compared to PSOFC parameters previously used by MSE and NASA-LaRC):

- The cruise-phase electrochemical efficiency is 55% (it had previously been 50%).
- The basic (long-duration, weight-basis) power density is 1 kW/kg (it had been 2 kW/kg).
- The climb-phase power level can be increased as much as 3-1/3 times or 333% (no such overrating was previously assumed possible).
- The electrochemical efficiency will decrease to 25% for the climb phase of the flight mission if the full 333% overrating is used. (MSE and NASA-LaRC are assuming now that the actual efficiency may be linearly interpolated (e.g., if the overrating is 267%, then the efficiency ***reduction*** will be 80% of (55% minus 25%) or 24%), thereby resulting in an electrochemical efficiency of 31% (i.e., 55% minus 24% is 31%).
- The descent phase of the flight mission could use as much as 83% of cruise power at an electrochemical efficiency of 65% (it had previously been 60%).

Obviously one big change based on the updated parameters is that the onboard weight of PSOFCs can be sized for cruise conditions (rather than climb conditions), which means considerable extra weight used for approximately 20 minutes (min) does not have to be carried for the duration of a long flight.

1.3.4 Updated Flight Optimization System Code Calculations

NASA-LaRC used the updated PSOFC parameters described above and recalculated the following:

- climb, cruise, descent, and total maximum range for emissionless operation (reaction product water stored onboard);
- climb, cruise, descent, and total maximum range for the water-emitting mode;
- onboard weight of PSOFCs; and
- power levels required for climb and cruise for both emissionless and water-emitting scenarios.

To clearly show the result of using these updated PSOFC parameters, Flight Optimization System (FLOPS) calculations were performed similar to those performed as described in a recent NASA CR (Ref. 1, pp. 22-35) (i.e., potential (weight basis) power density increases caused by innovative fuel cell materials were ***excluded***).

1.3.5 Procedure Used for FLOPS Code Calculations

Some of the items to be noted in the procedure used by NASA-LaRC to calculate aircraft ranges based on the updated PSOFC parameters are given below.

- The analysis had to be repeated a few times before proper convergence could be obtained.
- Planar solid oxide fuel cell weight was sized for cruise conditions (as explained above).
- The full 333% surge capability of the PSOFCs was not needed.
- There is a slight reserve of available power (for the climb phase of a flight mission) for both the emissionless and emitting scenarios.
- It was assumed that PSOFC power generation would instantly change from climb to cruise levels. In practice, there would be a transition; however, MSE and NASA-LaRC believe there would be no significant change in the calculation resulting from the extra computational effort.

1.3.6 FLOPS Code Results with Updated PSOFC Parameters

Using the updated PSOFC parameters and the NASA-LaRC FLOPS Code, the updated calculated ranges for emissionless operation are as follows:

- climb: 123 nmi
- cruise: 2,860 nmi
- descent: 225 nmi
- total: 3,207 nmi

The updated calculated ranges for water-emitting flight are as follows:

- climb: 147 nmi
- cruise: 18,759 nmi
- descent: 224 nmi
- total: 19,130 nmi

It should be noted that 19,130 nmi is approximately 89% of the distance around the Earth.

The required onboard weight of PSOFCs (calculated by the FLOPS Code) is 76,548 lb.

The required power levels are as follows:

- emissionless climb: 87.5 MW
- emissionless cruise: 31.4 MW
- emitting climb: 95.4 MW
- emitting cruise: 29.3 MW

1.3.7 Discussion of Updated Calculated FLOPS Results

The updated PSOFC parameters result in the following changes:

- total range for the emissionless scenario has increased 25%;
- total range for the water-emitting scenario has increased 27%;
- onboard PSOFC weight has decreased 11%;
- emissionless climb power has increased 4%; and
- emissionless cruise power has decreased 3%.

1.4 Controlled Water Expulsion

1.4.1 Introduction—Water Expulsion—Major Parameters Needing Investigation

Because of the very significant increase in calculated range when reaction product water does not need to be retained onboard the aircraft (for a transport aircraft fueled with hydrogen that is electrochemically reacted with atmospheric oxygen to produce water), MSE and NASA-LaRC conducted further investigations into water expulsion scenarios. Some of the major parameters identified to date are listed (some of these parameters will be discussed in more detail subsequently).

1) Critical Altitude

Above the critical altitude, it is important to prevent (or at least minimize) the introduction of water vapor. Below this altitude, the introduction of water vapor is not considered to be an environmental problem. As mentioned above, NASA-LaRC has recently stated that the critical altitude is 27,000 feet (ft). It is noted that this altitude is not constant but nominal (i.e., it can vary as a function of weather conditions).

2) Aircraft Cruise Altitude

Typical emissionless aircraft cruise altitudes (optimized for maximum aircraft range by NASA-LaRC with the NASA FLOPS Code) were in the range of approximately 39,000 to 43,000 ft (varying as a function of aircraft weight). Commercial airlines operate conventional GTE-powered transport aircraft at cruise altitudes that are typically 35,000 ft, plus or minus several thousand feet. This is because GTEs operate most efficiently (for the cruise part of a flight mission) at such altitudes.

If transport aircraft powered with hydrogen fuel electrochemically reacted in fuel cells were flown at a cruise altitude of 27,000 ft, water could be emitted as vapor and there would be no harm to the environment.

If it is determined that an HFC-powered transport aircraft should have a cruise altitude (significantly) higher than 27,000 ft, then expulsion of water as ***vapor*** may not be an option for an aircraft designed to protect the environment.

3) Water Phase and Particulate Size at Expulsion (if cruise altitude is higher than the critical altitude)

If water could not be emitted as vapor, then should the water be solid or liquid? In addition, what would the optimum particulate size be in order to minimize reevaporation while falling down to 27,000 ft ***and*** cause no damage when reaching the ground (i.e., be the same or very similar to ordinary rain or snow)?

1.4.2 The Advantages of Water Expulsion as Vapor

If water (produced by the electrochemical reaction of hydrogen fuel) could be expelled from a large transport aircraft as ***vapor***, there would be significant advantages.

1) The weight savings by not carrying (liquid) water to the conclusion of a flight mission would be ***highly*** significant (as previously mentioned).
2) Heat exchangers (and their associated weight) would not be required to condense water vapor.
3) As previously discussed, product water tanks (and their associated weight) would not be required.
4) The exhaust from the small turbines, which recover additional energy from the fuel cell exhaust gas, can now be used for ***thrust***. This is not possible when the exhaust from these turbines must be slowed down in heat exchangers that are required to condense water vapor to liquid (or solid) water. A more detailed discussion of this scenario and the thrust calculations is included in Section 1.5.

1.5 Thrust Produced by Power Recovery Turbine Exhaust

1.5.1 Introduction

Recognizing that if an HFC-powered transport aircraft maintained a cruise altitude no higher than 27,000 ft and therefore the exhaust from the power recovery turbines could be used to directly provide thrust, an effort was made to calculate the level of this thrust.

1.5.2 Thrust Calculation

Using the PSOFC P/P system block flow diagram and its previously calculated values as a starting point, MSE calculated the total amount of exhaust thrust available from the four power recovery turbines (Figure 3). This was done for the stated conditions on the block flow diagram (representing a cruise altitude of approximately 42,000 ft) and then repeated for the conditions at a cruise altitude of 27,000 ft.

The procedures used to calculate the thrust from the energy recovery turbine exhaust are summarized as stated below.

An emissionless aircraft core engine thrust was estimated using the Graphical Engine Cycle Analysis Tool (GECAT). GECAT's core computational code is the NASA Engine Performance Program (NEPP). The model constructed in GECAT was built using generic compressor and turbine maps and is a first attempt at estimating the amount of thrust that is possible in the core engine flow. The design point for the core engine was built using the conditions shown in the PSOFC P/P system flowchart. These conditions correspond to an altitude of 43,173 ft, flight Mach number of 0.85, and core engine airflow of 61 lb/second (s). The fuel cell power extraction was simulated using a hydrogen-fueled main burner and turbine shaft load. The turbine shaft load was increased until the desired turbine exit enthalpy was reached.

After a reasonable result was obtained from the design point calculations, an off-design calculation was performed at an altitude of 27,000 ft with the following assumptions:

- the fuel cell does not operate at constant inlet pressure;
- the turbine shaft load is constant (excluding the compressor horsepower); and
- the turbine entrance temperature is equal to the design point [1,661 Rankin (R)].

It is recognized that using a GTE computational code to calculate results when a fuel cell is (conceptually) integrated with a GTE is quite nonconventional. Nevertheless, at this time, NASA-LaRC and MSE believe the thrust calculations are reasonably accurate within the limitations of the assumptions as stated.

Note: The fuel cell/turbine airflow was calculated from the estimated hydrogen flow, which was based upon fuel consumption and calculated flight times.

Approximate calculated thrust values are as follows:

- 42,000-ft altitude gives 2,046 lb of thrust; and
- 27,000-ft altitude gives 2,576 lb of thrust.

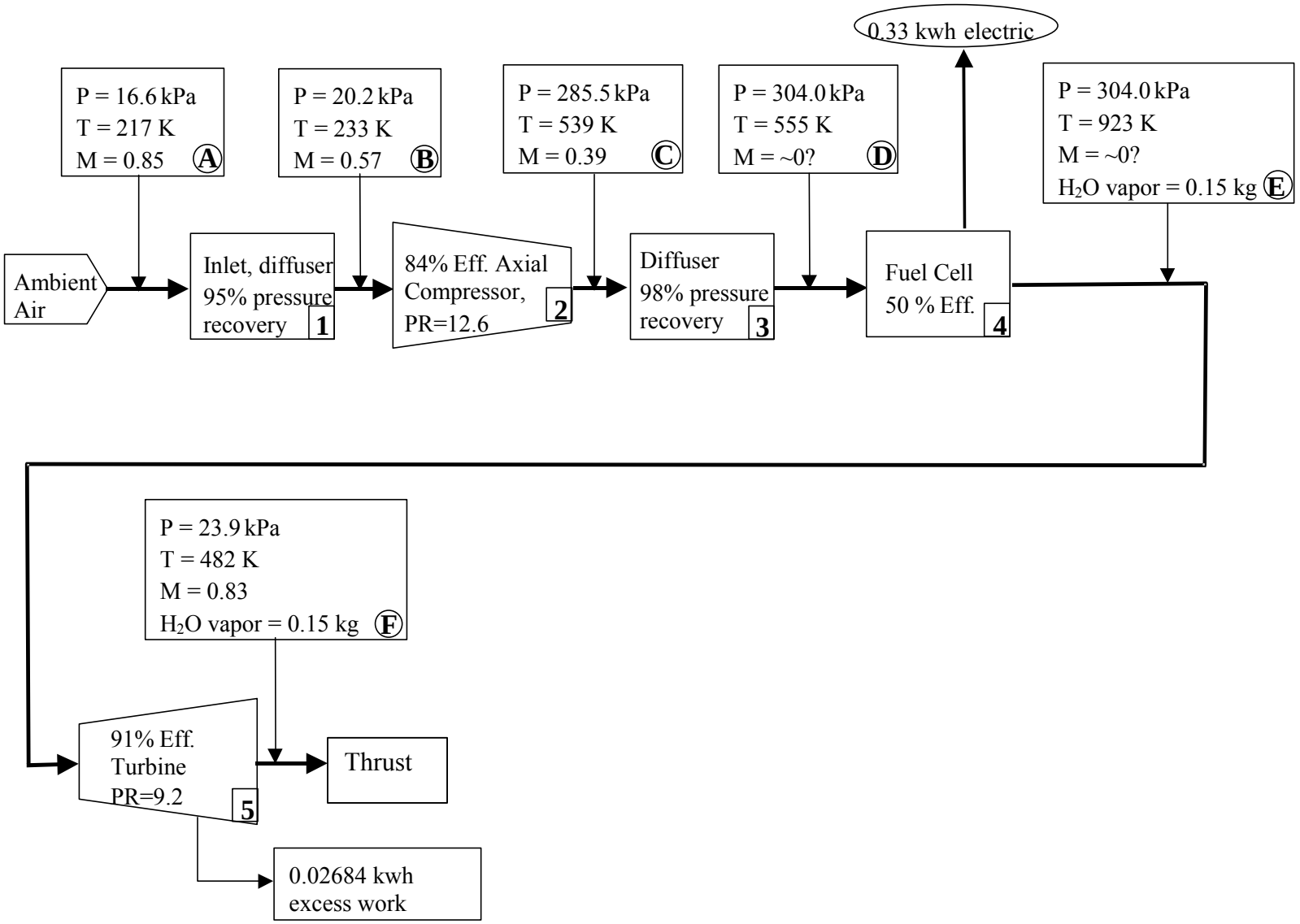

Figure 3. PSOFC P/P system.

1.6 Flight Optimization System Code Calculations for Various Water Expulsion Scenarios

A previous calculation performed by NASA-LaRC indicated that an HFC-powered transport aircraft, which would have a maximum gross takeoff weight of 655,626 lb and other parameters as described in the NASA-LaRC/MSE conceptual model, would have a calculated maximum range of 15,018 nmi if water expulsion were allowed (Ref. 1, p. 35). To achieve this range, the optimum cruise altitude of the aircraft would be in the range of approximately 39,000 to 43,000 ft (rising during the cruise phase of the flight mission as aircraft weight decreases). However, if the aircraft in this scenario were arbitrarily restricted to a maximum (cruise) altitude of 27,000 ft, then the calculated maximum range according to the FLOPS Code is 10,969 nmi, which is a decrease of approximately 27%.

At a 27,000-ft cruise flight altitude, the aircraft does not require heat exchangers to condense water vapor to liquid or solid. That weight difference can be hydrogen fuel, and a recalculation of the maximum range gives a value of 11,523 nmi, which is approximately 23% less than the previous 15,018-nmi calculated maximum range.

NASA-LaRC explains that the performance (maximum range) decrease caused by flying the cruise phase of a flight mission at approximately 27,000 ft (rather than approximately 39,000 to 43,000 ft) is largely caused by flying at nonoptimum aerodynamic conditions. At 27,000 ft, the aircraft is flying at a lift coefficient (C_L) below that which results in optimum aerodynamic performance. There is a mismatch between the optimum wing area for cruise at 27,000 ft and that necessary to meet landing and takeoff design requirements.

Another parameter calculated by the FLOPS Code at this time is the approximate value of thrust (provided by the ***primary*** propulsion system of fuel cells, electric motors, and fans). Of course, this value varies as a function of aircraft weight but is calculated to vary from 31,426 lb (start) to 28,645 lb (end) of the cruise phase of the flight mission at an altitude of 27,000 ft. The average of these values is 30,036 lb.

Because flying at 27,000 ft will allow the 2,576 lb of thrust from the power recovery turbine exhaust to augment primary thrust, the thrust from the primary propulsion system may be (computationally) "throttled back" in the FLOPS calculations, and the maximum aircraft range can be recalculated using both propulsion systems. This value is 12,463 nmi, which is approximately 17% less than the 15,018-nmi (higher altitude) value.

Therefore, the FLOPS calculations indicate that (within assumptions and the conceptual model as stated) restricting cruise-phase flight altitude to 27,000 ft will:

- not cause water-based damage to the upper atmosphere; and
- result in a maximum calculated aircraft range that is significantly more than one-half of the way around the Earth.

1.7 Circulation Control

1.7.1 Introduction

Improvement in low-speed aerodynamic capabilities beyond those assumed for this design could possibly enable a better match between cruise and takeoff/landing requirements and thereby regain lost range due to flying at 27,000 ft.

One of the aeronautical topics investigated by MSE to potentially enhance the performance of an emissionless aircraft is known as "circulation control." This section presents the result of the investigation.

1.7.2 Relevant Information

This information on circulation control was provided by Mr. Robert Englar of the Georgia Tech Research Institute during discussions with Mr. Mark Guynn of NASA-LaRC.

The concept known as "circulation control" refers to tangential blowing of a jet sheet over a rounded trailing-edge surface to augment airfoil circulation and lift.

A high-level review of information provided by Mr. Englar included the following (Refs. 10, 11, and 12):

- theory of circulation control; and
- application of circulation control to a 737 class aircraft.

Specific details included:

- The circulation control concept is based on the "Coanda Effect," which causes a downward deflection of the jet sheet by flowing over the rounded trailing-edge surface.
- A two-dimensional (2-D) airfoil C_L as high as 8.0 has been demonstrated using circulation control.
- The amount of lift augmentation obtained from circulation control is a strong function of the momentum coefficient ($C\mu$), which depends on the jet mass flow, jet velocity, and free stream dynamic pressure. The equation relating these parameters is:

$$C\mu = \frac{\dot{m} V_j}{\frac{1}{2} \rho_\infty V_\infty^2 S_{ref}} \qquad (1)$$

where:

$\dot{m}$ = mass flow of the jet

V_j = velocity of the jet

ρ_∞ = free stream density

V_∞ = free stream velocity

S_{ref} = wing reference area

- For application to aircraft, circulation control is achieved by bleeding off high-pressure air from the engine and sending it through a slot at the top of the trailing edge of the wings and then over a rounded flap. Due to the number of variables involved, Mr. Englar presented the impacts of circulation control on a 737 class aircraft in a series of curves reflecting various conditions.

Flight experiments on a U.S. Navy A6 aircraft, which was performed in 1979, had achieved the following results (using an older version of circulation control). These experiments demonstrated that the results obtained by this technology can be significant (Ref. 11):

- takeoff speed was reduced 35%;
- approach speed (landing) was reduced 35%;
- takeoff distance was reduced 60% to 65%; and
- landing distance was reduced 60% to 65%.

Mark Guynn used the NASA-LaRC FLOPS Code and computed what the maximum C_L would need to respectively be for takeoff and landing in order that the transport aircraft in the conceptual model being developed by NASA-LaRC/MSE could have aerodynamically optimum parameters for (cruise) flight at a 27,000-ft altitude.

The required C_Ls are:

- takeoff–$C_L \geq 4.0$; and
- landing–$C_L \geq 5.0$.

Mr. Guynn stated that based on his discussions with Mr. Englar, circulation control should enable these respective C_Ls to be achieved.

Mr. Guynn noted that diverting airflow for circulation control technology to increase lift will result in less thrust provided by the engines. This results in a (presently unknown) effect on engine performance that may increase power requirement at takeoff and landing.

Finally, assuming a maximum C_L of 4.0 for takeoff and 5.0 for landing, the maximum range with cruise at 27,000 ft was computed using the FLOPS Code to be 13,470 nmi. This is only 10% less than the maximum aircraft range (15,018 nmi) when the water-emitting aircraft would be flying at a cruise altitude of approximately 42,000 ft.

2. Breakthrough Fusion Reactors as Power Sources for Aircraft Propulsion

2.1 Introduction and Background

A recent NASA CR introduced the concept that a unique type of nuclear fusion reaction that is aneutronic (meaning it does not produce neutrons) could be used as a power source for the propulsion of an emissionless aircraft (Ref. 1, pp. 40-44). Currently, two distinctly different fusion systems have been theoretically examined, analyzed, and found capable of providing power that could potentially be used for aircraft propulsion. These systems are:

- Inertial Electrostatic Confinement (IEC) fusion that uses ***electric*** fields in a ***spherical*** geometry to confine radially oscillating ions until they fuse; and
- the Colliding Beam Fusion Reactor (CBFR) that uses ***magnetic*** fields in a ***cylindrical*** (annular) geometry to confine circulating ions until fusion occurs.

The preferred fusion reaction for either geometry is the one between ordinary hydrogen (H^1) and the most common isotope of boron with atomic weight 11 (B^{11}):

$$H^1 + B^{11} \rightarrow 3\ He^4 + 8.7\ \text{MeV energy} \qquad (2)$$

This energy is kinetic energy shared by the three helium nuclei. Each nucleus carries a double electric charge, thereby readily allowing that kinetic energy to be converted to usable electricity.

The following topics related to IEC fusion are presented in the above-referenced information (Ref. 1, pp. 40-44):

- concept origin and early history;
- concept development and commercialization;
- system description;
- operating principle;
- advantages of the H^1-B^{11} reaction;
- energy density and weight saving compared to chemical reactions;
- direct conversion of ion kinetic energy to useable electric power;
- an estimation of IEC system component weights; and
- the ***lack*** of a significant radiation hazard.

2.2 The Colliding Beam Fusion Reactor

2.2.1 Introduction

The concept of CBFR fusion was formally presented to the aerospace community as a P/P system for ***rocket*** propulsion in February 2004 (Ref. 13). MSE conceptually modified the original idea in order that it could provide power for emissionless ***aircraft*** propulsion. The most appropriate CBFR fusion reaction is (as it was for IEC fusion) the one between H^1 and B^{11}.

Subsequent sections present the MSE development of the original CBFR concept. Figure 4 is a schematic diagram depicting the CBFR Space Propulsion System (CBFR-SPS).

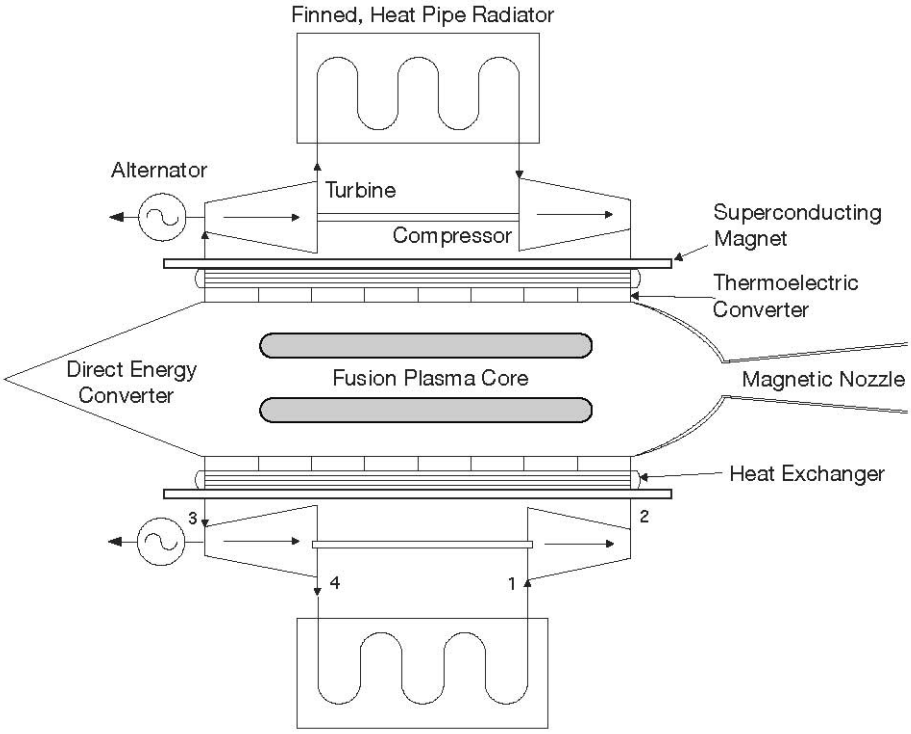

Figure 4. The CBFR-SPS.

2.2.2 Approach for Modifying the Original CBFR Concept for the Emissionless Aircraft Application

Major modifications required to the space propulsion CBFR so that it may be a power source adequate for emissionless aircraft propulsion are as follows:

1) Both ends of the CBFR would be "closed." The open-end configuration would not be functional in the atmosphere, and high energy ions (exiting the open end) suitable for space propulsion can be converted to electric power as is done (in the original concept) at the "closed" end. That is, it appears that the electric power output (produced by helium ion kinetic energy) may be readily ***doubled*** in a "fully closed" configuration.
2) Electric motors that drive fans would be used for propulsion, as previously presented.

3) There would be no cryogenic hydrogen (LH_2) onboard the aircraft. In the previous HFC-based approach, LH_2 cooled the aluminum windings and thereby greatly increased their electric conductivity, resulting in an extremely high power density electric motor. The superconducting magnet of the CBFR operates at 4.5 Kelvin (K); therefore, the liquid helium (LHe) cooling system of the CBFR could (in principle) be scaled up to cool the nonsuperconducting aluminum winding-based electric motors that were previously identified and had been built and tested at a 1-MW power level with LH_2 as the coolant.

4) There is no exhaust; therefore, no heat exchangers are required (as previously) to condense water reaction product in the exhaust.

5) The CBFR does produce some heat that must be removed. Some of this heat may be converted to additional electric power by conventional methods.

6) In addition to a negligible fuel weight, fuel tank weight is also negligible.

7) There is no reaction product tank weight.

8) Fuel cost will also be essentially negligible.

9) Unlike chemical reaction-based P/P systems, there would be no measurable aircraft weight change during flight.

10) It appears to be readily possible that the CBFR (within its physical operating restraints) is readily scaleable with respect to the net amount of electric power that would be produced.

2.2.3 Relevant Power and Weight Parameters of the Space Propulsion CBFR as Modified for the Proposed Emissionless Aircraft Application

The relevant parameters are stated below.

1) The fusion fuels are H^1 and B^{11}. This pair of reactants produces the least neutrons compared to the amount of charged ion reaction products but requires a longer reactor length to produce a given power level compared to other fuel choices.

2) The nominal system size is 100 MW. However, as will be subsequently explained, the ***net*** output power is less than this value.

3) The space propulsion energy balance of the proposed H^1-B^{11} reactor was stated as follows:

   - 50 MW of injected (ion) power is required to produce 100 MW of total output power.
   - The power produced by helium ion kinetic energy is 77 MW.
   - To produce thrust, half of the 77-MW power is used in the expelling of one-half of the helium 4 (He^4) ions out through a magnetic nozzle and into space.
   - The other half of the 77-MW ion power is recovered as electric power in a "direct-energy converter" (DEC) with 90% efficiency. This would produce 34.7 MW.

- Heat is produced by Bremstrahlung radiation (23 MW). It was proposed that the sequence of a thermoelectric converter (TEC) surrounding the reactor, which in turn would send lower temperature heat to a closed-cycle Brayton-heat engine, would provide sufficient electric power to sustain the 50 MW of required injected (ion) power.

4) Conceptually closing the open end of the reactor doubles the available electric power that may be produced. Therefore, at an estimated conversion efficiency of 90%, the net power outputs (before considering the usage of a TEC or Brayton engine) would be:

   - electric: 0.9 x 77 MW = 69.3 MW
   - heat: 0.1 x 77 MW + 23 MW = 30.7 MW

   Of course, heat must be transferred out of the power production system, and this will be subsequently explained.

5) The reactor chamber length is stated to be 6.9 meters (m).

6) The external reactor chamber's diameter (based upon the given wall radius and wall thickness) is 1.24 m.

7) The mass of niobium-tin (Nb_3Sn) superconducting wire required to produce the required magnetic field of the reactor is estimated to be 3,097 kg.

8) Two LHe pumps required to maintain the superconducting magnetic coils at their 4.5 K operating temperature have a total mass of 60 kg. For the emissionless aircraft application, it is assumed that the LHe pumps will also pump LHe through the four cryogenic electric motors. It is assumed that the total LHe pump mass required for this increased application will be 300 kg.

9) The outer structural shell of the reactor (made of 0.01-m-thick Kevlar/carbon-carbon composite) is estimated to have a total mass of approximately 772 kg.

10) The outermost layer (insulation jacket) has an estimated mass of 643 kg.

11) The total estimated mass of the ion injectors and ion sources is 60 kg.

12) The space-propulsion system concept used a cone-shaped DEC made of stainless steel, located at one end of the reactor. This converter has a base radius of R = 0.49 m and length of L = 2 m. The mass of this item is approximately 1,690 kg. For the emissionless aircraft application, one DEC would be placed on each end of the reactor. The total mass of two such units would be 3,380 kg.

13) A radio frequency (RF) power supply (inverter/converter) converts ion kinetic energy into electric power. The mass of this device is 30 kg; therefore, two would have a mass of 60 kg.

14) A storage battery for starting and restarting the CBFR has a mass of 500 kg.

15) A control unit to coordinate the operations of all the components has an estimated mass of 30 kg.

16) If none of the CBFR heat flux (produced from the electromagnetic emissions of the fusion core) is converted to additional electric power, then this heat must be removed from the system. This issue will be addressed in Section 2.3.

In summary, the net electric power produced by the CBFR configured for the emissionless aircraft application is 69.3 MW (gross output from DECs) minus 50 MW (required for ion injection) (refer to Items 3 and 4 in this section). Therefore, the ***net*** electric output of the CBFR, as described, is 19.3 MW.

The total estimated mass of the CBFR system is the sum of the masses of the nine components described in Items 7 through 15 in this section. This is a total mass of 8,842 kg. As masses were calculated and estimated, it is considered prudent to add an additional 10% as "contingency." Thus, the total mass is 9,462 kg, which is 20,860 lb.

(One such item in the contingency category would be equipment required to produce, or at least maintain, a sufficient vacuum inside the CBFR so it may operate.)

2.2.4 Component Masses and Power Levels for the Fusion-Powered Aircraft Performance Calculations

Table 2, derived from a table in a recent NASA CR that was used for presenting PSOFC P/P component weights per megawatt power level, has been modified by adding the CBFR weight-to-power ratio in an additional column, which also indicates the numerous items not required if the CBFR system is used (Ref. 1, p. 24).

Table 2. PSOFC P/P system and modified CBFR system component weights.

Component	Wt. per MW PSOFC Output	Wt. per MW CBFR Output
Inlet diffuser	Part of nacelle weight	N/A
Axial compressors	12.9 lb/MW	N/A
Pressure recovery diffuser	Relatively small	N/A
PSOFCs	1,102 lb/MW	N/A
Bottoming turbine	25.8 lb/MW	N/A
Pressure recovery diffuser	Relatively small	N/A
Exhaust-to-air heat exchanger	116 lb/MW	N/A
Exhaust-to-GH_2 heat exchanger*	16.9 lb/MW	N/A
Bottoming generators	22.9 lb/MW	N/A
Propulsion motors	66 lb/MW**	66 lb/MW**
Compressor motors	17.8 lb/MW	N/A
Modified CBFR	N/A	1,081 lb/MW
Total	1,385 lb/MW	1,147 lb/MW
*GH_2 = gaseous hydrogen **Based on propulsion motor output		

Even more important than the items in the table, there will be ***no*** weight requirements for LH_2 fuel, stored onboard water (for an emissionless mode of operation), or tanks.

Additionally, it will be assumed in the performance calculations presented subsequently that the propulsion fan efficiency is 85% and the percentage laminar flow is 20% (on the wing only).

2.3 Heat Transfer from the Colliding Beam Fusion Reactor Surface

2.3.1 Introduction

This section addresses the transfer of heat from the outside surface of the CBFR during the high-altitude cruise part of a flight mission.

2.3.2 Parameters for the Heat Transfer Calculation

At a conceptual level, the input parameters for the calculations of heat transfer from the outer surface of the CBFR are of the three general types listed below.

1) Dimensions and geometry of the outer surface of the CBFR (cylinder length = 6.9 m and cylinder diameter = 1.24 m).
2) Radiant heat flux (caused by internally produced Bremstrahlung) intercepted by the cylindrical shell of the CBFR [1.2 MW/square meter (m^2)].
3) Atmospheric parameters for air at a cruise altitude of 42,000 ft [these atmospheric values were used in prior system calculations related to PSOFCs providing propulsion power (Ref. 1, p. 23)]. The Mach number (M = 0.57) is significantly less than that of the aircraft with respect to the ambient air (M = 0.85) due to the (conceptual) slowing down of air entering a diffuser or moving near solid objects. The atmospheric parameters are:

   – pressure: 20.2 kilopascals (kPa) = 0.200 atmosphere (atm)
   – temperature: 233 K
   – velocity: M = 0.57, which is 174 m/s
   – flow direction and location (parallel to cylinder axis and surrounding the outside cylinder surface).

(For this analysis, the relatively smaller axial heat transfer from the ends of the cylinder are not included; the DEC converters are at these end locations, and their operating temperature is not presently known.)

The output parameter of the heat transfer calculation will be the cylindrical surface temperature at the trailing edge (exit end) of the flow. This would be the highest temperature of the cylinder as the moving air will produce more cooling on the leading edge of the cylinder.

2.3.3 Calculation Approach

In general, the following is a condensed and simplified conceptual explanation of how a heat transfer calculation (such as this one) is approached. The logic sequence is as follows:

1) Using the values of air density, air velocity, cylinder length, and air viscosity, calculate the dimensionless Reynolds number (R_e).
2) Examine the numerical value of R_e. If this number is sufficiently large, it indicates that turbulent flow methods and formulas will be required to calculate the heat transferred from the cylindrical surface (which in fact was the situation).
3) Calculate the dimensionless Grashoff number.
4) The numerical value of the Grashoff number indicates the significance of buoyancy effects. In this situation, the buoyancy effects are approximately 1%, and they can therefore be ignored as this amount of error is significantly less than other unavoidable calculation errors.
5) Calculate the dimensionless Eckert number.
6) The numerical value of the Eckert number indicates the significance of compressibility effects. In this situation, the compressibility effects are approximately 0.2%, and they can therefore be ignored as this amount of error is significantly less than other unavoidable calculation errors.
7) Assume that the model for calculating convective heat transfer from the outside of a cylindrical surface, where fluid is flowing parallel to the cylinder axis, is the same as if the convective heat transfer were occurring from a flat plate. This concept is explained in a standard heat transfer textbook (Ref. 14, pp. 358-376).
8) Include a term for the calculation of heat that is (electromagnetically) ***radiated***. Assume that this means of heat transfer is independent from heat transfer due to convection and that the hot surface of the CBFR is radiating heat to atmospheric air at the conditions stated previously.

2.3.4 Calculation Method

The method of doing these heat transfer calculations was to use an iterative mode of computer calculations to calculate the actual individual temperatures at which the ***sum*** of the radiative and convective heat fluxes equals the respective assumed total heat flux values (e.g., 1.2 MW/m^2).

2.3.5 Heat Transfer Equations

The total heat transfer is the sum of heat transferred by radiation and heat transferred by convection.

Heat transferred by radiation is calculated by Equation 3 (Ref. 14. pp. 10-11 and p. 670):

$$q_{rad} = \sigma\varepsilon\,(T_s^{\,4} - T^{4}_{free}) \qquad (3)$$

Where:

q_{rad} = radiated heat flux, W/m^2

σ = the Stefan-Boltzmann constant, which is 5.67×10^{-8} $\dfrac{W}{m^2 \times T^4}$

ε = an emissivity factor, assumed to be 0.8

T_s = the temperature of the solid surface that is radiating heat

T_{free} = ambient atmospheric temperature (233 K)

Heat transferred by convection is calculated by Equation 4 (Ref. 14, p. 360):

$$q_{conv} = h\,(T_s - T_{free}) \tag{4}$$

Where:

q_{conv} = convected heat flux [watts per square meter (W/m^2)]

h = a convective heat transfer coefficient with the units $\frac{W}{m^2 \text{ x } L}$

T_s = the temperature of the solid surface from which heat is being convected

In order to calculate the amount of convective heat transfer for a situation such as this (where the fluid flow is turbulent), the equation is modified to be:

$$q_{conv} = \frac{NuK}{L}\ (T_s - T_{free}) \tag{5}$$

Where:

Nu = the dimensionless Nusselt number

K = the mean temperature of the boundary layer surrounding the surface from which heat is being convected

L = the length (in meters) of the surface (cylinder) from which heat is being convected

The Nusselt number is defined (for these flow conditions but at the mean temperature of the boundary layer surrounding the surface from which heat is being convected) as follows:

$$Nu = 0.308\ R_e^{\frac{4}{5}}\ P_r^{\frac{1}{3}} \left(\frac{\mu_{free}}{\mu}\right)^{\frac{1}{4}}$$

(Note that the above Nusselt number relationship is an ***empirical correlation*** and subject to an unavoidable inherent error as large as $\pm$ 20%. It is ***not*** an equation).

The terms in the correlation (not previously defined) are as follows:

P_r = the dimensionless Prandtl number

μ_{free} = the viscosity of the ambient air at the given temperature (233 K)

μ = the viscosity of the air at the mean temperature of the boundary layer surrounding the surface from which heat is being convected

2.3.6 Calculation Results

The iterative computer calculation procedure, explained in Section 2.3.4, produced (for each value of heat flux originating inside the cylinder) a temperature of the outer cylindrical surface at the exit end of the cylinder. These results are as follows:

- 1.2 MW/m^2 = 1,947 K
- 1.0 MW/m^2 = 1,803 K
- 0.8 MW/m^2 = 1,623 K

2.3.7 Heat Conversion to Additional Electric Power

The maximum surface temperatures calculated for the CBFR are relatively high. A value of 1,947 K (for 1.2 MW/m^2) is 1,674 °C, which is higher than the melting point of pure titanium (1,933 K). A value of 1,623 K (for 0.8 MW/m^2) is well above the melting point of pure copper (1,357 K). Furthermore, the inner surface of the CBFR cylindrical shell will be somewhat hotter than the outer surface because the heat transfer is outward.

These high temperatures may potentially be addressed by the following approaches, which would each require a more detailed analysis:

- increase the cylinder diameter of the CBFR;
- reduce the CBFR power density;
- provide an alternate means of cooling such as fluid moving through channels; and
- fabricate the outer shell of the CBFR from a more refractory metal (e.g., niobium or zirconium).

However, if a lightweight conversion process is available, it would be advantageous to convert as much as possible of the internally generated heat into additional electric power rather than dissipate it into the atmosphere via radiation and convection.

Temperatures in the range of 1,800 K to 1,900 K are hot enough that ***thermophotovoltaic*** (TPV) conversion may be considered for generating additional electric power from heat. This technology (described in a recent NASA CR) would consist of enclosing the hot cylindrical surface of the CBFR with single crystal energy converter cells manufactured from an appropriate semiconductor such as gallium antimonide (GaSb). This conversion technology could have an efficiency as high as approximately 30% (Ref. 1, p. 5).

However, a difficulty with such an energy conversion is to ensure by materials selection and geometric design that the temperature gradient between the "front" and "back" is maintained within the thin layer of converting material. A more detailed analysis of this conversion would need to address this issue. Because of unknowns related to this temperature gradient, MSE chooses to conceptually incorporate a 20% efficient solid-state TEC as described by the authors of the CBFR-SPS paper, which would weigh 882 lb rather than the more efficient TPV system. This will produce an additional 4.6 MW of electric power from the 23 MW of intercepted heat flux.

2.4 Hybrid Colliding Beam Fusion Reactor Aircraft Propulsion—The "Turbojet" Concept

2.4.1 Introduction

This section presents a high level investigation and analysis of a concept of not merely ***removing*** CBFR surface heat but incorporating the CBFR into the equivalent of a turbojet engine so that this heat may provide some of the propulsive force required by the aircraft.

In this concept, the CBFR is to be thought of as a (nearly) fueless ***burner***. Ambient air is compressed, heated by the CBFR, expanded, and exhausted through a turbine and nozzle, thereby providing thrust. There are no combustion-related chemical compounds to change the composition of the air as it passes through the engine (the amount of nitrogen oxides that may be produced by heat-induced reactions of atmospheric nitrogen and oxygen may be estimated in a more detailed analysis).

By using unavoidable CBFR heat to produce propulsive thrust, it is potentially possible to downsize the primary P/P system, which uses electric power extracted from the ends of the CBFR to drive motors coupled to fans that provide propulsive force.

2.4.2 Input Parameters for Turbojet Calculations

The input parameters required for turbojet calculations are as follows (atmospheric parameters are for the cruise phase of a flight):

- ambient air pressure is 20.2 kPa = 0.200 atm;
- ambient air temperature is 233 K;
- aircraft velocity is Mach 0.85;
- the diameter of the CBFR cylindrical surface is 1.24 m; the length is 6.9 m;
- the heat flux at the (cylindrical) surface of the CBFR (for an electric power output of 23.9 MW) is 1.0 MW/m^2; total heat flux is 26.88 MW; and
- the weight of the CBFR is 22,412 lb.

2.4.3 General Assumptions for Turbojet Calculations

Additional assumptions required for subsequent calculations are given below.

- Conditions are steady state, continuous, and at cruise altitude.
- The CBFR may be (conceptually) "split" into thinner units so that the compressor may be shaft-driven with the turbine.
- The fraction of heat that leaves the CBFR surface and is transferred into air moving over this surface is 75%.

2.4.4 Turbojet Calculation Approach

The goal of the turbojet calculations was to determine net thrust. This was done by:

- Preliminary calculations used the total given heat flux to determine the inlet air mass flow rate to the engine that would be required to limit air temperature entering the turbine section of the engine.
- A standard turbojet code [with obvious modifications (e.g., zero fuel flow)] was then used to calculate the value of net thrust (Ref. 15).

2.4.5 Specific Turbojet Calculation Assumptions

To perform the turbojet calculations, it was necessary to incorporate assumptions that are based upon known parameters of state-of-the-art turbojet engines. These included:

- the total compression ratio is 28;
- the turbine inlet temperature must be limited to 2,600 ºF (~ 1,700 K); and
- there is a 6% pressure drop (in the direction of airflow) across the CBFR surface.

2.4.6 Calculations

This section is essentially an outline of the calculations that were used. Only some of the details are shown, but all calculation details are available at MSE. The equations and steps are as follows:

1) Adiabatic compression efficiency is calculated with Equation 6:

$$\mu_{comp} = 0.83 = \frac{h_{3s} - h_1}{h_{3a} - h_1} \tag{6}$$

where:

μ_{comp} = adiabatic compression efficiency
h_{3s} = air enthalpy after compression (isentropic)
h_{3a} = air enthalpy after compression (actual)
h_1 = air enthalpy (ambient)

2) By using the ambient cruise altitude air parameters (i.e., pressure and temperature) as a starting point and standard air property values published by the National Institute of Standards and Testing (NIST), the actual air temperature after compression and before adding heat (calculated by using Equation 6 above) is 669 K (Ref. 16).
3) Then, the CBFR is assumed to have a surface heat transfer efficiency of 75% (considered a typical value), which means that 0.75 x 1 MW/m^2 or 750 kW/m^2 of heat is added to the air that passes over the CBFR surface.

4) Using the NIST air property tables, the total increase in air enthalpy received from the entire cylindrical surface of the CBFR divided by the specific enthalpy for air at the selected turbine inlet temperature (at 1,700 K) minus the specific enthalpy for air after compression (at 669 K) results in a calculated mass flow rate for the heated air. This value is 37.12 lb/s.
5) The calculated air mass flow rate and other given parameters are then inserted into the standard turbojet code, which provides a calculated ***net*** thrust for the cruise altitude air pressure and air temperature conditions. This value is 6,227 lb force.

2.4.7 Turbojet Thrust Fraction

The results of NASA-LaRC FLOPS Code calculations showed that a 300-passenger, Mach 0.85 cruise velocity, emissionless transport aircraft with propulsion power provided by the electrical output of a CBFR would have the following parameters:

Aircraft weight: 275,019 lb (constant)
P/P system weight: 40,310 lb
Climb power: 35.3 MW
Cruise power: 16.8 MW
Energy per nautical mile (at cruise conditions): 34.4 $\frac{\text{kWh}}{\text{nmi}}$
Thrust for cruise conditions: 12,655 lb

Therefore, as a preliminary first approximation, calculations and stated assumptions indicate that using heat emitted by the surface of the CBFR in a modified turbojet engine can provide a significant fraction of the thrust required for flight as compared to a P/P system that merely rejected this heat. The amount that using this heat may change the parameters listed above is discussed in Section 2.4.9.

2.4.8 Estimated Total Engine Weight

The total estimated weight of the modified turbojet engine is derived as given below.

- A state-of-the-art comparable engine (with a similar air mass flow and identical pressure ratio (28) as that of the modified engine described in this report) is the General Electric (GE) CF34-8C5. The weight of this engine is listed as 2,470 lb.
- The estimated mass-basis power density of the CBFR is 938 lb/MW.
- Disregarding (for the present) the thrust resulting from heat in the turbojet concept, 35.3 MW power required for climb times 938 lb/MW results in a CBFR weight of 33,111 lb.
- Adding the weight of the state-of-the-art engine to the weight of the CBFR results in a weight of 35,581 lb.
- A contingency of 10% is then added to allow for (conceptually) connecting the compressor and turbine, as well for a cover over the entire engine that would be significantly larger than the conventional engine with a comparable compressor and turbine.

- The resulting total estimated engine weight is then 39,139 lb.

2.4.9 Effect of Turbojet Thrust on Aircraft Performance Parameters

The following factors would be included in a determination of how much aircraft performance factors are changed by augmenting the CBFR electric power output with thrust derived from the CBFR surface heat.

- As a result of FLOPS Code calculations performed by NASA-LaRC, it was determined that the weight of the CBFR-based P/P system (no turbojet concept) at 40,310 lb is only a relatively small fraction (14.7%) of the total aircraft weight (275,019 lb).
- It was also shown by these calculations that a 24% increase in CBFR electric power output (conceptually obtained by using a TEC on the CBFR surface) would reduce the P/P system weight by approximately 8,000 lb and the overall aircraft weight by approximately 10,000 lb (i.e., total aircraft weight is not a significant function of changes in mass-basis power density of this P/P system).
- As presented in Sections 2.4.6 and 2.4.7, thrust produced by CBFR surface heat is a significant fraction of the total thrust required for flight. As a first-order approximation, this suggests that the weight, size, and power capability of the electric power-related parts of the P/P system could be significantly reduced.
- However, as for any aircraft, a significantly higher thrust is required for takeoff and climb as compared to the requirement for cruise. For this high-level study, MSE has investigated a CBFR-turbojet concept that will operate at the stated cruise altitude air pressure and air temperature. Conditions involving lower altitudes and higher power levels could be included in a more comprehensive study.
- It is suggested that the most significant performance improvement obtained by using CBFR heat to produce thrust via a turbojet concept would be an increase in the calculated range per fuel mass, which, as presented in Section 2.5, is approximately 2.8 times around the Earth per pound of H^1-B^{11} fuel before considering the turbojet concept.

2.4.10 Comments on Power Levels

The first investigations reported herein on breakthrough fusion reactors were for a 100-MW (nominal) CBFR that would produce 19.3 MW of net electric power (subsequently increased to 23.9 MW by converting surface heat to additional electric power).

Later, FLOPS Code calculations using the previously determined pounds per megawatt value for the nominal CBFR determined that aircraft climb power would be approximately 35 MW (as shown in Section 2.4.7). This value was then used for fusor inner grid cooling calculations (Section 2.6.4).

2.5 Calculated Aircraft Range per Pound of Fuel

The energy per nautical mile described in Section 2.4.7 is electric energy output from the CBFR needed for each nautical mile the aircraft flies during the cruise phase of a flight.

The calculated aircraft range per pound of H^1-B^{11} fuel is determined by the following:

- Each pound of H^1-B^{11} fuel (i.e., 1/12 lb of H^1 and 11/12 lb of B^{11}) provides a theoretical energy output of 2.98×10^{10} British thermal units (Btu) if completely fused to He^4.
- When the heat-to-electric conversion is included at the CBFR surface, an internal (fusion) power level of 100 MW can theoretically provide 23.9 MW of electric power output. This can be restated as, "the overall energy efficiency of the CBFR is 23.9%."
- As presented in Section 2.4.7, the required electric energy ***output*** from the CBFR is 34.4 kilowatt-hours (kWh) for each nautical mile the aircraft flies during the cruise phase of a flight.
- One kWh is equivalent to 3,412 Btu.

Based upon the above parameters and relationships, the aircraft cruise range per pound of H^1-B^{11} fuel is calculated as:

$$\text{Range} = \frac{2.98 \times 10^{10}\ \text{Btu}}{3.412 \times 10^{3}\ \frac{\text{Btu}}{\text{kWh}}} \times 0.239 \times \frac{1\,\text{nmi}}{34.4\,\text{kWh}} = 60{,}681\,\text{nmi} \qquad (7)$$

This is a calculated cruise range of approximately 2.8 times around the Earth ***for each pound of fuel.***

2.6 Heat Transfer from the Inner Fusor Grid

2.6.1 Introduction

This updated information on IEC fusion examines a technological paradox that limits the power level of the system and then suggests a possible means of overcoming the limitation. The spherical ***electrostatic*** field, which confines H^1-B^{11} ions until they fuse, is produced by two open metallic wire grids. In the basic fusor design, a negative electric potential is placed on the inner grid and a positive electric potential is placed on the outer grid. Each grid is typically constructed from stiff wires formed into circles that are then welded into a three-dimensional (3-D) spherical shape resembling longitude circles of the Earth. The diameter of the inner grid is approximately one-fifth of the diameter of the outer grid. When the fusor is operating, the negative potential on the inner grid confines moving positive ions to the center of the device (Figure 5) (Ref. 1, p. 41).

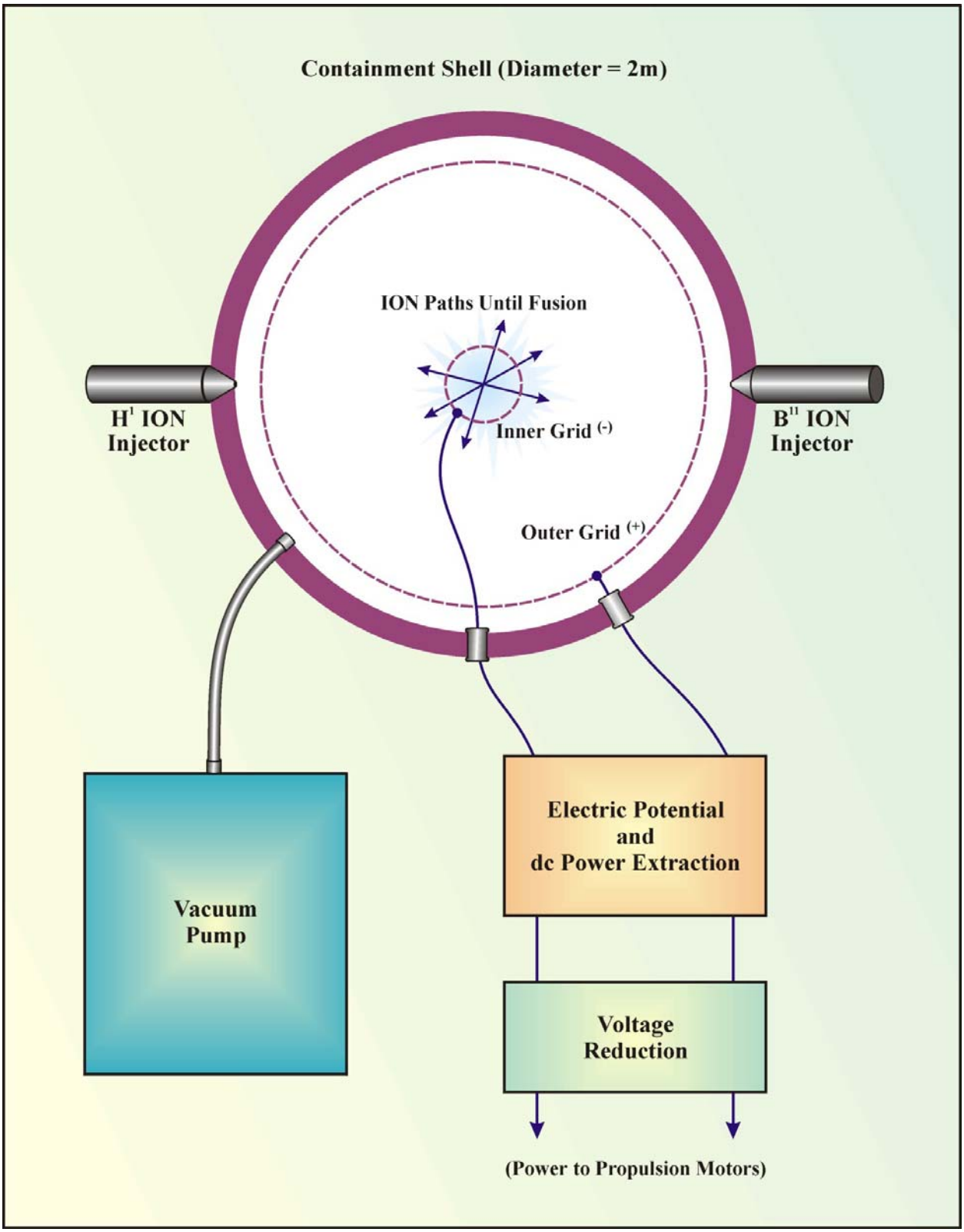

Figure 5. IEC fusion power generator concept.

The present technical difficulty is that:

- An inner conducting grid must surround the center of the device in order to establish a symmetric electric field (negative in the center of the sphere to positive at the edge of the sphere).
- Regardless of how "open" this inner grid is, it will inevitably be impacted by high-velocity ions traversing its location. These impacts of ions against the grid material produce heat and cause the grid to become hot.

Eric Dollard, an advanced energy researcher, stated that the fusor inventor (Philo T. Farnsworth), was able to operate one of his fusors at a power level of 100 kW for a time duration of 5 min, at which time the inner grid wire melted and the device consequently stopped functioning (Ref. 17).

The focus of this investigation is to examine if it is plausible to remove heat (i.e., control the temperature of) from the inner fusor grid in order that operation may be sustained at power levels that are even significantly into the megawatt range.

The approach will be to calculate heat transfer from the inner grid for a small fusor operating at a relatively low power level (as described above) and then to determine if this result can be scaled up for a larger system operating at a significantly higher power level.

The proposed conceptual method for removing heat from the inner fusor grid will be to construct it from small-diameter metal tubing (rather than stiff wire) and then pump a fluid (liquid) through the tubing in order to remove heat and control the temperature of the metal.

It is understood that this analysis is necessarily performed at a "high level," as some of the relevant parameters are only approximately known.

2.6.2 Calculation of Rate of Heat Produced in the Inner Wire Grid

The initial calculation is heat flux per area of metal that caused the inner grid of Farnsworth's fusor to melt in 5 min of operation at a 100-kW fusor power level.

The following assumptions are used in the calculations:

- the inner grid wire diameter is one-eighth of an inch;
- the total grid wire length is 1 m (before being configured into an "open-sphere" shape) (Ref. 18);
- the wire is pure copper;
- the initial temperature of the grid wire is ambient (289 K); and
- all of the ion-impact heat induced in the wire is retained in the copper (which is a "worst-case" assumption because even though the gas pressure in the fusor is very low, some amount of heat could be radiated from the wire, even in a vacuum).

Using properties of copper as found in a standard heat transfer text book and assuming no heat is lost, the calculated heat flux into the inner grid metal wire is 109 W (Ref. 14, p. 819 and 838).

2.6.3 Calculation of the Liquid Flow Rate Required to Control the Temperature of an Inner Grid Constructed of Tubing

Input parameters (not previously described above) are stated below.

- The OD of tubing (selected to be one-eighth of an inch) is to be equal to the wire diameter in Section 2.6.2. A standard wall thickness (0.03 in) then determines the inside diameter (ID) (0.065 in) (Ref. 19). The length is 1 m, which is equal to the wire length in Section 2.6.2.
- The design value of the coolant temperature rise within the tubing (assumed to be 100 degrees Fahrenheit (°F), which is 56 K).

The following assumptions (not previously described above) are used in the calculations.

- Water is the liquid selected to remove heat from the tubing.
- The concept used is that the tubing is one continuous length with one "entrance end" and one "exit end" (i.e., one acceptable pattern could be a 3-D spiral visualized as wound (increasing radius) from the "north pole" to the "equator" and then continuing with a (decreasing radius) spiral from the "equator" to the "south pole)."
- In practice, the inner grid of a fusor is electrically isolated (with insulation) from the rest of the system to prevent a short circuit. If water were pumped through the grid to control temperature, the water would need to be deionized (to have a high electric resistivity), and the pump and subsequent heat exchanger would also need to be electrically isolated.
- The tubing is a relatively good conductor of heat (i.e., all the heat entering the outside of the tubing is removed by means of the flowing water inside it). This tubing could also be assumed to be copper; however, this assumption will not directly affect this analysis.

Using properties of water as found in a standard heat transfer text book and assuming no heat is lost, the calculated flow rate of water in the tubing, to limit the water temperature rise to the design value, is 7.5×10^{-3} gallons per minute (gpm) (Ref. 14, p. 819 and 838).

The calculated pressure drop required to produce that flow rate is 0.238 pound per square inch (psi) (per the meter length of tubing).

2.6.4 Required Flow Rate and Pressure Parameters to Cool a High-Power Fusor Inner Grid

Information in Section 2.4 includes the results of a NASA-LaRC calculation which showed that the highest (climb) power required for the conceptual emissionless aircraft powered by the H^1-B^{11} aneutronic fusion reaction would be approximately 35 MW. Therefore, the intent of this section is to illustrate what is involved to (conceptually) control the temperature of a fusor inner grid when the reaction level is increased by 350 times, from 100 kW to 35 MW.

Based on the 1:5 ratio of inner grid diameter to outer grid diameter (described in Section 2.6.1) and the 2-m-diameter of a large (100-MW) fusor (Ref. 1, p. 42), it is estimated that the overall length of tubing in the inner grid of the 35 MW fusor is 10 m.

It is assumed that the heat removal rate (per area of metal) from the inner grid will scale in proportion to the fusor power level. An initial calculation using 1/8-in. tubing for the inner grid of a 35-MW fusor determined that the required water pressure drop would be excessive. Calculations determined that 1/2-in. (nominal) pipe would be adequate. (Heat rate from ion impact varies proportionately to pipe OD; however, liquid pressure drop varies approximately as the inverse fifth exponential power of pipe ID.) A summary of these scaleup ratios is as follows:

- fusor power: 350;
- overall pipe length: 10; and
- outside pipe diameter: 6.72.

The water volumetric flow rate as calculated in Section 2.6.3 must now be scaled up by a factor of 23,520, which is the product of the three factors listed above. The resulting value of the water flow rate is 176.9 gpm.

With the standard wall thickness (0.109 in) and a friction factor (at this turbulent flow condition characterized by a Reynolds number, $R_e = 1.4 \times 10^6$) determined from a Moody chart, the calculated pressure required to achieve the above-stated volumetric flow rate is 3,721 psi. The maximum allowable working pressure for 1/2-in. (nominal) schedule 40, type 304 stainless steel pipe is 4,660 psi. This value has a built-in safety factor of four (Ref. 20).

In principle, heat transfer liquids with operating temperature ranges significantly greater than that of water could be used, which would allow smaller flow rates and pressure drops to consequently be used because the temperature rise in the liquid could be significantly greater than the 100 °F chosen for water as the heat transfer fluid.

An alternative approach is to use multiple fusors, which would have a combined total output power of 35 MW. The advantages would be system redundancy and less technical constraints regarding heat removal from the inner grid; the disadvantage would be greater system weight.

2.6.5 Heat Exchanger Weight to Remove Fusor Inner Grid Heat from the Aircraft

The heat removed from the inner grid of a fusor providing propulsion power for an emissionless transport aircraft must subsequently be transferred to the ambient atmosphere. As explained above, when the fusor is operating at a power level of 35 MW (which is the highest power required for climb), the rate of heat removal from the inner grid must be 23,520 times the 109 W as stated in Section 2.6.2 (for the 100-kW prototype fusor). This value is 2.56 MW.

A recent NASA CR presented a pound per megawatt value for a conventional "automotive radiator" type of heat exchanger that would be designed to remove heat from hot water produced by a particular type of fuel cell used to provide propulsion power for a large emissionless aircraft. This value was 1,815 lb/MW (Ref. 1, p. 58). If the heat exchange process did use water as the heat transfer fluid, it could be estimated that (for a high-level approximate analysis such as this one), the same pound per megawatt value for the above-mentioned radiator would serve for the present example of heat transfer from the fusor inner grid. Therefore, the heat transfer rate of 2.56 MW times 1,815 lb/MW results in a heat exchanger weight of 4,646 lb. Adding additional weight for pumps, motors, tubing, controls, and contingency, the estimated total onboard weight required to transfer and remove heat from the fusor inner grid is 6,000 lb.

2.6.6 P/P System Weight and Effect on Aircraft Power Levels, Energy per Nautical Mile, and Cruise Range

Calculations included in Section 2.4 indicate that the conceptual (magnetic field) CBFR would have a weight of 22,412 lb for a net electric power output of 23.9 MW. This is a power density (mass basis) of 938 lb/MW.

The (electrostatic field) IEC fusion reactor described in the preceding sections will weigh less per megawatt of power output than the CBFR. A recent NASA CR presented the estimated weight of a conceptual IEC fusor as 9,330 lb for an electric power output of 100 MW (Ref. 1, p. 42). Most of the inside of a fusor is "empty" (actually low-pressure plasma while operating); therefore, the weight of a fusor does not scale linearly with power output. However, one could estimate that a fusor designed to produce 35 MW electric power output would weigh approximately one-half of the 9,330 lb as described above. Adding 10% for contingency and then 6,000 lb more for the inner grid heat removal system results in a fusor (including heat removal) system weight of approximately 11,100 lb. The results of the NASA-LaRC FLOPS Code calculations, which are presented in Section 2.4, show that conceptually increasing the CBFR electric power output by a value that reduced the P/P system weight by approximately 8,000 lb resulted in a reduction of the overall aircraft weight by approximately 10,000 lb.

In other words, when an aircraft has propulsion power provided by an extremely high power density fuel (e.g., H^1-B^{11}), the P/P system weight is a relatively small percentage of the total (constant) aircraft weight (less than 15% in this example). Consequently, it is to be expected that (conceptually) replacing a CBFR with an IEC fusor (while reducing the aircraft weight by many thousands of pounds), will not significantly change the climb power, cruise power, or energy per nautical mile values. However, it is also to be expected that the calculated cruise range per pound of H^1-B^{11} fuel would increase slightly from the (CBFR) value of 60,681 nmi.

3. Advanced Electric Concepts

3.1 Introduction and Overview

MSE has presented high-level overviews of on-going research in areas of breakthrough propulsion and energy technologies (Ref. 1, pp. 71-86).

Many of these breakthrough technologies share the common characteristic of being "electric" in nature. Obviously, it would be electric motors powered by fuel cells, which (in turn) drive propulsion fans for the baseline emissionless aircraft concept being developed by MSE and NASA-LaRC. However, "electric" in the context of this report refers to a characteristic of more advanced concepts such as deriving energy from the zero point energy (ZPE) field, present everywhere, and directly propelling an aerospace vehicle (for example) by means of high-voltage electric fields.

The topics included in this section are:

- Dr. Charles P. Steinmetz's theories of electricity;
- longitudinal and transverse electric waves; and
- scalar waves.

Sections 3.1.1 through 3.1.3 briefly introduce these topics and describe some of the ways they are connected.

3.1.1 Dr. Charles P. Steinmetz's Theories of Electricity

Dr. Steinmetz was the Chief Scientist of the GE Corporation approximately a century ago when large-scale alternating current (ac) electric technology was being rapidly developed and applied throughout the civilized world. Dr. Steinmetz also taught advanced courses to graduate electrical engineering students of that time so they could take part in the ongoing development of the electric power industry.

Additionally, those who are currently exploring the potential for accessing ZPE recognize that Steinmetz had valuable insights on electric characteristics and phenomena (not formally taught today) that could potentially help in the discovery and development of such breakthroughs.

One of these advanced topics taught by Steinmetz was electric transients (Section 3.2.2), and another is the characteristics of an electric field in the space surrounding an energized electric conductor (Section 3.2.3).

3.1.2 Longitudinal and Transverse Electric Waves

The traditional teaching on electric waves is actually on ***transverse*** electric waves in which the wave vibration is transverse to the direction of wave propagation. However, contemporary experimenters have found it possible to reproduce the remarkable experiments and results described by Dr. Nikola Tesla more than a century ago on ***longitudinal*** electric waves (in which the wave vibration is in the same direction as wave propagation, provided the experimental apparatus is built exactly according to the principles that Tesla described). Some experimenters have performed side-by-side demonstrations that clearly show that the characteristics of longitudinal and transverse electric waves are quite different.

Section 3.3 will compare the properties of longitudinal and transverse waves and furthermore suggest how the former type will potentially allow ZPE to be accessed and advanced propulsion concepts to be achieved.

3.1.3 Scalar Waves

Scalar waves is the name of a phenomena associated originally with the research of Dr. Nikola Tesla and other pioneering researchers of advanced electric topics. Research into and the recognition of the importance of scalar waves is now significantly growing worldwide.

Section 3.4 will present the topic of scalar waves from the perspective of:

- Dr. Thomas Valone, who has written extensively on ZPE and related phenomena; and
- Dr. Konstantin Meyl, who has written an extensive book on scalar waves in which he uses that phenomena as his basis for describing the properties of matter and energy from a viewpoint that is different from what is commonly accepted.

3.2 Teachings on Electric Phenomena by Dr. Charles P. Steinmetz

3.2.1 Introduction

In the early 1900s, Dr. Charles P. Steinmetz, Past President of the American Institute of Electrical Engineers, was GE Corporation's Chief Scientist for the development of long-distance ac high-voltage power transmission lines.

A series of graduate student university lectures given by Dr. Steinmetz on electric transients was collected and published in book form and was titled *Electric Discharges, Waves and Impulses, and Other Transients* (Ref. 21).

In this book, Dr. Steinmetz teaches what was known at that time regarding what would cause electric transients in electric transmission lines and the consequences of such transients, once formed.

This report includes information from Dr. Steinmetz's first two lectures (i.e., first two chapters of the book). The first chapter is titled *Nature and Origin of Transients*, and the second chapter is titled *The Electric Field*. A brief introduction for each respective chapter will be presented subsequently in this report.

Various claims for advanced energy and propulsion breakthroughs state that transient, high-voltage, or electric discharge phenomena were involved. The intent of this report is not to teach electrical theory but to show that selected electrical phenomena (which in general could be called "electric transients") could ***potentially*** lead to significant breakthroughs in aerospace technology.

3.2.2 Dr. Steinmetz's Teaching on Electric Transients

In the first chapter of the above-referenced book, Steinmetz introduces the question of why electric transients are ***not instantaneous***, with the following quotation (Ref. 21, p. 2):

> *The question then arises, why the effect of a change in the conditions of an electric circuit does not appear instantaneously, but only after a transition period, requiring a finite, though frequently very short time.*

The answer is that electric energy is stored in the electric system (e.g., voltage source, transmission line, and load), and a finite time is required to store energy in (or use energy that has been stored in) the system. With the following quotation, Steinmetz explains that in addition to mechanical energy storage (as in generators and motors) and thermal energy as in light bulb filaments, energy is stored electrically in the space around conductors:

> *While electric power flows over the line, there is a magnetic field surrounding the line conductors, and an electrostatic field issuing from the line conductors. The magnetic field and the electrostatic or "dielectric" field represent stored energy. Thus, during the permanent conditions of the flow of power through the circuit, there is electric energy stored in the space surrounding the line conductors.*

Dr. Steinmetz explained that one type of electric transient consists of one type of stored electric energy changing into another:

> *Thus in electric circuits containing energy stored in the magnetic and in the dielectric field, the change of the amount of stored energy - decrease or increase - frequently occurs by a series of successive changes from magnetic to dielectric and back again from dielectric to magnetic stored energy. This for instance is the case in the charge or discharge of a condenser through an inductive circuit.*

The storage of energy in the dielectric and magnetic fields of an electric circuit is subsequently discussed by Steinmetz in Chapter 2 of his book.

3.2.3 Dr. Steinmetz's Teaching on the Electric Field

In the second chapter of his book, Dr. Steinmetz presents his view on the component parts of the "electric field" surrounding a conductor through which electric power is flowing. Dr. Steinmetz stated that (Ref. 21, p. 10):

> *…in the space surrounding the conductor certain phenomena occur: magnetic and electrostatic forces appear.*

In the following quotation, Steinmetz provides more detailed information regarding the "magnetic field" and "dielectric field," which are the two components of the "electric field":

> *The conductor is surrounded by a magnetic field, or a magnetic flux, which is measured by the number of lines of magnetic force. With a single conductor, the lines of magnetic force are concentric circles, as shown in Figure 8. By the return conductor, the circles are crowded together between the conductors, and the magnetic field consists of eccentric circles surrounding the conductors, as shown by the drawn lines in Figure 9.*
>
> *An electrostatic, or, as more properly called, dielectric field, issues from the conductors, that is, a dielectric flux passes between the conductors, which is measured by the number of lines of dielectric force. With a single conductor, the lines of dielectric force are radial straight lines, as shown dotted in Figure 8. By the return conductor, they are crowded together between the conductors, and form arcs of circles, passing from conductor to return conductor, as shown dotted in Figure 9.*
>
> *The magnetic and the dielectric field of the conductors both are included in the term electric field, and are the two components of the electric field of the conductor.*

Figures 8 and 9 from Dr. Steinmetz's book are shown here as Figures 6 and 7, respectively.

Dr. Steinmetz shows by simple analogous mathematical derivations that:

- the energy stored in the magnetic field surrounding an electrically energized conductor varies as the square of the ***current*** in the circuit; whereas,
- the energy stored in the dielectric field surrounding an electrically energized conductor varies as the square of the ***voltage*** in the circuit.

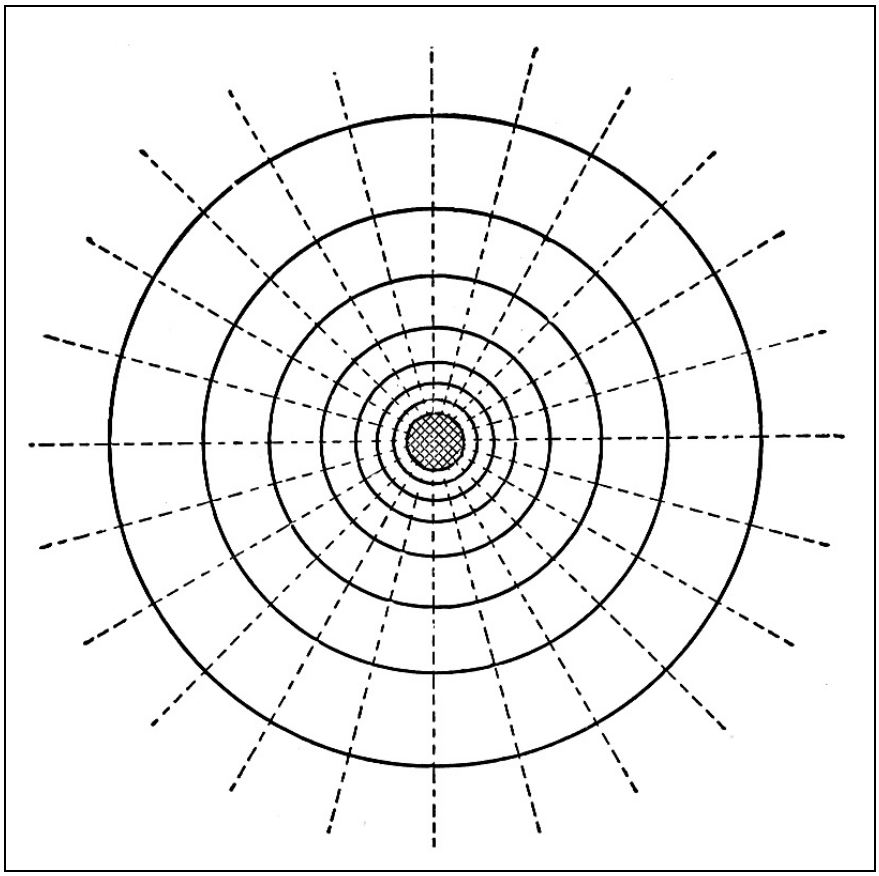

Figure 6. Electric field of conductor. Lines of magnetic force are shown solid; lines of dielectric force are shown dotted.

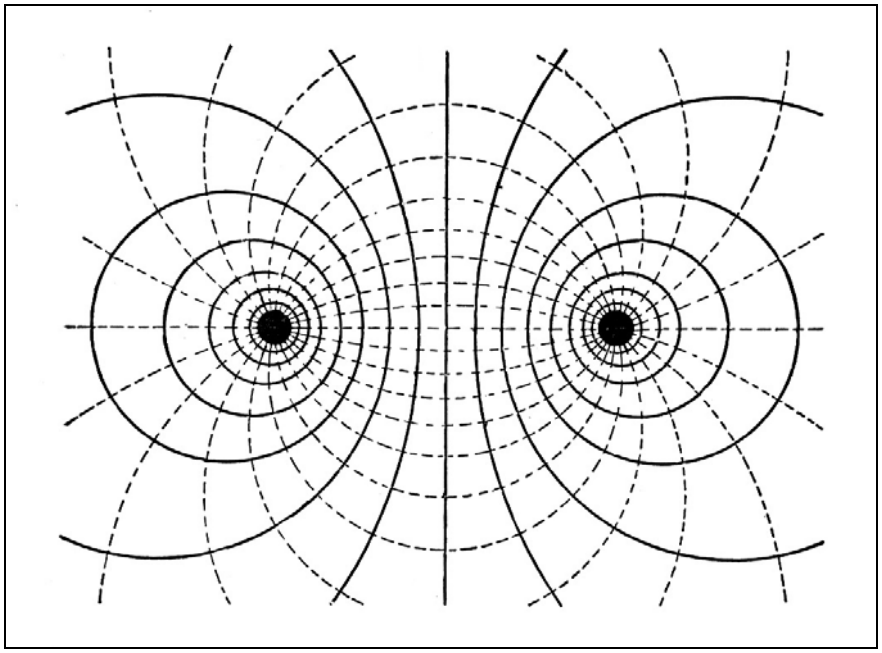

Figure 7. Electric field of circuit. Lines of magnetic force are shown solid; lines of dielectric force are shown dotted.

In the following quotation, Steinmetz teaches that the dielectric field surrounding an electrically energized conductor is not on the ***surface*** of the conductor but is in the space ***outside*** the conductor (Ref. 21, pp. 13-14):

> *Unfortunately, to a large extent in dealing with the dielectric fields the prehistoric conception of the electrostatic charge on the conductor still exists, and by its use destroys the analogy between the two components of the electric field, the magnetic and the dielectric, and makes the consideration of dielectric fields unnecessarily complicated.*
>
> *There obviously is no more sense in thinking of the capacity current as current which charges the conductor with a quantity of electricity, than there is of speaking of the inductance voltage as charging the conductor with a quantity of magnetism. But while the latter conception, together with the notion of a quantity of magnetism, etc., has vanished since Faraday's representation of the magnetic field by the lines of magnetic force, the terminology of electrostatics of many textbooks still speaks of electric charges on the conductor, and the energy stored by them, without considering that* ***the dielectric energy is not on the surface of the conductor, but in the space outside of the conductor, just as the magnetic energy*** *(emphasis added).*
>
> *All the lines of magnetic force are closed upon themselves, all the lines of dielectric force terminate at conductors, as seen in Figure 8, and the magnetic field and the dielectric field thus can be considered as a* ***magnetic circuit*** *and a* ***dielectric circuit****.*

As depicted in Figure 6 (Steinmetz's Figure 8), where there is a single conductor, an important difference between the magnetic field and the dielectric field is that the lines of magnetic force are ***finite***, whereas, the lines of dielectric force are ***infinite***.

3.3 Differences Between Longitudinal and Transverse Electric Waves

3.3.1 Introduction

The fundamental differences between "longitudinal electric waves" and what are commonly referred to as "electromagnetic waves" were first described by the inventor Dr. Nikola Tesla and the mathematician Dr. Charles P. Steinmetz approximately 100 years ago (Refs. 21 and 22).

Dr. Nikola Tesla invented the ac electric transmission system and its major components during the 1880s. At approximately 1890, Dr. Tesla began to investigate, write about, and demonstrate electric and electric transmission phenomena, which appeared unusual at that time and are very difficult to theoretically describe now based upon contemporary electric theory (Ref. 23). Over the years, investigators have ***claimed*** that Dr. Tesla was using a type of electric transmission referred to as longitudinal electric waves. It is to be understood that this claim (longitudinal electric waves) is applicable for the Tesla experimental phenomena replicated in the 1980s by a group of researchers in southern California who call themselves the Borderland Sciences Research Foundation (BSRF) (Refs. 17 and 24). These replications are described subsequently.

3.3.2 Definitions

Exact definitions of these two types of electric waves (from approximately 100 years ago) are as follows:

- Electromagnetic Waves = Transverse Electromagnetic Waves (TEM waves); for which the energy-related vibration is ***perpendicular*** to the wave propagation direction; and
- Longitudinal Electric Waves = Longitudinal Magneto-Dielectric Waves (LMD waves) for which the energy-related vibration is in the ***same*** direction as the wave propagation direction.

3.3.3 Wave Propagation Velocity Differences

The BSRF researchers claimed that they have demonstrated that the wave propagation velocities of transverse waves and longitudinal waves are significantly different, even when they are produced by the same signal source.

The wave velocity of transverse waves was determined by measuring the frequency for which low-power radio waves directly coupled to the end of a conductor of known length produced a resonance condition that resulted in a maximum voltage measured at the "far" (nonsource) end of the conductor. Wave velocity was calculated as (resonant) frequency times wave length, which was equal to frequency times conductor length times four. (The factor of four is included because reflected energy and input energy result in a maximum output when the conductor length is one-quarter of the full [electric] wave length.)

The wave velocity of longitudinal waves was determined in a very similar manner; however, the radio waves were ***capacitively*** (i.e., not directly) coupled to one end of a conductor equal in length to the conductor used for the transverse wave velocity measurement. As was done for transverse waves, wave velocity was calculated as (resonant) frequency times conductor length times four.

The results of these determinations were as follows:

- transverse wave velocity = 2.44×10^8 m/s = 0.81 x c; and
- longitudinal wave velocity = 3.74×10^8 m/s = 1.25 x c.

The velocity of transverse waves in "free space" (i.e., not confined to a conductor or other physical material) has been measured to be 3.00×10^8 m/s, and this value is commonly referred to as "the velocity of light, c" (Ref. 25).

The following points should be noted.

- Dr. Nikola Tesla described the propagation of some of the electric waves from his "Tesla Coils" as being "many" times the speed of light. [A Tesla Coil built ***as described by Tesla*** generates ***both*** transverse waves ***and*** longitudinal waves (Ref. 22)].

- Dr. James Clerk Maxwell's ***original*** electric wave equations (which he published in 1865, see Section 3.4.3.3 of this report) were written in a form of mathematics known as "quaternions" that predicted ***both*** transverse waves and longitudinal waves. Other researchers modified Maxwell's original equations to the vector form, as commonly taught in universities today, and in so doing ***arbitrarily*** discarded longitudinal waves. Nevertheless, longitudinal waves are believed to be a part of nature (Ref. 26).

3.3.4 Transverse Waves vs. Longitudinal Waves: Transmission Line Characteristics

The BSRF researchers demonstrated that the distribution of field strength and energy level along the length of a transmission line is fundamentally different when comparing transverse waves vs. longitudinal waves.

All electric transmission lines have electric properties referred to as "inductance" (associated primarily with coils) and "capacitance" (associated primarily with capacitors).

To illustrate the transverse configuration, a physical model of a two-element (two-wire) transmission line was demonstrated in which ***coils were connected in series*** in each wire and ***capacitors were connected in "shunt"*** from one wire to the other. Each coil had an inductance of 10 millihenry (mH), and each capacitor had a capacitance of 0.047 microfarad (μF). This model was several feet long. The analysis and understanding of this configuration is a well-accepted part of contemporary electric science and engineering.

The longitudinal configuration was illustrated with the identical coils and capacitors (in a model of equal length as for the transverse configuration); however, in this instance, the ***capacitors were connected in series*** in each wire, and the ***coils were connected in "shunt"*** from one wire to the other. Such a configuration would be considered "unconventional" according to contemporary electric science and engineering.

High frequency power from an audio oscillator was introduced to the "source" end of the model transmission lines; the other end will be referred to as the "far" end. The input power at the source end was stated to be essentially the same for both the transverse and longitudinal configurations.

The BSRF researchers showed that the distribution of magnetic field, dielectric field, capacitor temperature, and coil temperature along the length of the transmission lines was different for the two respective configurations. More importantly, it was shown that the electric energy transmitted to the far end of the transmission line was significantly more for the longitudinal configuration than for the (conventional) transverse configuration.

3.3.5 Unique Characteristics of Longitudinal Electricity

The BSRF researchers claim they have not only demonstrated fundamental differences between transverse and longitudinal waves but also refer to a number of phenomena they believe are unique to longitudinal waves.

It is important to understand that after Dr. Nikola Tesla invented the ac electric power distribution system and many of its essential components (e.g., alternators and motors), he began a lengthy series of experiments in which he perfected a power transmission system whose capabilities far exceeded that of alternating current. The key is believed to be that Tesla used ***longitudinal waves that he produced with high-voltage impulses of direct current (dc) electricity.*** The pulses were always of one polarity; therefore, they are defined as direct current, ***not*** alternating current (Ref. 23).

The BSRF experimenters built a transmitter coil and a receiver coil ***according to the information and specifications in Tesla's 1900 patent*** (Ref. 27). These coils were technically described as air-core transformers of an approximately 18-in-diameter flat spiral configuration. The coils (which will be subsequently described in more detail) are referred to as "pancake" coils due to their flat shape.

The major components of the longitudinal wave transmitting system were:

- a dc electric impulse generator (which was actually a small antique Tesla Coil manufactured in the 1920s);
- two "spark-gap" tubes as used in radar technology, which are now available in the electronic surplus market; and
- one of the pancake coils.

Initially, the BSRF researchers showed that with longitudinal waves, a standard incandescent electric light bulb is readily lit to normal brightness using ***only a single wire connection*** to energize the bulb.

The next demonstrations were based upon effects produced by small standard incandescent-type electric light bulbs (designed for household ac operation), which were powered instead by ***longitudinal electric impulses*** (Figure 8).

The light emitted by these bulbs (powered by longitudinal electric impulses) was described by the BSRF researchers as the color of natural daylight or "bluish" compared to identical adjacent bulbs powered by standard 120-volt (V) ac, 60-hertz (Hz) electric power, for which the emitted light was described as "reddish."

The BSRF experimenters placed their fingers approximately 1 in. from the bulbs lit by longitudinal electric impulses and claimed they could feel a ***mechanical force*** radiating from the bulbs and pushing against their fingers. However, when a piece of copper foil was hung from a piece of masking tape and brought to within approximately one-half inch of the same impulse-powered bulb, the copper foil was pulled ***toward*** the bulb. The BSRF researchers believe that this was not a mere high-voltage charge effect, as the copper foil was ***not*** pulled toward other high-voltage parts of the circuit.

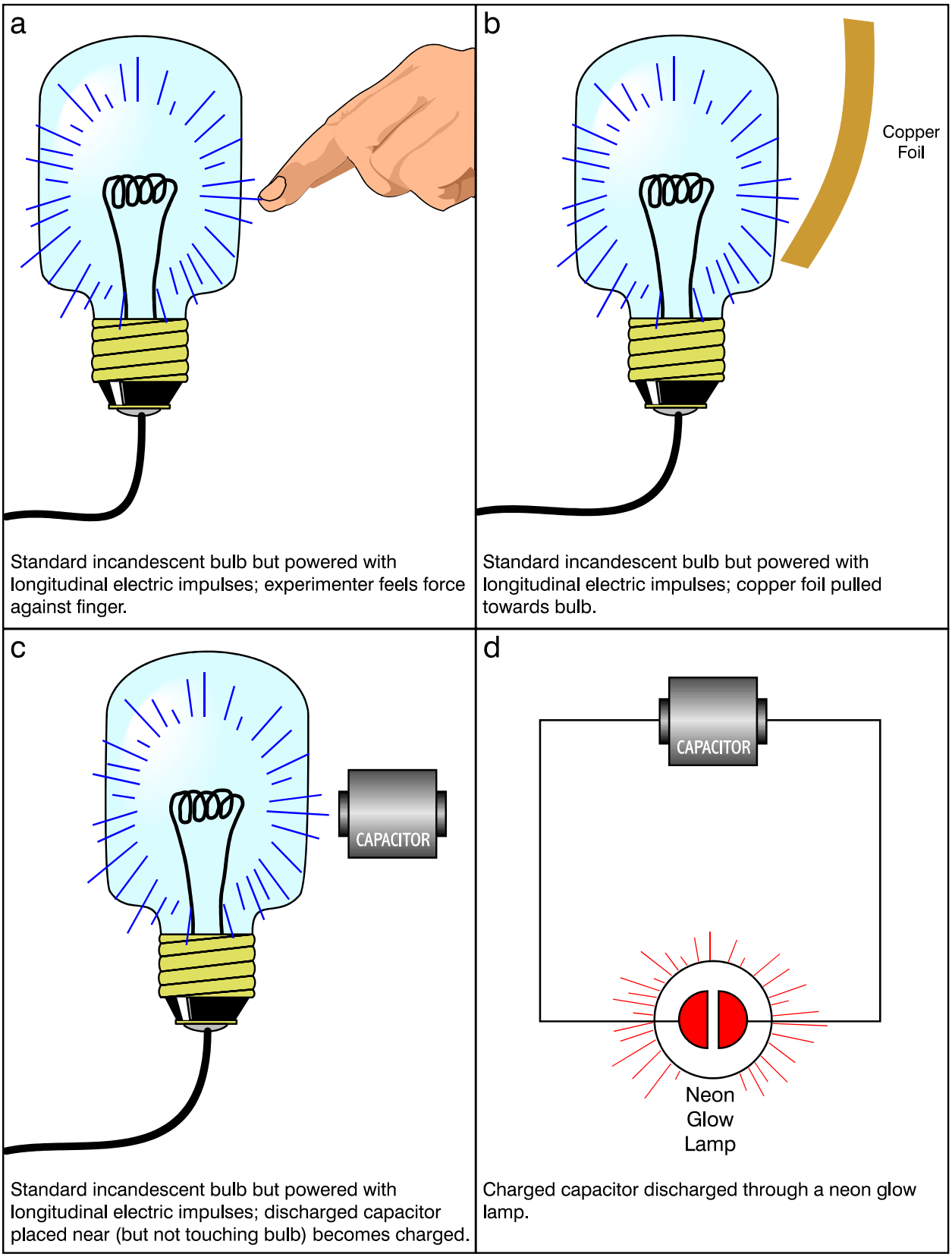

Figure 8 (a-d). Experiments with standard incandescent bulbs powered by longitudinal electric impulses.

The BSRF experimenters claimed that they were demonstrating what Tesla had described in patents and articles approximately 100 years ago, namely that dc electric impulses can produce not only visible light but also "rays" that exhibit mechanical action at a distance.

3.3.6 Demonstration of Tesla's Radiant Energy Patents

Next, the BSRF experimenters referred to the cover page of one of Dr. Tesla's "Radiant Energy" patents that described a form of rays that could charge a capacitor at a distance with no direct connection to the capacitor (Refs. 28 and 29).

This was followed with a demonstration of what the patents described. An electric device referred to as a "doorknob capacitor" (with a capacitance value of 500 picofarad, a voltage rating of 20 kilovolts (kV), and dimensions of approximately 1-in. diameter and 1 in. in length) was first shown to be discharged by momentarily shorting it out by means of a wire touching both terminals. Then, for a few seconds, this capacitor was brought near (***but not touching***) one of the incandescent electric bulbs operating on electric impulse energy. The capacitor was rapidly charged as shown by discharging it through a neon glow lamp (the neon glow lamp emitted a bright flash of light, and the spark where the connection was made was very audible as it made a "snapping" sound). When the capacitor was held near a high-voltage wire in the circuit (rather than the bulb operating on electric impulse energy), only a ***very small*** amount of charge was received.

This demonstrated capability of storing energy in a capacitor ***at a distance without using conventional electromagnetic technology*** is significant.

One of the BSRF experimenters gave some detailed information about the construction of the transmitter and receiver coils and the principles of construction (based upon information originally presented by Dr. Tesla) (Figure 9):

- The coil primary consists of two turns of bronze strap made from three layers of 1-in-wide by 0.010-in-thick metal.
- The ODs of the primary turns are 18 in.
- The coil secondary consists of 20 turns of Teflon-coated silver-plated coaxial cable (the inside conductor of the coaxial cable is not used; the outer sheath conductor is used).
- The secondary turns start inside the primary turns and spiral inward to a diameter of 13-1/2 in. (Coil turns are immobilized by placing them in notches cut in spoke-like wooden strips.)
- The secondary turns are actually ***double turns*** with one wire on top of another (when viewing the flat face of the coil). This is done to obtain the correct amount of capacitance in the coil to allow it to function as Tesla originally designed.
- The receiving coil is constructed identically to the transmitting coil but with its respective windings wound in a complementary direction.

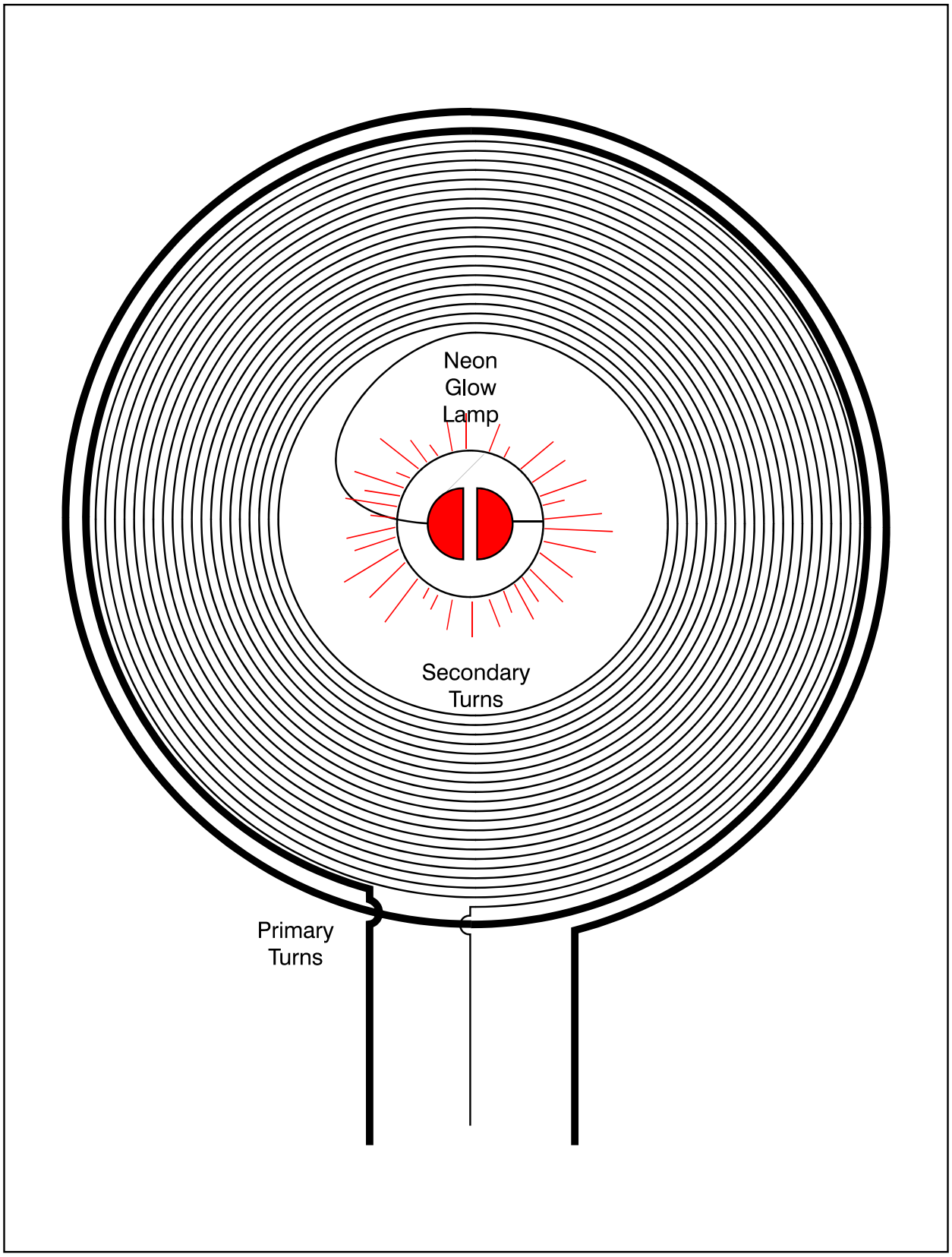

Figure 9. Flat spiral coil for transmitting/receiving longitudinal electric waves (not to scale).

- The coils are designed and built such that the total ***volume*** of metal material in the primary is equal to the total ***volume*** of metal material in the secondary. (Note that according to contemporary electric construction practice, such a requirement would appear to be strange; however, Dr. Tesla was researching different phenomena, and he precisely described what he found.)
- For both the transmitter and receiver coils, the interior end of the secondary winding terminates (with a one-wire connection) to a neon glow lamp (approximately 2 in. in diameter) that is located adjacent to the plane of the coil on the central coil axis. (The BSRF experimenters substituted an argon glow lamp rather than the neon type; the characteristics are very similar). For a very high-power system (such as the ones Dr. Tesla built), the experimenters stated that the interior coil termination should be a metal sphere.

3.3.7 Long-Range Longitudinal Wave Transmission

Finally, the BSRF researchers demonstrated longitudinal waves being transmitted and then received several thousand feet away.

Inside the BSRF laboratory building a conventional continuous wave (CW) radio transmitter was connected to the pancake transmitter coil. Outside (on the seashore beach 3,000 ft away), a conventional (shortwave) portable radio receiver was connected to the pancake receiver coil, which in turn was connected to a copper screen immersed in the ocean as an "antenna" for the longitudinal waves. The signal reception [at a frequency of 2.94 megahertz (MHz)] was shown. It was not demonstrated to what extent the screen immersed in the ocean was augmenting the reception process; however, it should be noted that there was no "line of sight" from the transmitter to the receiver and the transmission distance was too short to use reflecting the signal from the ionosphere. It was also stated that the transmitter location was not only 3,000 ft away but was behind a mountain. Therefore, the point of the BSRF demonstration was to show that longitudinal waves (at this frequency) can more readily penetrate matter than can transverse waves.

In their concluding comments, one of the BSRF experimenters pointed out that all the demonstrations they showed were done on a very low budget with "surplus" equipment or equipment fabricated from available materials and that anyone could reproduce the experiments. He went on to state that the key is that anyone attempting to replicate Dr. Tesla's experiments will be successful when they realize that Tesla ***did*** know what he was doing and his discoveries were ***not*** confined to generally accepted electric principles.

3.4 Scalar Waves

3.4.1 Introduction

Advanced energy researchers believe a phenomenon known as "scalar waves" may be an important key for accessing ZPE (Section 4) and achieving advanced propellantless propulsion. The following sections present information on this topic.

3.4.2 Dr. Thomas Valone's Writings on Scalar Waves

Dr. Thomas Valone has investigated, lectured on, and written about breakthrough energy, breakthrough propulsion, and advanced physics topics for nearly 25 years.

Dr. Valone defines the following terms in the glossary of one of his books (Ref. 30):

Comments are provided beneath some of these quoted definitions.

> *Longitudinal Wave—A pressure type of wave, similar to sound, in which the vibrations are along the direction of travel, a sequence of compressions and rarefractions...Scalar waves are longitudinal, as contrasted with EM 'Hertzian' waves which have transverse oscillations. Longitudinal waves are non-Hertzian as a result, as Tesla said many times, regarding his magnifying transmitter.*

"EM" is an abbreviation for electromagnetic. One may suggest the sound-like waves are propagated in the "aether." E.Y. Webb carefully explains in his book (as presented in Section 5.3.4) that the experiments done in the 1880s, which caused many physicists to conclude that there was no aether, were faulty, being based on a false premise (Ref. 31).

> *Scalar Field—In physics, each point in space for a particular potential is assigned a magnitude but no direction. The scalar potential is just the Coulomb potential due to a charge density...While EM (electromagnetic) waves travel at light speed, 'the scalar potential propagates instantaneously everywhere in space'.*

The concept of "instantaneous" propagation is supported mathematically, as explained in Section 3.4.2.4.

> *Scalar Wave—(see Longitudinal Wave.) Also Tesla Wave. An oscillating field of pure potential without E and B (electric and magnetic) fields. X is a scalar wave varying harmonically in time but only longitudinal fields exist...In quantum mechanics (e.g., Aharonov-Bohm experiment) it has real effects on the electron wave function. Because no energy or momentum transfer occurs, X fields can penetrate all objects and in fact can traverse the whole universe. Scalar waves thus may in fact, travel faster than light speed c, since no c-limited fields are involved.*

Even though scalar waves can "penetrate all objects," they can nevertheless sometimes interact with matter in certain specific situations, explained subsequently in this report.

> *Transverse Wave – A standard Hertzian EM vector wave which oscillates laterally, as contrasted with a Tesla electrostatic scalar wave which vibrates longitudinally.*

To date, almost all of the world's electric and electromagnetic (EM) technology is based upon transverse EM waves. Longitudinal wave technology and its unique proven capabilities are not as widely known or used.

3.4.2.1 Scalar Potentials, Fields and Waves – Their Scientific Basis

Dr. Valone has also published a report on scalar waves and related phenomena, which is a collection of articles and patents by researchers of this topic (Ref. 32). The remainder of Section 3.4.2 consists of material quoted from Valone's report with explanations added.

The first (overview) article of this report is by Dr. Valone. Selected excerpts from this article follow; comments are provided after some of the selected excerpts:

> *A scalar field can be defined as a physical influence pervading an area, analogous to a voltage field, but without a direction. Scalar fields are everywhere.*
>
> *Without showing the physics, which can be found in the references, we start with the famous Aharonov-Bohm experiment which brought the Vector Potential into prominence. (A "vector potential" is analogous to a voltage or electric field that has direction.) Up until this experiment, the Vector Potential was relegated to electromagnetic textbooks as a mathematical concept without physical effects. Once Aharonov and Bohm set up a long coil with no leaking magnetic field outside the coil, they found that they could change the interference pattern of an electron beam source which went **around** the coil. This was unexplainable except that the Vector Potential was outside the coil.*

The physics concepts underlying the Aharonov-Bohm experiment are the basis of patented communications systems, which cannot be shielded and are described subsequently.

> *By using special coils to create internal magnetic fields, scientists have suggested that we can create scalars. Toroids (e.g., Coil #69370 from PICO Electronics, Mt. Vernon, NY) have the unique geometry of being a long coil that touches both ends together, like a donut. This ensures that the magnetic field does not stray outside the coil. In my paper to the 1992 Tesla Symposium, I tested the PICO coil in a backwound or caduceus mode, since it has two layers which can be backwound, for scalar generation.*

As an example, Valone is referring to the manner in which half of a (continuous) length of wire wound into the shape of a coil may be wound (on the same coil form) in a direction opposite that of the first half. Another way to describe this is to visualize a ***pair*** of wires connected together at one end. The ***pair*** is then wound in the shape of a coil. The magnetic field produced by electric current flowing ***to*** the connected end ***cancels*** the magnetic field produced by the return current ***from*** the connected end (because the respective currents are flowing in opposite directions). This method of winding is often referred to as "***bifilar***." Such a coil cannot generate a net magnetic field; however, the more subtle scalar fields may be generated.

Dr. Jack Dea, from the Arizona State University, writes in 1985 that...the (longitudinal) "phase field" (of scalar waves) has a l/r dependence and that more intriguing is their property of passing right through matter since information is carried rather than energy. He predicts that (scalar waves)...can penetrate all objects and in fact can traverse the whole universe.

The term "l/r dependence" means that the magnitude of the scalar wave varies inversely as the distance from the transmission source. In contrast to this, the magnitude of the better known transverse wave varies inversely as the ***square*** of the distance from the transmission source.

3.4.2.2 Dr. Hal Puthoff's U.S. Patent for a Potential-Based Communication System

One of the leading proponents of ZPE is Dr. Harold E. Puthoff of the Institute for Advanced Studies at Austin, located in Austin, Texas. Dr. Puthoff has published a number of papers and articles on the theoretical physics supporting ZPE.

Additionally, Dr. Puthoff obtained a U.S. Patent on a ***nonelectromagnetic*** communication system that cannot be shielded. The cover page of Puthoff's U.S. Patent (5,845,220) is included in Valone's report. The title of this patent is *Communication Method and Apparatus with Signals Comprising Scalar and Vector Potentials without Electromagnetic Fields*. MSE spoke with Dr. Puthoff about his invention and briefly described it in the prior work (Ref. 1, pp. 85-86):

It is important to note that the Aharonov-Bohm effect is the basis of a unique communication system patented by Dr. Harold E. Puthoff of the Institute for Advanced Studies at Austin, located in Austin, Texas.…The patent abstract reads, "Information that changes as a function of time is communicated from a transmitting site to a receiving site by transmitting a signal comprising scalar and vector potentials without including any electromagnetic field...The patent diagrams depict alternating voltage from a signal generator coupled to two essentially square metal plates at right angles to each other and alternating current from the same signal generator coupled to an electric coil located where the two metal plates would intersect.

*The receiver is **electromagnetically shielded** and uses a cryogenic superconductor device known as a "Josephson Junction." The Josephson Junction converts the electrostatic scalar and magnetic vector potentials that **do** penetrate the shielding into conventional electromagnetic waves that can then be subsequently detected by an ordinary radio receiver.*

The importance of this invention is that it is a nonelectromagnetic communication system and cannot be shielded.

In response to specific questions from MSE, Dr. Puthoff stated the following:

- *as the patent states, only **potential** is being transmitted and received;*
- ***no energy** is transferred from the transmitter to the receiver. (Energy would be the sum of the squares of the individual electrostatic and magnetic fields, and these fields cannot be transferred, as they are shielded); and*
- *the system has been built and tested "as part of a classified project."*

Raymond C. Gelinas received U.S. Patent 4,429,288 for a nonshieldable communication technology that is apparently very similar to that invented by Dr. Puthoff.

3.4.2.3 An Excerpt from One of Dr. David Bohm's Quantum Mechanics Lectures

Dr. David Bohm was one of the two scientists who predicted that there would be an effect from potentials (when fields are shielded), which has become known as the Aharanov-Bohm Effect (briefly described in Section 3.4.2.1).

Valone included a brief excerpt from one of Dr. Bohm's books, *Lectures on Quantum Mechanics*, in which Bohm points out that elementary particles may have ***scalar interactions***, as well as the (classical) ***electromagnetic interactions***.

3.4.2.4 Excerpt from "Classical Electrodynamics"

Valone includes several pages on vector and scalar potentials excerpted from the textbook, *Classical Electrodynamics*, by Jackson.

It is noted that in his final comments on this topic, Jackson points out that even though "electromagnetic disturbances propagate with finite speed," (one of the equations he presents) "indicates that the scalar potential 'propagates' instantaneously everywhere in space." Jackson states that this characteristic is "puzzling."

3.4.3 Dr. Konstantin Meyl's Teachings on Scalar Waves

3.4.3.1 Introduction

Professor Dr.-Ing. Konstantin Meyl began to lecture on scalar waves in Germany in 1996. Dr. Meyl published a book compiled from a series of lectures on scalar waves and related topics that he gave from 1996 to 2003. This book has subsequently been translated from German to English (Ref. 33). Dr. Meyl was also one of the speakers at the Extraordinary Technology Conference held in Salt Lake City, Utah, in August of 2004, and he presented experimental demonstrations of scalar wave phenomena as part of his lecture on that topic.

3.4.3.2 Scalar Wave Concepts from Dr. Meyl's Book

Dr. Meyl's book is comprehensive and lengthy as it attempts to explain (by means of a scalar wave approach) a very wide spectrum of topics that include physics, electric phenomena, cosmology, biology, and Earth history.

In the following sections, this report will focus on those topics in Dr. Meyl's book related to the properties of scalar waves and how they may potentially be used for both advanced energy and advanced propulsion applications. As additional disclaimers, it is to be understood that:

- it is Dr. Meyl's ***personal hypotheses*** or ***postulates*** that are being reported and they may not agree with those of other researchers nor are they necessarily endorsed by NASA-LaRC/MSE; and
- Dr. Meyl's original book has been translated from German to English, and the resulting translation may not be communicating precisely what Dr. Meyl intended.

3.4.3.3 Longitudinal Electric Waves

In the late 19th century, scientists were trying to understand the electric wave phenomena discovered by Dr. Heinrich Hertz. The properties of electric wave phenomena claimed by Dr. Nikola Tesla were totally different than the properties of the electric wave phenomena claimed by Dr. Hertz, and this lead to contention between the competing viewpoints (Ref. 33, p. 191).

Because of the controversy, the eminent scientist, Professor William Thomson of Glasgow University, Scotland (also known as Lord Kelvin) traveled to New York in 1897 to see Tesla's experiments and, as a result, he concluded that ***both*** Tesla and Hertz were correct. The explanation is that Hertz experimented with ***transverse*** waves, whereas Tesla's waves were ***longitudinal***.

Hertz claimed that the transverse electric waves he discovered could be calculated with Dr. James Clerk Maxwell's electrodynamic equations, and scientists of that time accepted the experimental agreement with mathematical calculations as proof Hertz was correct.

However, as explained in a recent NASA CR, almost no scientists or engineers today have even ***seen*** (much less understood) Dr. James Clerk Maxwell's ***original*** electrodynamic equations, published in 1865, which ***did*** predict longitudinal waves, transverse waves, and much more (Ref. 1, p. 81). What scientists and engineers today refer to as "Maxwell's Equations" is an extremely simplified set of electrodynamic equations that is quite different than what Maxwell published. A more correct name for what is taught today would be Maxwell-Heaviside equations, as Oliver Heaviside was the major adversary of Maxwell who removed the capability to calculate ***longitudinal*** electric waves and electric ***potentials*** from Maxwell's ***original*** equations.

However, Tesla's claims were backed up with documented experimental demonstrations rather than mathematical equations. In the following quotation, Meyl describes one of Tesla's demonstrations and states that Hertz's technology could ***not*** have accomplished such a demonstration:

> *In Colorado Springs he had built a 10 kW transmitting installation and lighted 200 fluorescent lamps of 50 Watt each on a mountain in the Rocky Mountains in a distance of 25 miles. With that he had completely transmitted the transmission power of 10 kW, as can be inferred from the press reports at that time. With Hertzian waves, which propagate spatially, this experiment even today, after over 100 years, wouldn't be realizable technologically. According to the law of the square of the distance one isn't even able to let glow a tiny little lamp in such a distance.*

Meyl helps resolve the controversy between longitudinal and transverse waves by explaining that the high-voltage "spark" transmitters used in the early days of radio actually transmitted ***both*** longitudinal ***and*** transverse waves (Ref. 33, p. 459). The characterization of the type of radio technology employed was in the ***receiver***, not the transmitter. Tesla's equipment would only receive longitudinal waves, whereas the equipment of Hertz and other pioneer radio inventors (such as Marconi) were designed to receive only transverse waves. Because both types of waves (longitudinal and transverse) were being transmitted, ***both*** viewpoints of how the technology functioned were correct.

3.4.3.4 Dr. Meyl's Personal Tesla Coil Experiments

Dr. Meyl describes how he personally constructed and experimented with a small-scale version of a Tesla flat ("pancake") coil in 1995 (Ref. 33, pp. 405-407). By adding:

- a spherical electrode (approximately 6 in. in diameter);
- a spirally wound flat Tesla Coil (approximately 4 in. in diameter);
- a two-turn coil to electrically couple to the outer turns of the flat coil; and
- an old interleaved metal plate variable capacitor (formerly used in broadcast radio receivers)

to the input of an oscilloscope, Meyl could readily receive, detect, and analyze scalar wave signals originating from (unspecified) sources of interferences and distant thunderstorms. Compared to what he had learned in his prior training and expertise in electrical engineering, Meyl stated that he was totally surprised at the large magnitude of the scalar wave signals displayed on the oscilloscope screen. Meryl also stated that he and his colleagues had to repair their oscilloscope several times due to scalar wave energy spikes that had entered the equipment but were too brief to be visually observed on the oscilloscope screen.

3.4.3.5 Differences Between the Near-Field and Far-Field of a Transmitted Signal

Meyl explains that the properties of waves in the "near-field" and "far-field" with respect to the transmission source are quite different (Ref. 33, p. 463).

According to Meyl, Hertz used relatively short waves that were only a few meters in length, whereas Tesla typically used frequencies of approximately 100 kilohertz (kHz) and wave lengths of several kilometers and, in some cases, Tesla used frequencies as low as 6 Hz with a wave length as large as the entire Earth. Meyl states that the characteristic distance that distinguishes near-field from far-field is the wave length divided by 2 π. According to this definition, the Tesla experiments were near-field (characterized by longitudinal waves) and those of Hertz were far-field (characterized by transverse waves).

Meyl adds the insight that ***scalar*** wave technology is by no means obscure but is in widespread commercial use in the anti-theft system in the doorways of stores. Unless a small passive coil (in a package wrapper) has been deactivated at the point of sale, that coil will be a scalar wave receiver and couple energy back to the scalar wave transmitter at the door, be detected, and thereby activate a security alarm.

3.4.3.6 Variable Velocity of Scalar Waves

Meyl states that unlike transverse waves moving through a given medium, scalar (longitudinal) waves have a nonconstant velocity (Ref. 33, p. 469). The velocity of propagation of a scalar wave oscillates at double the frequency of the wave and with opposite phase to the corresponding field. This means that when the field is maximum, the wave velocity is minimum, and vice versa. However, an ***average*** velocity of propagation of a scalar wave may be determined and stated.

3.4.3.7 Potential Efficiency of Scalar Waves for Communications

Meyl points out the wastefulness of Hertzian wave technology for communicating point to point (Ref. 33, pp. 482-485). With conventional Hertzian waves, only a very small fraction of transmitted energy arrives at the intended point of reception. In contrast to this, scalar wave communication, where the energy couples to the receiver (at resonance), could (according to Meyl) allow one to "carry out a telephone call right through the Earth" with the power expenditure of only a few ***microwatts***.

3.4.3.8 Comparison of Scalar Wave Propagation with Nerve Conduction

The final information chosen from Meyl's book, which is related to the preceding section, is on the biophysical process of nerve conduction (Ref. 33, pp. 519-521). Meyl states that nerve conduction is a form of "single-wire transmission," and the segmented (interrupted) geometry of the insulation sheath surrounding nerves (which makes nerve signal transmission efficient and selective) was very similar to one of the single-wire transmission concepts described by Dr. Tesla approximately a century ago.

3.4.3.9 Vortices as a Link Between Scalar and Transverse Waves

Dr. Meyl postulated in his talk given at the August 2004 Extraordinary Technology Conference that conventional linear (i.e., nonspherical) transmitting antennas emit scalar waves ***at the surface of the antenna***. A vortex shape energy flow then transforms the longitudinal scalar waves into conventional (Hertzian) transverse waves as the energy traverses the "critical" distance from the near-field to the far-field, which is the wave length divided by 2 π.

Note: For this reason, Dr. Meyl is deeply concerned that cell phone users are directly coupling scalar waves from the phone's near-field directly into their brains, potentially causing brain damage. Many researchers and engineers are not even aware of the existence of scalar waves. ***Conventional*** measuring techniques and measurements at greater than the critical distance, where only transverse waves occur, do ***not*** indicate the presence of scalar waves.

At the receiving antenna, another set of energy vortices forms and transforms the transverse waves back into scalar waves that enter the antenna, (i.e., essentially the inverse of what happens at the transmitter). However, when spherical antennas are used for the transmitter and receiver (Tesla's method), the scalar waves do not transform into transverse waves.

3.4.3.10 Dr. Meyl's Scalar Wave Demonstration Device

Dr. Meyl and his university students built a miniature transmitter and receiver to demonstrate (within a distance of approximately 20 ft between these two units):

- properties of scalar waves; and
- a comparison between the properties of scalar waves and transverse waves in the same environment.

These researchers used principles (except for those related to voltage and size) from the writings of Dr. Nikola Tesla in the design of this equipment. For affordability and portability, the miniature transmitter and receiver "towers" have a maximum dimension of approximately 1 ft. Each tower has a horizontal flat Tesla "pancake" coil in the base (with an approximate diameter of 6 in) and a "Tesla" sphere on top (with an approximate diameter of 4 in). For the purpose of making accurate frequency measurements, the researchers incorporated up-to-date technology, namely a digital frequency readout display. Because of the relatively small size of the equipment, a frequency range of approximately 4 to 8 MHz was used rather than the very low frequencies Tesla used with his relatively large systems. Additionally, Meyl stated that these small-scale demonstration devices operated at an electric potential of 2 V, in contrast to potentials in the range of 60 kV as Tesla used in his large equipment.

3.4.3.11 A Demonstration of (Average) Scalar Wave Velocity

As explained in Section 3.4.3.6, even though the velocity of scalar waves can vary, the ***average*** velocity of these waves may be determined.

If wave length is considered constant, velocity is proportional to frequency. With his transmitter and receiver spaced approximately 20 ft apart, Meyl demonstrated that the (digitally read) resonant frequencies for reception were:

- transverse waves: 4.6 MHz; and
- scalar waves: 7.1 MHz.

Meyl claimed that the ratio of the scalar to transverse resonance frequencies (7.1 MHz/4.6 MHz), which is 1.54, is the ratio of the respective velocities. That is, for the conditions of the demonstration, the average velocity of the scalar waves was 1.54 times the velocity of the transverse waves, or 1.54 times the (commonly understood) "speed of light."

3.4.4 The Polarization Synchrotron

3.4.4.1 Introduction

Apparently, the functioning of a recently described device ***cannot*** be explained by EM theory as presently taught. However, it is suggested that scalar wave concepts may allow this technology to be more readily understood.

3.4.4.2 Background Information

A recently published article titled, "Table-Top Synchrotron Defies Convention," (which has been accepted for publication in *The Journal of Applied Physics*) is quoted in its entirety, as follows (Ref. 34):

> *A group of physicists in the UK and US has built a device which they claim generates radiation that circumvents the inverse square law. John Singleton of the Los Alamos National Laboratory in New Mexico and colleagues say that their table-top machine works by rotating a pattern of polarization at faster than the speed of light, and that it could be used as a new type of low-power or long-range radio transmitter. But other researchers believe that they have got their physics wrong.*
>
> *The device, dubbed a polarization synchrotron by its inventors, consists of a 2 metre-long gently curving arc of alumina (a dielectric material), with a series of electrodes fitted at regular intervals along its length. Applying a sinusoidal voltage across each electrode and displacing the phase of the voltage very slightly from one electrode to the next generates a sinusoidally-varying polarization pattern that propagates along the device. By carefully adjusting the frequency of the voltage and the phase displacement the researchers say they can make the wave travel at greater than the speed of light (even though no physical quantity of charge travels superluminally).*
>
> *This principle is based on a model of pulsars—rapidly spinning neutron stars—developed by one of the group, Houshang Ardavan of Cambridge University. Ardavan believes that the well-defined pulses of radio waves emitted by these astronomical objects are caused by the pulsar's rotating magnetic field polarizing the surrounding plasma. As the magnetic field sweeps round so too does the region of polarized plasma, and far enough away from the pulsar this region will sweep round at faster than the speed of light.*

Singleton's group—which includes Ardavan's son, Arzhang Ardavan (of Oxford University)—believes that its polarization synchrotron, like a pulsar, emits radiation in a well-defined beam. They argue that the electromagnetic wavefronts generated by each point within the polarization pattern build up behind that point like sound waves from a supersonic aircraft. Interference between these wavefronts then reinforces the radiation along a spiral trajectory—the beam—that travels away from the source.

The researchers claim that the intensity of this beam is proportional to 1/r, where r is the distance from the transmitter, rather than the $1/r^2$ associated with spherically decaying radiation. They carried out tests on their device at the Turweston Aerodrome in Northamptonshire between May 2003 and February 2004, measuring the intensity of the emitted radiation at a range of distances up to 900 metres and mapping the three-dimensional shape of the emission.

According to Singleton, the polarization synchrotron could transmit radio messages with very little power or over vast distances. A scaled-down version of the device could be used in mobile phones to allow direct communication with satellites, rather than having to rely on relay stations. He says the device could also be used in radar systems, since the beam's unusual shape would make it difficult to trace the beam back to its source.

However, other researchers are skeptical. John Hannay, a theoretical physicist at Bristol University points out that conventional radio sources can generate slowly decaying radiation over limited distances. He has previously said that Singleton and co-workers must test their device over tens of kilometres rather than hundreds of metres.

3.4.4.3 Unusual or Anomalous Features of the Polarization Synchrotron

The unusual or anomalous features of the polarization synchrotron, as described in the above article, are listed as follows:

- the beam intensity is proportional to 1/r, (not $1/r^2$, as for more conventionally known forms of radiation), where r is the distance from the transmitter;
- the beam is generated by a "polarization pattern," and one may suggest that this is describing a "wave of potential";
- the wave can be made to travel at greater than the speed of light; and
- there is a capability to transmit messages with very little power or over vast distances.

3.4.4.4 Possible Explanation of the Unusual or Anomalous Features of the Polarization Synchrotron by Means of a Scalar Wave Approach

The unusual or anomalous features of the polarization synchrotron are not readily explainable by conventional EM theory as presently taught; therefore, the claims were perceived by some as controversial. However, each of the unusual features matches exactly (at a qualitative level) with the respective described properties of scalar waves, as described in this report, namely:

- beam intensity varying as 1/r;
- beam as a "wave of potential";
- wave velocity greater than the speed of light; and
- capability to transmit messages with very little power or over vast distances.

Therefore, because the unusual features of the polarization synchrotron qualitatively match the properties of a scalar wave generator, it is possible to suggest that the operation of this device is based upon scalar wave principles and not conventional EM technology.

3.4.4.5 Astronomical Implications of the Polarization Synchrotron

It is stated in the article quoted above that the operating principle of the polarization synchrotron is based on a model of pulsars.

If the suggestion in the preceding section is correct, namely that the operation of this technology is based upon scalar wave principles, it is possible to further suggest that pulsars emit scalar waves (in addition to conventional transverse waves).

4. Breakthrough Energetics—Zero Point Energy

4.1 Introduction and Overview

MSE published information on ZPE that included the following quotation (Ref. 1, p. 79):

> *According to the principles of quantum mechanics, the seemingly empty vacuum between atoms, when considered at small enough dimensions (orders of magnitude smaller than atoms), contains an exceedingly high energy density (as large as 10^{94} ergs/cm^3). This energy is referred to as zero-point energy because it is believed to exist even at a temperature of absolute zero. This energy can be thought of as electromagnetic radiation of all frequencies or even as fluctuations of spacetime itself. Because of the totally random characteristic of this energy, it paradoxically appears to cancel itself out or not exist. Most physicists believe that the randomness of this energy does not allow any of it to be tapped for any practical use (one exception is a recent acknowledgment by developers of nanoscale microelectromechanical systems that the zero-point energy (which has been conclusively proven to exert the measurable Casimir Force when micromechanical parts are within 1 micron or less of each other) can prevent such devices from functioning, unless means are introduced to overcome this phenomenon).*

The existence of this type of energy is not immediately obvious, and it is difficult to detect because it is incoherent. The energy is everywhere–its detection requires measuring an energy ***difference***, and the extremely high frequencies of this energy do not readily interact with matter (Ref. 1, p. 79).

4.2 Accessing or "Tapping" Energy from Zero Point Energy

4.2.1 Specific Disclaimer Regarding ZPE Plausibility

For more than 100 years, a number of people have claimed to have invented energy conversion technologies that would deliver an output energy greater than the input energy. Of course, it is not considered controversial that the common "heat pump" does this routinely; one unit of electrical energy is used to transfer approximately three units of heat into a selected location (i.e., within a building). The heat (of course) is simply being transferred either from the air or the ground.

However, when it appears that one unit of electrical energy has been put into a device that delivers more than one unit of electrical output, many scientists and engineers consider this to be an example of measurement error, fraud, or an accomplishment that goes against the accepted Laws of Thermodynamics.

It should be noted that the science of thermodynamics originated nearly 200 years ago in an attempt to compare quantities of heat with an equivalent quantity of mechanical work. As (classical) thermodynamics is generally taught today, a (conceptual) "boundary" is drawn around a system being investigated, and (by ***definition***), if the boundary is drawn large enough, the energy within the system is ***conserved*** (i.e., ***constant***). However, if nuclear reactions are involved, then the term "mass-energy" (based upon Dr. Albert Einstein's equation $E = mc^2$) must be used rather than "energy."[2] Dr. Ilya Prigogine won the Nobel Prize in Chemistry in 1977 for describing an "open" form of thermodynamics that predicts nonclassical behavior when a source of energy is available to continue flowing through a system (Ref. 35). According to Prigogine's theory, outputs and inputs do not need to be equal.

One can put forth the hypothesis that ZPE is potentially such an energy source that can possibly explain the "excess output" inventors have claimed to observe. The calculated spatial density of ZPE is incomprehensibly large (as described in Section 4.1). If these calculated values are correct and a ***very small fraction*** of ZPE could be obtained in a system output, then this output could readily exceed the conventional types of energy entering the system. The working hypothesis in this report is that (excluding claims associated with poor measurements and intentional fraud) ZPE has been demonstrated a number of times, and that an examination of what is common or similar between claimed technologies could lead to a theoretical understanding of the science involved. Once the underlying scientific theory is understood, it may be possible to derive a short-list of "principles" that could be used to develop ZPE technology.

4.2.2 ZPE Credibility Breakthrough

The concept of accessing a significant amount of useful energy from the ZPE gained much credibility when a major article on this topic was recently published in *Aviation Week & Space Technology*, a leading aerospace industry magazine (Ref. 36).

4.2.3 ZPE Access Principles Stated by Moray King

According to Mr. Moray King, who has been studying and lecturing on ZPE for more than 30 years and has published two books on this topic, there are a few basic principles that do allow ZPE to be tapped, and these principles have been incorporated in technology that inventors have ***claimed*** achieved this result (Refs. 37 and 38).

One of the principles that Mr. King claims may allow ZPE to be tapped is that of the nonequilibrium thermodynamics advanced by Ilya Prigogine who won the Nobel Prize in Chemistry for this work in 1977. Mr. King explains Prigogine's work and its importance in the following (Ref. 1, pp. 79-80):

- The standard scientific belief is that the Second Law of Thermodynamics must cause systems to become more random and disordered; however, nonlinear systems (e.g., ionized plasma) are not restricted to this "law."

[2] Mr. Gloyd Simmons, Staff Engineer, U.S. Air Force Programs Manager, MSE Technology Applications, Inc., April 1, 2003.

- The addition of energy to a plasma can sometimes form a metastable vortex ring called a plasmoid. According to Mr. King, "such a structure cannot be predicted by a linear thermodynamic model, but it can be predicted by a nonlinear magnetohydrodynamic model. The nonlinear interactions produce macroscopic coherence from random turbulence."
- The persistence of "ball lightning," which has been modeled as a vortex ring plasmoid, is cited by Mr. King as evidence that such structures are cohering some ZPE (which maintains the stability of the structure) and then radiating excess energy as light and heat.

Mr. King has stated that many inventors who have claimed to build devices that produce "anomalous" excess energy have been doing the following:[3]

1. *Use ions in a plasma to 'tap' ZPE, because the electric field lines are highly concentrated where they enter the nucleus of an atom.*
2. *Induce a shock-wave into the plasma to cause a sudden motion of ions.*
3. *Tap ZPE via what could be called a 'rebound effect'.*

Mr. King has shown many connections between advanced physics concepts and ZPE claims; however, his views (like that of other ZPE researchers) should be considered as a "work in progress."

4.2.4 Dr. Thomas Valone's Overview of ZPE Approaches

4.2.4.1 Introduction

Dr. Thomas Valone has been researching and teaching advanced energy concepts (mostly related to tapping ZPE) since 1980. Valone founded the Integrity Research Institute (IRI) in Washington, DC in order to provide a focus for his publishing, research, and teaching activities.

Dr. Valone has released a sample chapter of his forthcoming book, which included the following excerpts (Ref. 39):

> *With the discovery of ZPE, scientists find that space is rich with activity from* ***virtual particles*** *and full of energy. Therefore, physicists like to call it the "physical vacuum" when they want to talk about ZPE. Furthermore, the vacuum also vibrates and "fluctuates." In fact, that is the essence of ZPE. Vacuum fluctuations are even predicted by a branch of physics, started by Albert Einstein, Neils Bohr, and Werner Heisenberg, called quantum mechanics.*

[3] Moray B. King, "Advanced Work of Dr. T. Henry Moray," Presentation at the Institute of New Energy Symposium, September 2003.

Even the energy density of the limited zero point field is amazing. It is much more than we humans normally can comprehend. For example, if we presume that the minimum possible wavelength is limited to the size of the proton, the famous Nobel Prize winning physicist, Richard Feynman, calculated that the energy density of ZPE would be ten raised to the 108^{th} power joules per cubic centimeter (10^{108} J/cc).

Quantum electrodynamics (QED) predicts that the vacuum spawns particles that spontaneously pop in and out of existence. Their time of existence is strictly limited by the ***uncertainty principle*** *but they create some havoc while they bounce around during their brief lifespan, from virtual existence to real existence and back. The churning 'quantum foam,' as it is popularly called, is believed to extend throughout the universe even filling the empty space within the atoms in human bodies.*

4.2.4.2 Dr. Valone's Concepts for Accessing ZPE

The following ZPE access concepts are described in two of Dr. Valone's books published on this topic (Refs. 39 and 40).

Nonconservation

Zero point energy consists of random EM waves of all possible frequencies or can be considered to be random fluctuations of the vacuum itself. Researchers believe that ZPE is ***not*** conserved. If correct, so-called "conservation laws" do ***not*** apply to ZPE. Experiments have been performed that readily show that small amounts of ZPE are being tapped, and these experiments have been replicated. Other researchers are developing concepts to access appreciably larger power levels (e.g., kilowatts) of ZPE, and key ideas of some of these were presented by Valone.

The Lamoreaux Experiment

In 1997, Dr. Lamoreaux accurately measured the force (caused by ZPE) between two conducting objects separated by a short distance (on the order of microns) (Ref. 41). The force (known as the Casimir Force because it was predicted by the physicist Casimir approximately 50 years earlier) occurs because random ZPE EM waves larger than the distance between the conducting objects are essentially "shorted out" and cannot exist within that small space. Therefore, the ZPE in the vacuum ***outside*** the two close objects, which has a very slightly greater energy density, will have an effective pressure ***slightly*** higher than between the objects and produce an attractive force between these objects. The force Lamoreaux measured agreed with the theoretically predicted value within 5%.

Laboratory ZPE Measurement

Valone described a recent technical report that claimed to detect ZPE in a laboratory experiment. The spectral density of energy across a superconducting "Josephson Junction" was stated to match the spectral density predicted by Planck's second radiation law, thereby measuring the effect of ZPE (Ref. 42).

Solid-State Diode ZPE Converter

Finally, Valone referred to the pioneering concepts for producing electric power by rectifying thermal noise (derivable from ZPE), which were developed by Joseph Yater (Ref. 43). Yater "theorized that a Schottky diode, formed between a semiconductor and a metal, with nonlinear rectifying characteristics and fast switching speeds, could be the diode of choice for rectifying thermal noise." Yater states in the above-referenced patent that "for the long range design goals, submicron circuit sizes are required if all the high power goals of megawatts per square meter are to be achieved."

4.3 Zero Point Energy Principles in the Similar Technologies of Nikola Tesla and E.V. Gray

4.3.1 Dr. Peter Lindemann

Dr. Peter Lindemann has been researching, writing about, and lecturing on advanced electric and ZPE principles for approximately 25 years. Lindemann was the first to recognize that the technology ***principles*** used to achieve what Dr. Nikola Tesla ***claimed*** in the 1890s were the same as those used by E.V. Gray to achieve the accomplishments Gray ***claimed*** in the 1970s and 1980s. However, the hardware used by the respective inventors was different, as will be described in subsequent sections (Ref. 23).

4.3.2 ZPE Principles Suggested in E.V. Gray's Technology

E.V. Gray, Sr. announced an electric engine using capacitor discharges and electromagnets in 1973 (Ref. 23). Gray claimed the engine running on batteries could produce 100 horsepower (hp) and recharge the batteries. Gray claimed that this was possible because he had discovered a new "cold" form of electricity, and he received a patent for this technology in 1975 titled, *Pulsed Capacitor Discharge Electric Engine* (Ref. 44). In 1978, it was evident to advanced energy researcher Dr. Peter Lindemann that though the patent protected the design of the motor, it did not reveal the ***technique*** of its operation.

In 1999, Dr. Lindemann learned that Gray had received two other patents for his capacitor discharge technology in the late 1980s (Refs. 45 and 46). Dr. Lindemann contends that these two patents describe the core secret of what Gray had discovered, essentially the same technology (but accomplished in a different manner) that Dr. Nikola Tesla had discovered in 1890. Even though the wording of these patents described energy derived from electric impulses and suggested that the circuit diagram shown could generate far more output energy than the energy put into it, the operating principles were not explained.

4.3.3 The Energy Science of Dr. Nikola Tesla

Dr. Lindemann claims that information from Chapter 1 of a book recently written by Gerry Vassilatos enabled him to understand the similarities between the discoveries of E.V. Gray and those of Tesla (Ref. 47). This section presents the important points of what Lindemann wrote, which in turn was based on the studies of Vassilatos.

In 1889, Dr. Nikola Tesla began a series of experiments in an attempt to produce EM waves, which were theoretically predicted years earlier by Dr. James Clerk Maxwell. Tesla used what he called "disruptive discharges" obtained by charging a powerful capacitor bank, then discharging through copper bus bars, thereby explosively vaporizing the copper.

Tesla noted that these explosive discharges produced shock waves that could be felt as stinging sensations in his body. He further realized that these effects were similar to shock wave or "surge" effects that occurred during an extremely brief time interval when technicians would close an electrical circuit energized by a ***dc*** dynamo. Dynamos rated at a few thousand volts produced electrical impulses (or shock waves) as high as ***millions*** of volts for the brief interval when they were switched into load circuits.

Tesla learned how to intensify this effect by keeping the electrical surge ***unidirectional (i.e., preventing any back-oscillations)***. He also found that something like "rays" emanating from the discharges could easily penetrate insulators like glass or metals (like copper). Then Tesla searched the scientific literature and learned that such phenomena had only been previously described on two occasions.

By experimentation, Tesla learned that the parameters related to this phenomenon that produced penetrating rays from electrical discharges were:

- abruptness—the instantaneous switch closure was important;
- impulse time—which had to be brief;
- a single direction of current—there could be no reversal or "backflow"; and
- a considerable enhancement was achieved by placing an electrical capacitor between the disrupter and the dynamo.

Tesla initially used motor-driven, high-speed rotating contact switches to produce his unidirectional impulses. Later he used an automatic magnetic quench method (that he invented) to continually (i.e., repetitively) "blow out" (i.e., disrupt or terminate) an electric arc almost immediately after it would reestablish itself.

Tesla realized he had discovered a previously unknown electrical phenomenon: "radiant electricity," and furthermore, that this transmitted energy consisted of ***longitudinal waves (not alternating waves)***.

By experimenting, Tesla learned how to either project electrical charge into or withdraw electrical charge from objects that were ***not*** physically in contact with the rest of the apparatus. A modern demonstration of this phenomena, charging a capacitor at a distance, is described in Section 3.3.6. Tesla additionally discovered (and publicly demonstrated) the information given below.

- Peculiar lighting and heating effects could be obtained from radiant electricity by choosing appropriate pulse durations.
- "Radiant shock waves actually auto-intensified when encountering segmented objects," (e.g., the turns of an air-core coil).

- The electrical discharges traversed coils in the manner of gases moving over surfaces rather than behaving according to the "normal" EM laws.
- When the discharge stream was directed at a distant metal plate, electronic charges would be produced in the metal.
- Tesla measured zero current in the secondaries of his coils; however, he did measure a voltage rise along the length of the coil. His system was dynamic, yet it behaved like an electrostatic field, producing voltage without current.
- It was possible to illuminate incandescent lamps connected to the circuit disrupter producing the electrical discharges even when these lamps were electrically shorted out by means of a heavy U-shaped copper bus bar. Tesla showed that there was another type of energy flowing in the circuit that took the path of highest resistance (not lowest resistance) to light the bulbs.
- His high-voltage coils were inadvertently "fractionating" electrons (which could not leave the metal of the coil from "something else") that traveled like a gas ***over the surface of the coil***. Thus, "electrical discharges" were "composed of several simultaneous mobile species."
- ***Abrupt unidirectional impulses*** were the key to releasing this second type of energy inherent in electricity. Merely alternating the current direction would ***not*** be sufficient to do this.

Tesla realized that the nonelectron part of electricity released by abrupt impulses, which was capable of penetrating many forms of matter, would be a key to tapping into immense amounts of energy. One can hypothesize that the controlled release of this nonelectron component of electricity was the means used by Tesla to access practical quantities of ZPE.

Tesla's experiments guided him to understand that the nonelectron energy flow he was researching ***exhibited characteristics of a gas*** (though it was not a gas). Tesla's coils ***(built and operated as he described)*** are best understood from a fluid dynamics (not electrical) perspective.

Tesla experimented with ways in which to transmit power from his coils while at the same time minimizing the electrical arcs projected from them.

The important points of Tesla's research on electrical impulse phenomena (as described by Dr. Lindemann) can be summarized as follows:

1) What we call electricity consists of the flow of charged particles (generally electrons) that have mass and "something else" (an energetic or "neutral component"), which is normally associated with (somehow bound to) the charged particles, and therefore not normally detected.
2) If dc electricity at a sufficiently high voltage undergoes an abrupt explosion-like event such as a discharge (spark), the charged and neutral components of electricity are momentarily separated.
3) The separation process must be completed by forcing the electrons "out of the way" (such as by using a magnetic arc quench technique like the one invented and used by Tesla).

4) A radiant form of energy (termed by Tesla as "Radiant Energy") then proceeds on a straight line trajectory (at superluminal velocity, according to Tesla) and penetrates many (but not all) forms of matter.
5) Radiant Energy then releases electrons (i.e., reconstitutes "normal" electricity when it impacts a metallic conductor).
6) Tesla stated that this overall process was ***magnifying energy***; he assigned the name "magnifying transmitter" to the system that he designed, built, and tested and that he ***claimed*** accomplished this goal (Ref. 23).
7) It should be noted that according to classical "closed-system thermodynamic theory," energy in a system can never be "magnified." However, it should also be noted that with an "open thermodynamic system" with sufficient energy available from the ZPE field, which according to accepted principles of physics exists everywhere in the universe, it would be ***possible*** to have a measured energy output greater than the measured energy input, ***provided that*** the unidirectional electric impulse and longitudinal electric wave phenomena used by Tesla was converting merely an ***extremely small*** fraction of (unobservable) ZPE to observable energy.
8) One hypothesis is that Tesla experimentally discovered a way to separate a neutral "mass-free" component from the charged "mass-bound" component of electricity, thereby allowing this mass-free component to magnify or grow as it traversed space (which contains the incomprehensibly large amount of ZPE) then (when intercepting a metallic conductor) forming a greater amount of electric energy than was used to initiate the process. This statement will be explained in increasing detail in subsequent sections.

4.3.4 Dr. Lindemann's Definition of "The Electro-Radiant Event"

Dr. Lindemann refers to the process discovered, developed, and used by Tesla in his magnifying transmitter as "The Electro-Radiant Event," and he summarizes its characteristics as follows (in Dr. Lindemann's words) (Ref. 23, p. 44):

> *The Electro-Radiant Event is produced when a high-voltage, direct current is discharged across a spark-gap and interrupted abruptly before any reversals of current can occur.*
>
> *This effect is greatly increased when the source of direct current is a charged capacitor.*
>
> *The Electro-Radiant Event leaves wires and other circuit components perpendicular to the flow of current.*
>
> *The Electro-Radiant Event produces a spatially distributed voltage that can be thousands of times higher than the initial spark discharge voltage.*
>
> *It propagates instantaneously as a longitudinal, electrostatic "light-like ray" that behaves similarly to an incompressible gas under pressure.*

Electro-Radiant effects are solely characterized by impulse duration and voltage drop in the spark-gap.

Electro-Radiant effects penetrate all materials and create "electronic responses" in metals like copper and silver. In this case, "electronic responses" means that an electrical charge will build up on copper surfaces exposed to Electro-Radiant emissions.

Electro-Radiant impulses shorter than 100 microseconds are completely safe to handle and will not cause shock or harm.

Electro-Radiant impulses shorter than 100 nanoseconds are cold and easily cause lighting effects in vacuum globes.

Dr. Lindemann claims the Electro-Radiant Event is the "gain mechanism" that Tesla discovered and then used in his magnifying transmitter. According to Dr. Lindemann, "it is the foundation of his claim that he was able to create more energy in his output than it took to initiate it in his input" (Ref. 23, p. 43).

4.3.5 Comparing E.V. Gray's Technology with that of Tesla

Dr. Lindemann states that the energy magnification results E.V. Gray demonstrated and claimed to achieve in the 1970s were based upon the same principles used by Tesla (making similar claims) in the 1890s. However, each inventor used a somewhat different approach. Fundamentally important principles can be learned by examining what is ***common*** to both approaches.

Dr. Lindemann lists the important common features between the technology of Tesla and Gray as follows (Figure 10) (Ref. 23, pp. 47-53):

- They both start with a source of high-voltage direct current.
  - Tesla used a high-voltage dc generator (dynamo); and
  - Gray used the sequence of a battery, multivibrator, transformer, and rectifier to obtain high-voltage direct current.
- Both inventors used their respective high-voltage direct current sources to charge a capacitor repeatedly.
- In both circuits, the next component is a spark-gap.
- The spark in the gap must be ***unidirectional***.
  - Tesla's circuit had the continuous voltage from the dynamo to ensure the unidirectional discharge of his capacitor; and
  - Gray used an electronic vacuum tube to ensure there would be no current reversal.

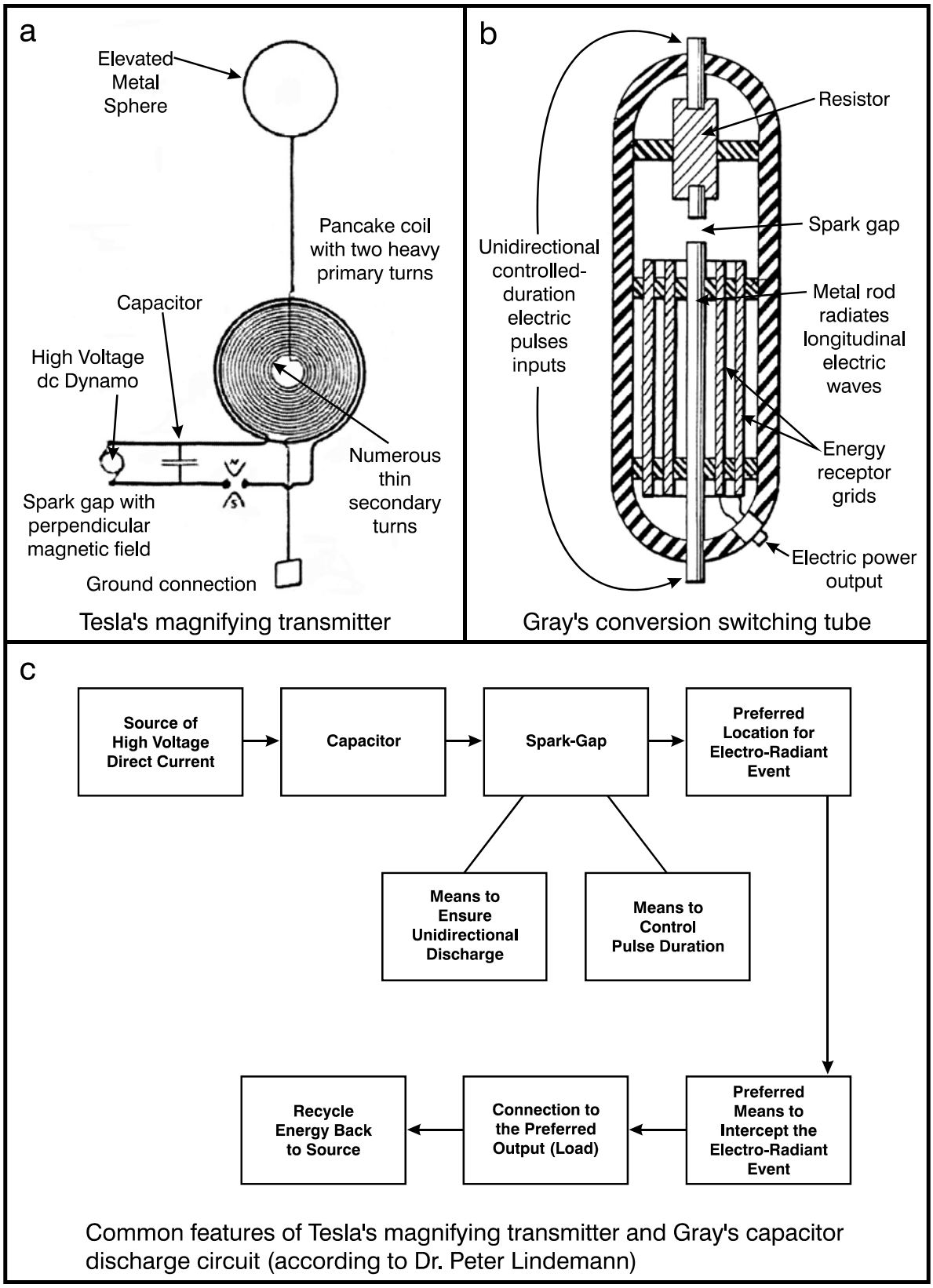

Figure 10 (a-c). Technologies of Tesla and Gray and common features of both.

- The spark duration must be controlled.

  – Tesla used a magnetic field to quench the arc in his spark-gap. He could determine the time before quench by adjusting the magnetic field strength (and capacitance of his capacitor); and
  – Gray used a resistor to limit discharge current, and the discharge duration was controlled by means of the same electronic vacuum tube referred to above.

- The respective circuits then have what Dr. Lindemann calls the "preferred location for the Electro-Radiant Event."

  – Tesla used two turns of very heavy (thick) copper wire as the "primary" of his magnifying transmitter. (It is to be understood this transformer (a small working model is described in Section 3.3.6) is not a normal transformer primary based upon conventional EM induction); and
  – Gray used what he called a "conversion switching element tube." As described in his patent, this device is essentially a metal can "specifically designed to have an explosive, electrostatic event radiate away from its central chamber."

- The next element common to the two technologies being compared in Dr. Lindemann's analysis is the "preferred means to intercept the Electro-Radiant Event."

  – Tesla used the "secondary" coil located within the outer thick primary turns as in his magnifying transmitter; and
  – Gray used charge-receiving grids within his "conversion switching element tube."

Dr. Lindemann points out that there is no direct connection in either technology between the source of energy and the "receiver element."

- Next in the sequence is what Dr. Lindemann calls the "connection to the preferred output."

  – Tesla used a ground connection at one end and an elevated metal sphere connected to the other end of his magnifying transmitter secondary. His intention was to transmit electrical power to the world; Tesla did demonstrate the transmission of 10 kW of electric power (which lit a bank of 200 lamps) with no wires at a distance of 26 miles during his experiments conducted in Colorado Springs, Colorado, in 1899 (Ref. 30, p. 123); and
  – Gray connected his charge-receiving grids to an inductive load (i.e., an output circuit that performed useful work and also served to recharge the batteries).

(It should be noted that Tesla's long-distance transmission of 10 kW was efficiently accomplished by using resonance principles rather than by a high-power EM energy "beam" such as engineers would consider using at this time.)

Dr. Lindemann explains (and Gray's patent drawings indicate) that Gray's conversion switching element tube contained concentric metal cylinders surrounding one of the two high-voltage electrodes that formed a spark-gap in the interior of the device. Dr. Lindemann refers to Gray's conversion switching element tube as an "electro-radiant transceiver" because it both broadcasts and receives the "Electro-Radiant Event."

Based upon statements made by Gray in the 1970s, as well as photographs of his technology also from that time, Dr Lindemann presents more technical details of Gray's work (Ref. 23, pp. 55-59).

- Three conversion switching element tubes were used with each being approximately 3 in. in diameter, and (according to patent drawings) the length of each is several times the diameter.
- Each conversion switching element tube was fed by discharges from a single large capacitor. The labels on the capacitors stated their rating was a capacitance of 2 μF and a voltage rating of 4,000 V dc. (Dr. Lindemann states that Gray had claimed in newspaper articles from the 1970s that the electric discharges in his system were from a potential of 3,000 V.)
- The output pulses from the switching tubes were fed into the primary turns of an air-core transformer (wound on a 4-in-diameter polyvinyl chloride pipe), and electrical power from the secondary turns was then available to be used. An air-core (not iron-core) transformer was used because of the high operating frequency.
- Pulse durations used by Gray were in the 10- to 50-microsecond range. This is ***postulated*** by Dr. Lindemann; however, he bases this upon statements made by both Tesla and Gray concerning their respective technologies.
- The charge-receiving grids in Gray's conversion tubes are copper. (As previously stated, Tesla had learned in his experiments that when "radiant electricity" is intercepted by a metallic conductor, "normal" electricity is produced.)

Dr. Lindemann summarizes Gray's cold electricity circuit as follows:

> *It starts with power out of the battery; he raises it to 3,000 volts DC that he stores in a very large capacitor. He then discharges impulses through a spark-gap, clipped by a vacuum tube, such that the impulse duration is less than 50 microseconds. This staccato of impulses flows through the Electro-Radiant Transceiver, which creates a series of radiant, electrostatic fields of spatially-distributed voltage that is picked up by the charge-receiving grids. As soon as the Electro-Radiant Event ceases, these charged grids discharge to ground through the primary of the "inductive load." The output recovery system is inductively coupled to this discharge primary with a voltage step-down to run light bulbs and other medium voltage appliances, as well as another step-down transformer to recharge the secondary battery. By switching the batteries back and forth periodically, Gray could keep the system going indefinitely, and still produce a sizable output* (Ref. 23, p. 59).

4.3.6 Summary of Principles for Accessing ZPE

It is possible to summarize the respective principles used by Dr. Nikola Tesla and Edwin V. Gray to release what each inventor ***claimed*** was an output energy greater than the input energy, as follows:

1) Generate a relatively high voltage by an applicable method.
2) Discharge the voltage across a spark-gap.
3) Control the duration and ***direction*** of the discharge.
4) Capture (with a metallic receiver that is not directly connected to the spark-gap) a (postulated) "mass-free" component of electricity that is radiated from the discharge.
5) Feed a sufficient fraction of the captured energy back to continue Step 1.

One can hypothesize that the "mass-free" "radiant electricity" ***momentarily*** coheres and collects a very small amount of the ZPE field as it traverses the space between the discharge and the metallic receiver and that the collected energy is significantly larger than the energy dissipated in the initial spark discharge.

4.4 Additional Inventions and Discoveries Claiming "Excess" Energy

4.4.1 Introduction

The objective of this ZPE information is to present ideas, based upon what experimenters and inventors have ***claimed***, so that new ZPE-related technology might potentially be developed. It is suggested that comparing related information from similar sources allows general principles to be better understood, and that approach has been used. If it does become possible to use ZPE for practical applications, numerous breakthroughs will occur in many other areas of technology, including emissionless aircraft.

4.4.2 Disclaimer

It is to be understood that this information is exploratory, a "work in progress," and intended to present what ***may be technologically possible*** provided that claims that have been put forth by inventors and researchers can be validated.

4.4.3 The Papp Engine

Disclaimer: It is recognized that the claims for and description of the Papp engine are (to a great degree) not readily explainable by a conventional understanding of chemistry and physics. The information on this unusual engine is included because it represents another example of a form of advanced energy technology in which it is ***claimed*** an electric discharge (by a presently unknown process) results in a significantly larger release of energy compared to the energy that provided that discharge. It is recognized that claims such as these should be independently replicated.

Mr. Josef Papp obtained a U.S. Patent for an unusual engine he invented in the 1970s (Refs. 48 and 49). The ***claims*** made for this device were extraordinary. The external dimensions, weight, and power output were comparable with that of a four-cylinder, internal-combustion, reciprocating engine similar to that currently used for automotive applications. However, the internal structure and functioning of the engine were quite different, as indicated in the following patent descriptions and claims.

- There was no introduction of either fuel or air, no combustion, and no emission of reaction products.
- Each of the four cylinders was hermetically sealed with a metallic bellows seal to allow for piston reciprocation. There were no engine valves.
- Power was delivered (via crankshaft rotation) at angular velocities of hundreds of revolutions per minute.
- The gases sealed within each cylinder were stated to be a mixture of the "inert gases" (i.e., these would include helium, neon, argon, krypton, and xenon).
- When operating and producing power, the engine became warm but not hot.
- For the purpose of this report, the point of potential importance is that power production in each respective cylinder was initiated by a high-voltage electric discharge that then briefly converted the inert gas mixture in that cylinder into expanding plasma (which pushed the piston in that cylinder, providing useful power).
- Papp stated that his engine could provide power continuously for "thousands" of hours.
- Papp's patent states (with obscure wording) that ***the excess power generated by the plasma was significantly greater than the initiating electric discharge*** because he was using a proprietary method of treating the inert gas mixture with radioactive elements.

However, another possible explanation could be (as explained in Section 4.3.6) that Papp's engine was using the high-voltage electric discharge to transmit longitudinal waves (radiant electricity) into the inert gas mixture, and a small amount of the ZPE (from the "vacuum" between the gas atoms) was cohered and added to the plasma energy in the initial electric discharge.

4.4.4 The Graneaus' Water Arc Explosion Experiments

Disclaimer: Dr. Peter Graneau and his son Dr. Neal Graneau were also using electric discharges in their experiments and ***claiming*** to achieve "excess" energy output. Similar to that of other researchers whose work is presented in this report, the Graneau work should be independently replicated.

A typical "Graneau" experiment (originally conducted at the Massachusetts Institute of Technology) would release an abrupt electric discharge (from an 8-μF capacitor bank charged to 75 kV) through a column of water in a heavy wall steel "cannon" (1.2-cm bore diameter and 10-cm height) then use high-speed photography to investigate the resulting blast of ejected water.

The Graneaus claimed that the (1-km/s) water blast from this cold electric explosion punches a 1.2-cm-diameter hole through a 0.6-cm-thick aluminum plate (placed near the cannon opening).

What is more interesting (from an energy comparison perspective) is that the Graneaus claim that the kinetic energy of the expelled water is significantly greater than the electric energy released from the capacitor bank. Depending on experimental conditions, Peter Graneau claimed that the ratio of output kinetic energy to input electric energy was in the range between approximately 3 and 20 (Ref. 50). High-speed photographs reveal that the water is emitted as a cold ***fog*** (not liquid or steam). The Graneaus claim that there is a (presently unknown) intermolecular bond energy released when bulk water is converted into small fog droplets, which provides the "unexplained" energy. (This claim is ***not*** supported by other physical chemistry evidence).

However, one could hypothesize that these water arc explosion experiments could be (unknowingly) replicating "electric discharge excess energy" experiments performed by a number of other researchers including Nikola Tesla, Edwin Gray, and Josef Papp.

4.4.5 Dr. T. Henry Moray's Energy Device

Disclaimer: The extraordinary energy claims made for Dr. T. Henry Moray's energy device should also be independently replicated. Contrary to what Dr. Moray stated, it appears that his technology used radioactive materials in order to function. It is preferable to avoid using any radioactive material in an energy-producing device; however, Dr. Moray's research is included because it illustrates ***principles*** in common with other research described in this report.

Throughout the 1930s and 1940s, advanced energy researcher Dr. T. Henry Moray gave numerous demonstrations of an energy device he invented that he claimed was producing an energy output from a nonconventional source (Ref. 51).

Dr. Moray's device was contained in a wooden box of several cubic feet volume. In a typical demonstration, Dr. Moray would carry the device into rural areas, away from all power lines (from which it might be possible to induce electric energy), and he then showed that his invention could operate a number of conventional electric appliances (whose total power consumption was several kilowatts) for several hours. Dr. Moray showed witnesses that his device contained no "hidden batteries."

The Moray technology was never developed because:

1) Dr. Moray's claim that the device was operating from a previously unknown form of energy arriving from "space" was not scientifically defensible.
2) Dr. Moray never revealed (or perhaps did not know) a plausible explanation of how the device did operate.
3) The functioning of the device was claimed by Dr. Moray to be based upon an amplifying effect in a resonant electronic circuit that contained 29 cold plasma (argon and mercury vapor) tubes connected in series. The U.S. Patent Office arbitrarily stated that an electronic tube had to have a heated filament in order to be functional, and therefore, would not issue Dr. Moray a patent. Without a patent, Dr. Moray never obtained significant investor support.

However, advanced energy researchers (who have investigated Dr. Moray's work) have stated that the "electrotherapeutic tube" for which Dr. Moray was able to receive patent protection was identical (or very similar) to the tube in his energy technology (Ref. 52). The "secret" (as described in that patent) is that these tubes were coated on the inside with uranium compounds, which are of course radioactive. It is ***not*** stated in the patent, but is suggested in this report, that charged particles (alpha particles and beta particles) emitted by the nucleus of uranium atoms could have initiated another form of the so-called "Electro-Radiant Event" (see Section 4.3.4).

It is also suggested that the radiated change in electric potential (i.e. "radiant electricity," as explained in Section 4.3.3, that would accompany the radioactive emission of charged particles) could be cohering a very small fraction of the ZPE and carrying that "excess" energy into the oscillating plasma in Dr. Moray's tubes.

After Dr. Moray briefly initiated the energy transfer in his device (from an external source), each of the 29 stages in the oscillator circuit would cause the energy from the preceding stage to be slightly increased. The output of the last stage would yield enough energy to operate appliances after conversion of this electricity to a suitable voltage and frequency. A small fraction of the final stage output was fed back to the first stage to maintain the system oscillation. It is suggested that the abrupt change in electric potential "radiated" into an ionized plasma by radioactive atoms is a "catalyst" that initiates a release of energy significantly greater than the radioactive energy, which causes the change in potential.

4.4.6 Summary

Dr. Nikoa Tesla, Edwin V. Gray, Josef Papp, Drs. Peter and Neal Graneau, and Dr. T. Henry Moray all ***claimed*** to have energy technology that produced "excess" energy. The devices or experiments of the first four inventors or teams featured high-voltage electric discharges, whereas Dr. Moray used radioactive materials (which emitted high-energy charged particles).

It is suggested that ***either*** an electric discharge ***or*** emission of a charged particle from a radioactive material could cause what Dr. Peter Lindemann refers to as an "Electro-Radiant Event" (as described in Section 4.3.4).

It is further suggested that the radiated electric potential of the "Electro-Radiant Event" could possibly cohere a very small amount of the immense ZPE and thereby produces a measurable "excess" energy in a suitable material (or electronic circuit).

These suggestions are not research per se but are hypotheses presented in an attempt to show that what inventors in the past have claimed is plausible and could ***possibly*** be replicated or extended if ***apparently*** common principles used by different inventors are more widely understood.

Another way to summarize these concepts is to suggest that what could be called "moving electric potential" or "radiant electricity," which is initiated with either an electric discharge or emission of a charged particle from a radioactive material, could cohere or convert a very small fraction of ZPE and carry it into an appropriate energy "receiver" where it is measured as "excess" energy.

5. Other Research Relevant to Advanced Energetics

5.1 Introduction

MSE investigated additional research topics that add relevant background and supporting information to the advanced energy concepts presented in Sections 2, 3, and 4. These topics are listed below.

- The Fourth Law of Motion, which is relevant to a better understanding of higher derivatives of motion, shock waves, reactionless propulsion systems, and possibly accessing ZPE.
- The Scientific Theories of Edwin Yates Webb, Jr., which includes Webb's explanation of the flaw in 19th century experiments that "disproved" the aether, as well as Webb's hypothesis to explain gravitational attraction between masses.
- An update on Condensed Matter Nuclear Science, sometimes referred to as low energy nuclear reactions (LENR), acquired from information presented at an international conference on this topic in 2003.
- High frequency gravitational waves (HFGWs) acquired from information presented at an international conference on this topic in 2003.

5.2 The Fourth Law of Motion

5.2.1 Introduction

This report presents an introduction and overview to a topic with many fundamentally far-reaching implications and applications. The Fourth Law of Motion is so-named because it has been applied to measurable physical phenomena that are not accurately explained by Sir Issac Newton's classical Three Laws of Motion.

The application of the Fourth Law of Motion could potentially lead to a better understanding of many topics, including but not limited to, transient phenomena, shock waves, thermodynamics, some of the approaches used to attempt to access ZPE, and some of the approaches used to attempt to construct a propellantless (i.e., reactionless) propulsion system.

5.2.2 Specific Disclaimer for the Fourth Law of Motion

Of course, scientists and engineers are aware that physical systems (e.g., electrical, hydraulic, mechanical, etc.) may sometimes be subject to transient phenomena and that furthermore, phenomena related to shock waves are a major topic studied in aerospace science. Nevertheless, it may be a new concept to many scientists and engineers that a formal extension to Newton's classic Three Laws of Motion is ***required*** (and has been postulated) in order to adequately mathematically describe and understand transient and shock wave phenomena. The truth or falsity of scientific postulates (hypotheses) such as this one can only be determined by published experimental results that are replicable by other experimenters.

5.2.3 The Origin of the Fourth Law

In 1962, Dr. William O. Davis published an article entitled *The Fourth Law of Motion* for an audience interested in advanced space propulsion (Ref. 53, pp. 83-109). Prior to his writing of the article, Dr. Davis (in addition to obtaining a Ph.D. in physics) had commanded a U.S. Army Air Corps Bombardment Squadron at the close of World War II. Davis had also served at executive levels in corporations and was involved in research that (according to his biography) "covered the fields of cosmic ray neutrons, special weapons development, and the management of government and industrial research programs." His last military assignment was as Assistant to the Director of Laboratories, Wright Air Development Center (now Wright Patterson Air Force Base) from 1957 to 1958.

Dr. Davis also formally presented his research on the Fourth Law of Motion to meetings of professional scientists in the 1960s (Refs. 54 and 55).

Dr. Davis begins his presentation of the Fourth Law by stating the three classical Laws of Motion originally published by Newton (Ref. 53, p. 86):

> *First Law: Every body tends to remain at rest or in uniform motion in a straight line, unless acted upon by an outside force.*
>
> *Second Law: An unbalanced force acting on a body causes the body to accelerate in the direction of the force, and the acceleration is directly proportional to the unbalanced force and inversely proportional to the mass of the body.*
>
> *Third Law: "For every action, there is an equal and opposite reaction."*

Davis states that Einstein postulated Relativity Theory where Newtonian physics apparently could not explain some astronomical phenomena, and Quantum Theory was postulated to explain what was discovered in atomic physics. However, it was widely assumed that Newton's three equations of motion could mathematically explain the mechanics and motions of "everyday" objects and systems.

Davis explains that this assumption is not always true. There are often anomalies involving rate of strain in mechanical materials and systems. For example, the strength of many materials is not time independent but is a function of ***how fast*** a stress (force) is applied. This is generally difficult to explain with Newtonian mechanics.

Specifically, Davis refers to research conducted by the U.S. Air Force (USAF) in the 1950s in which USAF Flight Surgeon Colonel John Paul Stapp rode on a rocket propelled sled in order to study the effect of high forces on the human body. The rocket sled was rapidly accelerated (maximum acceleration was positive 12 Gs) to a velocity of 421 miles per hour within 5 s, then rapidly decelerated to a stop by water brakes (maximum deceleration was negative 22 Gs). However, the measured forces were significantly greater than what would be calculated from a simple application of Newton's Second Law of Motion (i.e., "force equals mass times acceleration," or F = Ma). A mathematical approach more detailed than that of Newtonian physics is required to understand such phenomena, and some of this topic is presented in the next sections.

5.2.4 Nonsimultaneity

As Davis explains it, Newton had no way to measure the "anomalous" forces that occur in high-speed impacts, shock waves, and starting transients. It is implicit in the Newtonian equations of motion that either bodies would be infinitesimal (points), or bodies would be perfectly rigid (meaning that changes in density would be propagated instantaneously). In the "real world," these criteria do not exist.

As an example, Davis suggests that one may consider a force applied to the end of a steel rod (1 m long) in order to accelerate that rod. Assume that compression waves (sound waves) in that steel travel at a velocity of 5,000 m/s. From the instant in time when the force is applied to the end of the rod, a 5,000-m/s compression wave travels to the far end of that rod and then reflects back to where the force was applied. The time interval for the transmission and reflection of the compression wave is 4 ten thousandths (0.0004) of a second.

Quoting Dr. Davis (Ref. 53, p. 91):

> *Until the wave returns, 4/10,000 of a second later, the rod as a whole cannot move according to the Second Law! No matter how much force is applied, the center of gravity of the rod cannot obey F = Ma in less than this time.*

The force applied to the rod and subsequent acceleration of the rod are not ***simultaneous.*** There is a starting transient inherent to the system, or to state it another way, a critical action time separates the application of force and the resulting response. They are ***not*** simultaneous. Davis states that even though it is often ignored by theoreticians, for real world (e.g., mechanical or electrical) systems, the third derivative "surge" (rate of change of acceleration) is often more important than the actual ultimate second derivative "acceleration."

5.2.5 Third Derivative Equations of Motion

To develop equations of motion that use the third derivative, Davis postulates that a system would be subject to a force proportional to surge as well as a force proportional to acceleration. As a result of (unstated) laboratory experiments, Davis says the two forces are additive; therefore, he states the third derivative form of the law of motion force equation should be:

> *F = Ma + a term consisting of "critical action time," times system mass, times the rate of change of* ***acceleration.***

5.2.6 Third Derivative Reactionless Propulsion System

In the following quotation, Davis explains the logical consequence of the functioning of a mechanical system constructed so that the critical action time is not the same in all directions (Ref. 53, p. 99):

If, for example, we build a mechanical oscillator such that the critical action time is short compared to the period of oscillation in one direction, the mass will appear to be approximately Newtonian and the phase angle of reaction will be negligible when the oscillator is moving in that direction. If we now change the system to make the critical action time much longer during the time the oscillator is moving in the opposite direction, the mass will appear to be greater and the phase angle larger, even though the total applied force is exactly the same in the two directions. Thus there will be a net unidirectional acceleration of the driven mass in the direction of the least apparent mass even though the applied force is balanced!

The next sections examine the possibility that this may have been accomplished.

5.2.7 Overview of Patented Reactionless Propulsion Devices

Advanced energy researcher Dr. Thomas Valone has collected a database of (primarily United States) patents of inventions that ***claim*** to be reactionless propulsion devices (Ref. 56). These devices are typically mechanical and describe a means of converting an internal motion into a unidirectional (i.e., reactionless) force that would thereby propel the entire device (and anything fastened to it). Obviously such a device clearly violates Newton's Third Law because the force produced appears to be unbalanced; there is an "action," but no "equal and opposite reaction."

However, if one considers effects allowed by the third derivative of motion, such devices could be possible. Dr. Valone's database of patent cover pages includes 65 devices, and a preliminary analysis indicates that these inventions appear to use some form of the third derivative of motion by incorporating either impact or a change in a (circular) state of motion. For example, one can readily feel or measure the force produced when a functioning gyroscope is tilted. This is a third derivative effect. Therefore, it should be considered ***possible*** that correctly designed systems may be reactionless if they use third derivative effects. However, it would not be scientifically defensible to claim a propulsion device is reactionless unless this can be experimentally validated.

5.2.8 Analogy with Work Produced by Electrical Alternating Current

Davis uses some analogies with electric technology to explain more about the Fourth Law of Motion and third derivative effects. For example, in the 1800s when direct current was being used to run electric motors it was believed that alternating current would not be capable of operating a motor because the average current was zero. The point Davis makes is (Ref. 53, p. 99):

Although the current in one direction is balanced by an equal flow in the opposite direction, the flows are not equal and opposite simultaneously and thus work can be done.

5.2.9 Statement of the Fourth Law of Motion

Davis states that for systems with significant third derivative effects, it is the ***rate of change of energy*** that is critical. He therefore postulates the Fourth Law of Motion as follows (Ref. 53, p. 103):

> *The energy of a given system can only be changed in some finite length of time depending on the system, and never in zero time.*

5.3 The Scientific Theories of Edwin Yates Webb, Jr.

5.3.1 Introduction

Edwin Yates Webb, Jr. was the chief of research and development for the U.S. Signal Corps Intelligence Agency during World War II. In 1949, Webb wrote a book called *Origin of the Universe and the Secret of Light and Magnetism*, which is a statement of his scientific theories (Ref. 31). This report presents some of Webb's theories (considered most relevant for achieving breakthroughs in aerospace applications) and briefly discusses them. It is believed that Webb's ideas will provide helpful insights that may possibly lead to accessing ZPE (Section 4) or achieving advanced (propellantless) propulsion.

5.3.2 Specific Disclaimer for Webb's Theories

It is to be understood that Webb's scientific theories are not the present paradigm of physics as it is taught today. Nevertheless, an open-minded consideration of what Webb wrote can stimulate breakthrough ideas related to energy and propulsion. The truth or falsity of scientific postulates such as these can only be determined by published experimental results that are replicable by other experimenters.

5.3.3 Webb's Electric Field Interpretation of Matter and Energy

Webb's theories began with his attempt to understand both light and radio waves. Webb's view was that neither a particle nor wave theory correctly describe the known properties of light.

Even though he describes it in different terms, Webb postulates a "primordial" electric field permeating all of space, which is seemingly like the so-called "aether," or, as it is currently described, the field of ZPE. According to Webb, all matter and radiant energy are caused by different densities of this universal electric field, which is flexible, compressible, and lossless to any electric disturbance propagated through it (i.e., a perfect electric conductor) with zero resistance but containing inductance due to the magnetic component of light (Ref. 31, p. 11).

5.3.4 Webb's Analysis of the Null Results of Classical Aether Detection Experiments

A key topic in Webb's book is his interpretation of why one of the most famous experiments in physics produced a null result (Ref. 31, pp. 37-51).

Prior to and during the early 1880s, physicists and astronomers believed that light was propagated by a tenuous fluid filling all of space, which they referred to as the "aether."

Since it was known that the average velocity of the Earth in its orbit around the Sun is approximately 18 miles per second (30 km/s or 3×10^4 m/s) and the velocity of light is 3×10^8 m/s), it was believed possible that a sufficiently sensitive optical experiment could use the properties of light itself and produce an observably different result between a time when the optical apparatus (on the Earth) would be "aimed" in a given direction as compared to a fraction of a day (or year) later when the Earth's rotation (or revolution around the Sun) would cause the alignment of the optical apparatus to be different.

In 1887, the physicists Michelson and Morely devised an experimental apparatus in which a single beam of light was projected at a 45-degree angle against a semitransparent mirror (consisting of a thin silver film on glass). The mirror produced two light beams (one transmitted through the mirror and the other reflected from it) that were perpendicular to each other. Each of these beams was reflected from separate opaque mirrors back to its respective source (the semitransparent mirror).

In theory, Michelson and Morely hypothesized that the amount of displacement of optical interference fringes produced when the beams recombined at the source mirror could readily measure the velocity of the apparatus through the aether, which was postulated to be at rest.

Michelson and Morely conducted this experiment for a long time but obtained a null result (i.e., there was no shift in the optical interference fringes); therefore, no motion of the Earth through the aether was observed. Since the Earth is in motion, Michelson and Morely concluded that no aether existed.

Other physicists postulated that there was an aether but that the (massive) experimental apparatus used by Michelson and Morely ***shrank*** (as a result of moving through the aether) by the exact amount required to give a null result.

In 1905, Albert Einstein ***postulated*** that there was no universal reference frame from which the motions of objects could be measured in an ***absolute*** sense (i.e., any motion of any object could only be measured in a ***relative*** sense in reference to another object). This represented the beginning of Einstein's Relativity Theory.

The implication of the null result in the Michelson-Morely experiment and the subsequent belief that only ***relative*** motion could be measured between objects lead to the idea that there was no universal aether. Many variations of the original Michelson-Morely experiment (as described by Webb in his book) were performed over a number of years and all of them resulted in null results, which only strengthened physicists belief that no aether exists.

However, Webb carefully explains that in spite of the attention experimenters paid to taking careful measurements in all of their attempts to detect the aether, they all made a fatal mistake in the ***logical premise*** of these experiments.

Webb points out that all these experimenters believed they were measuring a difference between the condition of the apparatus "in motion" as compared to the apparatus "at rest"; however (according to Webb), their original postulate was wrong. ***There never was a condition of "at rest."*** Therefore, all such experiments could only yield a null result.

Finally, Webb states that if one of the two opaque mirrors used by Michelson and Morely had had a surface that was curved (e.g., spherical) rather than the planar surface they used, they could have observed a reflected light ray "considerably displaced …… measurable even in inches" from the outgoing beam (Ref. 31, pp. 50-51).

As described in the next section, the absence of the aether in 20th century theoretical physics has had profound effects.

5.3.5 Consequences of Removing the Aether from 20th Century Theoretical Physics

The removal of the aether concept greatly impacted 20th century theoretical physics. However, the implications were much greater, as shown below.

- If there were no aether, then the "vacuum" between material particles would be truly empty.
- Thus (and for other reasons also), the earlier view that light was propagating waves was replaced with a "photon" theory.
- Without an aether, there was no apparently possible way that experimental claims for "excess" energy produced from nonconventional sources could be plausible.
- However, in the latter part of the 20th century, the aether (now referred to as ZPE) was gaining reacceptance in theoretical physics. Some ZPE concepts are presented in Section 4.

5.3.6 Webb's Theory of Gravity

(Some information related to gravity is presented in Section 5.5).

Issac Newton was the first person to correctly state that the force of gravity between two masses is proportionate to the product of the two masses and inversely proportionate to the square of the distance between these masses.

It is natural to assume that some property of matter causes the observed force of gravitational attraction. To date, there is no widely accepted explanation of what causes this attractive force. Contemporary physics postulates that "curved space-time" near a mass causes gravitation, but this is ***not*** a description of the physical mechanism involved.

The following is a restatement of Webb's postulated ideas on gravity. The restatement has been done for the purpose of clarification. Currently, this should be considered a qualitative explanation rather than a mathematical theory (Ref. 31, pp. 86-94).

- "Empty" vacuum is (paradoxically) filled with an extremely high density of energy (equivalent to a high density of matter). In recent decades, this energy has been referred to as ZPE. At this time, there is experimental evidence that proves ZPE does in fact exist (Ref. 1, pp. 79-80). The classical name for ZPE had been "aether." This term will be used in the remainder of this section.
- In empty space (away from observable massive objects), there is an extremely high pressure of the aether "fluid" (i.e., the extremely high density of energy or matter referred to above); however, all vector components of the force produced by this pressure are equal and therefore cancel each other out. As a result, there is no net force vector (direction).
- Observable matter (atoms, molecules, and large objects composed of these) is slightly ***less dense*** than the uniform aether of the vacuum.
- Therefore, the surrounding aether (vacuum) will (paradoxically) create a force vector ***pushing*** (not pulling) from the high pressure in the space away from observable massive objects and toward the lower pressure near observable massive objects. That is, a pressure gradient in the aether is established toward "matter."
- The inverse square relationship for the gravitational force as a function of distance between two masses is due to geometry (i.e., at twice the distance from an object, the "intercepted" area would be one-fourth, etc.).

5.3.7 Comments on Webb's Theory of Gravity

The following comments are intended to augment Webb's ideas on the force of gravity and furthermore show the relationship between some advanced energy concepts ("tapping" energy out of the ZPE) and advanced propulsion concepts.

Some inventions that have been ***claimed*** to produce (excess) "nonconventional" energy did so by producing a ***force***. Webb's insights (interpreted together with recent ZPE ***claims***) suggest that it may be possible to directly produce relatively large forces in a device or system simultaneously with the production of excess energy. Such forces could potentially levitate and/or propel aerospace vehicles ***directly*** without expelling mass from the vehicle. Such technology would not be limited to aerospace applications.

It is possible that examples of such technology may include the Papp engine (Section 4.4.3) and the "water arc explosion" experiments performed by Dr. Peter Graneau and Dr. Neal Graneau (Section 4.4.4). It should be noted that both of these technologies had mechanical energy outputs claimed to be significantly larger than the respective electrical energy inputs, and both processes apparently produced force directly, as they were inherently essentially ***cold*** (i.e., produced little or no heat).

5.4 Condensed Matter Nuclear Science

5.4.1 General Background and Introduction

Scientists studying what has come to be known as "cold fusion" meet annually at an international conference to present the most recent research findings. MSE attended the Tenth International Conference on Cold Fusion (ICCF-10), which was held in Cambridge, Massachusetts, in August 2003, and was attended by more than 100 researchers. The 111 research papers (in 34 different categories) given at this conference represent a considerable expansion of the research field opened by Drs. Pons and Fleischmann, as well as Dr. Steven Jones, in March 1989.

Some key organizers and participants of ICCF-10 stated that terms such as "Condensed Matter Nuclear Science," "low energy nuclear reactions," or "chemically assisted nuclear reactions" more accurately describe this new field of research as compared to the old (and often misleading) term "cold fusion." A considerable number of research reports are now readily accessible on this topic (Ref. 57).

5.4.2 Disclaimer for Condensed Matter Nuclear Science

There are common misunderstandings about this topic. What is reported here are ***claims*** made by researchers at an international conference. It is understood that many of these recent research findings do not agree with what is currently taught in universities.

5.4.3 Electrochemically Induced Deuterium Fusion in Palladium

The first-discovered form of solid-state fusion (part of condensed matter nuclear science) was that achieved by electrochemically splitting heavy water in order to cause the deuterium to absorb into pieces of palladium metal (Ref. 1, pp. 44-47). When this experiment is conducted according to procedures that have resulted from the work of many researchers since 1989, it is reproducible.

The evidence that a nuclear process is occurring is that excess energy in the form of heat (greater than what could be produced by any possible chemical reaction in the system) and He^4 (in quantities exceeding any possible contamination) occur. The primary nuclear reaction (shown in Equation 8) is:

$$ {}_1D^2 + {}_1D^2 \rightarrow {}_2He^4 + \text{heat} \qquad (8) $$

Unlike plasma-phase fusion reactions, the very low production of neutrons and gamma rays (for the amount of excess energy produced) is very noteworthy. Even though the heat originates in palladium metal, the process produces warm liquid electrolyte at temperatures significantly less than the normal boiling point of water. Because the fraction of heat that can be converted into electrical or mechanical energy at this relatively low temperature is small, aircraft propulsion using such an aqueous-phase system is probably not practical. (Pressurization, to achieve a "steam" cycle with the associated steam condenser, would be heavy.)

5.4.4 The ICCF-10 Paper by Drs. Dennis G. Letts and Dennis J. Cravens, "Laser Stimulation of Deuterated Palladium: Past and Present"

A notable recently claimed breakthrough in research with the "classical" heavy water electrolytic cells (Section 5.4.3) is that such cells will generate a significant amount of excess heat when the palladium cathodes are illuminated with a relatively small amount of visible light.

Letts and Cravens have tested numerous experimental parameters for influencing the generation of excess heat in these types of electrolytic cells, including changes in temperature, gas pressure, acoustic stimulation, numerous different additives, intentional defects in the palladium cathode, magnetic fields, pulsing the electrolysis current, and most recently, visible (laser) light.

Dr. Letts observed that by shining the beam from an ordinary 1-milliwatt red laser pointer (as commonly used by lecturers) on the cathode of a functioning heavy water electrolytic cell, as much as 1/2 W of excess heat would immediately begin to be released from the cell. The ratio of power released to stimulation power is 500:1. At this time, many other researchers have reproduced the "Letts Effect," as it is known.

Drs. Letts and Cravens have noted that laser light is ***coherent***, which means that the photons in the laser beam are all in phase with each other as well as all having the same frequency and wavelength. Some theoretical physicists are attempting to explain (from a quantum mechanical viewpoint) how such a relatively weak stimulus can intensify the (now well proven) fusion of deuterium nuclei within the palladium lattice.

5.4.5 The ICCF-10 Paper by Dr. Yasuhiro Iwamura, et al., "Low Energy Nuclear Transmutation in Condensed Matter Induced by D_2 Gas Permeation through Pd Complexes: Correlation Between Deuterium Flux and Nuclear Products"

The results of this highly significant transmutation experiment were first mentioned by Dr. Iwamura at ICCF-9 but were presented in much greater detail at ICCF-10.

Iwamura's research team implanted a layer of cesium atoms on the surface of a thin mixture (several hundred angstroms) of palladium and calcium oxide that had been sputtered onto a metallic palladium substrate.

The palladium substrate with the above-described layers was then placed in an experimental apparatus that applied a low pressure of deuterium gas to the (top) cesium layer while pulling a vacuum on the (bottom) metallic palladium substrate layer. Deuterium (or other hydrogen isotopes) can readily diffuse through palladium. Therefore, a small (but significant) flow of deuterium was established between the top and bottom of the above-described layers and substrate. The entire experiment was conducted at the relatively low temperature of only 70 °C, and there was no electric current involved.

After several days of deuterium permeation, Dr. Iwamura claimed that time of flight secondary ion mass spectrometry (TOF-SIMS) and inductively coupled plasma-mass spectrometry (ICP-MS) analyses of the top layers revealed that the cesium was no longer present, but that a "new" element, praseodymium, had appeared. Cesium (atomic number 55 and atomic weight 133) had apparently transmuted to praseodymium (atomic number 59 and atomic weight 141). Therefore, the atomic number had increased by four and the atomic weight had increased by eight.

When Iwamura's team performed a nearly identical experiment, but with strontium on the top layer rather than cesium, the results are claimed to have been even more remarkable. At the completion of this second version of the experiment, they claim that analyses revealed that the strontium was no longer present but instead the "new" element, molybdenum, had appeared. Most significant of all is that (unlike cesium) strontium has not one but several stable isotopes (^{86}Sr, ^{88}Sr). The transmutation reaction (as it did with the previous cesium experiment) added four to the atomic number and eight to the atomic weight. The important point is that the abundance ratio of the resulting ^{94}Mo and ^{96}Mo isotopes is totally different than it is for molybdenum as found in nature. Therefore, any argument that the molybdenum somehow came from a source of contamination is totally refuted.

The fusion of a single deuterium atom with another element would result in an atomic number increase of one and an atomic weight increase of two. Therefore, theorists are attempting to not only explain how nuclear fusion can occur with such an extraordinarily low energy input but how (apparently) ***four*** deuterium atoms simultaneously fuse with another element.

5.4.6 The ICCF-10 Paper by H. Yamada, et al., "Analysis by Time-of-Flight Secondary Ion Mass Spectroscopy for Nuclear Products in Hydrogen Penetration through Palladium"

The Yamada team, from the Electrical and Electronic Engineering Department of Iwate University in Morioka, Japan, reported results of their experiment, which consisted of permeating normal hydrogen through a piece of 12.5-millimeter (mm) x 12.5-mm x 0.1-mm-thick palladium foil. A pressure up to 10 atm was applied to one side of the foil, and hydrogen was evacuated from the system after permeating through the palladium and exiting the "back" side of the foil.

The team used TOF-SIMS to analyze the sample surface both before and after the hydrogen permeation and reported that the hydrogen flow through the palladium resulted in a "considerable increase" in the amount of chromium, iron, copper, manganese, and nickel. The isotope ratio of the newly produced chromium was reported to be different than the natural ratio (as found on Earth).

The significance of these results (which of course need to be replicated) is that they were obtained with ***normal hydrogen*** not deuterium.

5.5 High Frequency Gravitational Waves

5.5.1 Introduction

This report focuses on the state of GW research in general, and specifically on HFGWs, which were the topic of an international conference held near Washington, DC in early 2003, which MSE attended.

Some items pertaining to gravity research were presented in a recent NASA CR (Ref. 1, pp. 82-85). In that reference, it was pointed out that no one has yet been able to measure the velocity of gravity or GWs; however, experimental evidence supports the hypothesis that the force of gravity is transmitted at a velocity significantly faster than the velocity of (transverse) light waves (c). In fact, logical conclusions derived from the stability of the Earth's Solar System and other astronomical observations support the hypothesis that the speed of gravity is ***at least*** $2 \times 10^{10} \times c$.

5.5.2 Disclaimer for HFGWs

No one has ever obtained direct, conclusive proof that they have detected GWs. Nevertheless, for more than 40 years, physicists have been attempting to detect GWs, as such waves are theoretically predicted based upon the mathematical theories of Dr. Albert Einstein and other researchers. If GWs can be generated in a controlled manner, their unique properties could ***possibly*** enable the development of technological breakthroughs related to communications, imaging, and propulsion.

5.5.3 Extreme Weakness of Gravity and GWs

The ratio of forces between gravity and typical electric forces is an extremely small number. If one could place two electrons a given distance apart, the ratio of the calculated force of gravitational attraction between the electrons to the calculated force of electric repulsion (the two like charges repel each other) would be approximately 2.4×10^{-43} (Ref. 58).

Whatever gravity "is," it is known that the strength of this force and therefore the power density of GWs (if they exist) will be an incomprehensibly small value, at least by any technology that will be available in the foreseeable future.

The extremely low power density of GWs (if it ever becomes possible to generate them) provides a very small "signal" that would compete with a "noise" consisting of thermal motion in solids, interference caused by electromagnetic radiation, and interference caused by mechanical vibrations. The successful generation and then detection of HFGWs (if it is possible) will be quite challenging and very expensive.

5.5.4 GWs

No one has yet detected GWs in an Earth-based experiment. Two researchers ***claimed*** that they showed GWs were radiated by the binary pulsar PSR 1913 + 16. It must be noted that their proof was indirect.

For more than a century, by using an ***analogy*** with electric waves being emitted by moving charges, physicists have ***postulated*** that moving (neutral or uncharged) masses will emit GWs. The inverse is also postulated that GWs will cause a mass to vibrate as they pass through that mass.

As some speakers at the recent HFGW conference stated, various researchers have attempted to ***generate*** GWs by rotating multi-hundred pound masses of metal. The large mass of the metal limits rotation speed. Gravity waves emitted from such an apparatus would be (arbitrarily called) ***low*** frequency gravity waves (LFGW).

Since no one has directly detected GWs, it follows that the velocity of such postulated waves has never been determined. Physicists have hypothesized that the velocity of GWs is that of transverse EM radiation, referred to as "c." It is emphasized that this is an ***assumption***.

5.5.5 HFGWs

Gravity waves at frequencies higher than 10^5 Hz are classified as ***high*** frequency. Physicists have speculated that such waves may possibly be generated by vibrations of significantly less massive bodies than have been used for attempts to generate LFGWs. For example, whereas LFGW research would use masses of metal in the multi-hundred pound range rotating several times per second, HFGW research would use very small (perhaps microscopic) masses vibrating at frequencies that may be as high as a gigahertz (10^9 cycles per second) or even higher. This would be a branch of nanotechnology referred to as micro-electromechanical systems (MEMS).

5.5.6 Applications of HFGWs

The force of gravity affects neutral (uncharged) mass. If GWs exist, it is hypothesized that they would likewise interact with matter in a manner not directly related to electric or magnetic forces. The implication of this is that matter is ***almost*** totally transparent to GWs. In principle, communication and imaging are possible for depths deep into (or all the way through) the Earth (or other astronomical bodies). However, this very ultra-transparency means that the reception of a transmitted GW "signal" would be extremely challenging.

If GWs could be focused into a (unidirectional) beam, the reaction force to the momentum propagated in the beam could potentially propel a space vehicle. This concept was described in a recent NASA CR (Ref. 1, p. 83).

5.5.7 Selected HFGW Conference Papers

A paper by H. David Froning, Jr. and Terrence W. Barrett presented mathematical concepts developed by Dr. Barrett that indicate that the generation of GWs by masses is mathematically more complex than the generation of EM radiation by moving charges. Barrett suggests that if a beam of microwave or laser radiation has its plane of polarization continually ***rotated***, it could potentially exhibit (some) of the characteristics of a beam of GWs.

It should be noted that the four equations often referred to as "Maxwell's equations" came from Oliver Heaviside, who simplified Maxwell's original (more complex) equations. In general, one can say that the mathematical development and addition of terms to the ***Heaviside*** equations may result in equations similar to what Maxwell published in 1865. MSE has been analyzing these issues and discussed them with both Dr. Froning and Dr. Barrett at the HFGW Conference. This is important because once it is understood, a number of "electromagnetic anomalies" and possibly GWs will be based on a firm theoretical foundation.

Two of the concepts Froning and Barrett are attempting to develop are:

- The elimination of aerodynamic shock waves (and the resulting "sonic boom") from aerospace vehicles by projecting "specially conditioned" EM waves ahead of the vehicle.
- The attempted generation of "electromagnetic radiation" that can penetrate metal shielding and possibly generate GWs by putting RF energy into a bifilar-wound (toroidal) coil (see Section 3.4.2.1). A bifilar-wound coil has no inductance because it is wound with a pair of wires (connected at one end) and therefore carries current in opposite directions in adjacent wires (such technology was used by Dr. Nikola Tesla more than 100 years ago). The results of the Barrett-Froning experiments are inconclusive at this time.

A paper by Harold E. Puthoff and Michael Ibison presented extensions of their Polarizable Vacuum (PV) theory related to the generation of HFGWs. This theory predicts results that are numerically and directionally different than what would be predicted by general relativity. Therefore, in principle, a discriminatory test between the two competing theories could be possible.

Dr. Puthoff's theory treats empty space (the "vacuum") as a variable dielectric medium. In Einstein's General Relativity Theory, the Sun's gravity bends light (of a distant star) passing near the edge of the Sun. In Puthoff's PV Theory, the Sun's gravity polarizes space near the Sun, increases the refractive index of vacuum (slightly) higher than one, and thereby slightly slows light passing by the edge of the Sun, which causes the light to bend.

Dr. Puthoff further stated that GWs predicted by general relativity would be transverse, whereas GWs predicted by his PV Theory would be longitudinal.

It may be possible that the PV Theory could explain the anomalous claimed behavior of torsion pendulums during eclipses; however, Puthoff said he is still investigating that possibility.

6. Conclusions

The conclusions of prior MSE Emissionless Aircraft/Advanced Energy research published in NASA/CR-2003-212169 remain valid. In the past 2 years, this exploratory research has been continued, and conclusions in each topic area are stated as given below.

Emissionless Aircraft Innovations

- Some issues related to reaction product water expulsion below an environmentally critical altitude were presented. However, other issues remain to be investigated.
- Water expulsion as vapor could potentially significantly augment thrust required for aircraft propulsion.
- It is potentially possible to fabricate planar solid oxide fuel cells (PSOFCs) from materials, which will significantly increase the electric power density of this technology.
- Conceptual emissionless aircraft performance calculations have been performed using actual PSOFC parameters from a company that fabricates these devices.
- An aerodynamic concept known as "circulation control" is capable of significantly extending aircraft range by providing a better match between cruise and takeoff/landing requirements.

Breakthrough Fusion Reactors as Power Sources for Aircraft Propulsion

- A published concept for an aneutronic fusion reactor based upon principles of magnetic confinement has been modified so that it would be suitable as an aircraft propulsion power source.
- It is potentially possible to use the byproduct heat that would be emitted from a magnetic confinement fusion reactor to heat ambient air and thereby provide significant additional thrust for an aircraft propulsion application.
- An investigative study showed it should be possible to remove potentially damaging heat from the inner grid of an aneutronic fusion reactor based upon principles of electrostatic confinement and thereby potentially scale up the power output of such a device so it may be suitable for the propulsion of a large aircraft.
- Performance calculations based upon NASA Langley Research Center (NASA-LaRC) codes and stated assumptions indicate that merely 1 pound of aneutronic fusion fuel (hydrogen and boron) could provide the energy to propel a large transport aircraft, at normal cruise speed, around the Earth nearly three times.

Advanced Electric Concepts

- MSE investigated breakthrough areas of electric and energy technology in order to surpass current fuel and thermodynamic based limitations for aircraft propulsion.
- Dr. Charles Steinmetz's views on the nature of the electric field provide valuable insights for those developing advanced electric concepts at this time.
- Dr. Nikola Tesla's longitudinal electric wave experiments are reproducible and could also be developed into advanced electric technology.
- The topic of "scalar waves" is another means of using longitudinal electric waves and is being applied commercially.

Zero Point Energy (ZPE)

- There is a significant growth in the awareness that ZPE is real and not confined to the presently understood "laws" of thermodynamics and therefore could potentially be accessed for practical applications.
- A number of technologies that claimed to access a nonconventional source of energy (which, if validated, could very well be ZPE) have been compared and found to have common operating principles. These principles were stated.

Advanced Physics Concepts

- Selected advanced physics topics (including higher than normal derivatives of motion, aether theories, condensed matter nuclear science, and high frequency gravity waves) have been investigated to some extent in order to augment the understanding of breakthrough technologies applicable for aircraft propulsion. Major findings of these topics were reported.

7. References

1. Alexander, David S., *Advanced Energetics for Aeronautical Applications*, NASA/CR-2003-212169, February 2003.
2. www.cmse.ed.ac.uk/AdvMat45/SuperEng.pdf.
3. Carrette, L., K.A. Friedrich, and U. Stimming, *Fuel Cells—Fundamentals and Applications*, Fuel Cells 2001, 1, No. 1.
4. DOE/FETC-99/1076, *Fuel Cell Handbook*, 4th Edition, U.S. Department of Energy, pp. 5-4, November 1998.
5. MIL-HDBK-5D, *Metallic Materials and Elements for Aerospace Vehicle Structures*, U.S. Department of Defense, pp. 2-194, June 1983.
6. "Properties and Selection of Metals," *Metals Handbook*, 8th Edition, Vol. 1, American Society for Materials, p. 490 and 519.
7. *Metals Reference Book*, 7th Edition, Butterworths London & Boston, pp. 27-1.
8. www.matweb.com/search/GetProperty.asp.
9. Hartvigsen J., S. Elangovan, and A. Khandkar, *Selection of SOFC Stack Operating Point for Optimal Balance of Efficiency and Power,* 3rd European SOFC Forum, Nantes, France, 1999.
10. Englar, R.J., M.J. Smith, S.M. Kelly, and R.C. Rover, III, *Development of Circulation Control Technology for Application to Advanced Subsonic Transport Aircraft*, AIAA 93-0644, 1993.
11. Englar, R.J., *Circulation Control Pneumatic Aerodynamics: Blown Force and Moment Augmentation and Modification; Past, Present, & Future*, AIAA 2000-2541, 2000.
12. Englar, R.J., *Continued Development and Application of Circulation Control Pneumatic Technology to Advanced Transport Aircraft*, NASA CR-1998-207471, 1998.
13. Cheung, A., et al., "Colliding Beam Fusion Reactor Space Propulsion System," *Space Technology and Applications International Forum—STAIF*, M.S. El-Genk (Ed.), 2004.
14. Incropera, Frank P. and David P. DeWitt, *Introduction to Heat Transfer*, 2nd Ed., John Wiley & Sons, New York, NY, 1990.
15. GECAT Cycle Design and Analysis, NEPP Test Version 4.1, June 1994.
16. National Institute of Standards and Technology (NIST), Standard Reference Database 23.
17. Borderland Science Research Foundation, *Tesla's Transverse & Longitudinal Electric Waves*, Adventures Unlimited, 1988.
18. Farnsworth, Elma G., *Distant Vision*, PemberlyKent Publishers, Inc., p. 294, 1990.
19. http://www.phillips-johnston.com/prod_copper.html.
20. http://www-training.llnl.gov/wbt/hc/PressureInterm/AppendixD.pdf.
21. Steinmetz, Dr. Charles Proteus, *Elementary Lectures on Electric Discharges, Waves, and Impulses, and Other Transients*, 2nd Edition, McGraw-Hill Book Company, Inc., 1914.

22. http://jnaudin.free.fr/html/lmdtem.htm.

23. Lindemann, Peter, *The Free Energy Secrets of Cold Electricity*, Clear Tech, Inc., 2001.

24. Borderland Science Research Foundation, "Tesla's Longitudinal Electricity," *Adventures Unlimited*, 1988.

25. Halliday, David and Robert Resnick, *Fundamentals of Physics*, Revised Printing, John Wiley & Sons, p. 657, 1974.

26. http://www.cheniere.org/references/maxwell.htm.

27. Tesla, Nikola, *Apparatus for Transmission of Electrical Energy*, U.S. Patent No. 649,621, May 15, 1900.

28. Tesla, Nikola, *Apparatus for the Utilization of Radiant Energy*, U.S. Patent No. 685,957, November 5, 1901.

29. Tesla, Nikola, *Method of Utilizing Radiant Energy*, U.S. Patent No. 685,958, November 5, 1901.

30. Valone, Thomas, *Harnessing the Wheelwork of Nature, Tesla's Science of Energy,* Adventures Unlimited Press, Kempton, IL, pp. 325-326, 2002.

31. Webb, Edwin Yates, Jr. *Origin of the Universe and the Secret of Light and Magnetism,* 1949 and 1951, Republished by Mark E. Foster, 1993.

32. Valone, Thomas, *Scalar Potentials, Fields and Waves,* Integrity Research Institute, Washington, DC, ~1999.

33. Meyl, Konstantin, Professor Dr.-Ing., *Scalar Waves*, INDEL GmbH, Verlagsabteilung, Villingen-Schwenningen, 2003, (translated out of the German language).

34. http://physicsweb.org/articles/news/8/7/16.

35. Prigogine, Ilya, *Time, Structure and Fluctuations*, Nobel Lecture, December 8, 1977.

36. Scott, William R., "To the Stars," *Aviation Week & Space Technology*, pp. 50-53, March 1, 2004.

37. King, Moray B., *Quest for Zero-Point Energy*, Adventures Unlimited Press, Kempton, IL, 2001.

38. King, Moray B., *Tapping the Zero-Point Energy*, Adventures Unlimited Press, Kempton, IL, 2002.

39. Valone, Dr. Thomas, *Zero Point Energy: Fuel of the Future!*, publication pending.

40. http://integrityresinst.crosswinds.net/FEASIBILITYofZPEStudy-Valone-2004.doc.

41. Lamoreaux, "Demonstration of Casimir Force in the 0.6-6 mu m Range," *Phys. Rev. Lett.*, Vol. 78, Issue 1, pp. 5-8, January 6, 1997.

42. *Nature*, Vol. 430, No. 6996, p. 126, July 8, 2004.

43. Yater, *Reversible Thermoelectric Converter with Power Conversion of Energy Fluctuations*, U.S. Patent No. 4,004,210, January 18, 1977.

44. Gray, Edwin V., *Pulse Capacitor Discharge Electric Engine*, U.S. Patent No. 3,890,548, June 17, 1975.

45. Gray, Edwin, V., *Efficient Power Supply Suitable for Inductive Loads*, U.S. Patent No. 4,595,975, June 17, 1986.

46. Gray, Edwin V., *Efficient Electrical Conversion Switching Tube Suitable for Inductive Loads*, U.S. Patent No. 4,661,747, April 28, 1987.

47. Vassilatos, Gerry, *Secrets of Cold War Technology—Project HAARP and Beyond*, Adventures Unlimited Press, 2000.

48. Papp, Josef, *Method and Means of Converting Atomic Energy into Utilizable Kinetic Energy*, U.S. Patent No. 3,670,494, June 20, 1972.

49. Papp, Joseph, *Inert Gas Fuel, Fuel Preparation Apparatus and System for Extracting Useful Work from the Fuel*, U.S. Patent No. 4,428,193, January 31, 1984.

50. Graneau, Peter, "Extracting Intermolecular Bond Energy from Water," *Proceedings of the Fourth International Symposium on New Energy*, May 1997.

51. Manning, Jeane, *The Coming Energy Revolution*, Avery Publishing Group, 1996.

52. Moray, T.H., *Electrotherapeutic Apparatus*, U.S. Patent No. 2,460,707, Feb. 1, 1949.

53. Dr. William O. Davis, *The Fourth Law of Motion,* Analog Vol. 69, No.3, May 1962.

54. Davis, W.O., G.H. Stine, E.L. Victory, and S.A. Korff, "Aspects of Certain Transient Mechanical Systems," *Bulletin of the American Physical Society*, No. 4, Series II, Vol. 7, p. 284, April 23, 1962.

55. Davis, William O., "The Energy Transfer Delay Time," *Annals of the New York Academy of Sciences*, Vol. 138, Art. 2, pp. 862-863, February 6, 1967.

56. Cox, James and Thomas Valone, P.E., *Inertial Propulsion Patent Collection*, Integrity Research Institute, Washington, DC, 1995.

57. www.lenr-canr.org.

58. http://www.fnal.gov/pub/inquiring/questions/strong_force.html.

REPORT DOCUMENTATION PAGE

Form Approved
OMB No. 0704-0188

1. REPORT DATE *(DD-MM-YYYY)*	2. REPORT TYPE	3. DATES COVERED *(From - To)*
01- 04 - 2005	Contractor Report	

4. TITLE AND SUBTITLE
Advanced Energetics for Aeronautical Applications: Volume II

5a. CONTRACT NUMBER

5b. GRANT NUMBER
NAG1-02048

5c. PROGRAM ELEMENT NUMBER

6. AUTHOR(S)
Alexander, David S.

5d. PROJECT NUMBER

5e. TASK NUMBER

5f. WORK UNIT NUMBER
23-090-2048

7. PERFORMING ORGANIZATION NAME(S) AND ADDRESS(ES)
NASA Langley Research Center
Hampton, VA 23681-2199

MSE Technology Applications, Inc.
200 Technology Way
P.O. Box 4078
Butte, MT 59702

8. PERFORMING ORGANIZATION REPORT NUMBER

9. SPONSORING/MONITORING AGENCY NAME(S) AND ADDRESS(ES)
National Aeronautics and Space Administration
Washington, DC 20546-0001

10. SPONSOR/MONITOR'S ACRONYM(S)
NASA

11. SPONSOR/MONITOR'S REPORT NUMBER(S)
NASA/CR-2005-213749

12. DISTRIBUTION/AVAILABILITY STATEMENT
Unclassified - Unlimited
Subject Category 44
Availability: NASA CASI (301) 621-0390

13. SUPPLEMENTARY NOTES
Langley Technical Monitor: Dennis M. Bushnell
An electronic version can be found at http://ntrs.nasa.gov

14. ABSTRACT

NASA has identified water vapor emission into the upper atmosphere from commercial transport aircraft, particularly as it relates to the formation of persistent contrails, as a potential environmental problem. Since 1999, MSE has been working with NASA-LaRC to investigate the concept of a transport-size emissionless aircraft fueled with liquid hydrogen combined with other possible breakthrough technologies. The goal of the project is to significantly advance air transportation in the next decade and beyond. The power and propulsion (P/P) system currently being studied would be based on hydrogen fuel cells (HFCs) powering electric motors, which drive fans for propulsion. The liquid water reaction product is retained onboard the aircraft until a flight mission is completed. As of now, NASA-LaRC and MSE have identified P/P system components that, according to the high-level analysis conducted to date, are light enough to make the emissionless aircraft concept feasible. Calculated maximum aircraft ranges (within a maximum weight constraint) and other performance predictions are included in this report. This report also includes current information on advanced energy-related technologies, which are still being researched, as well as breakthrough physics concepts that may be applicable for advanced energetics and aerospace propulsion in the future.

15. SUBJECT TERMS
Aerodynamics; Aircraft propulsion and power; Propellants and fuels; Energy production and conversion; Environment pollution; Advanced physics; Advanced electric concepts; Zero point energy

16. SECURITY CLASSIFICATION OF:			17. LIMITATION OF ABSTRACT	18. NUMBER OF PAGES	19a. NAME OF RESPONSIBLE PERSON
a. REPORT	b. ABSTRACT	c. THIS PAGE			STI Help Desk (email: help@sti.nasa.gov)
					19b. TELEPHONE NUMBER *(Include area code)*
U	U	U	UU	114	(301) 621-0390